Dissertations (2016-Present)   Dissertations

8-2021

Bacteria Assessment of Soil Samples in Houston Watersheilds; Impact of Heavy Metal, and Stress Responses in an Eukaryotic Co-Culture System.

Folasade Adedoyin

Follow this and additional works at: https://digitalscholarship.tsu.edu/dissertations

Part of the Microbiology Commons, and the Toxicology Commons

BACTERIAL ASSESSMENT OF SOIL SAMPLES IN HOUSTON WATERSHEDS; IMPACT

OF HEAVY METAL, AND STRESS RESPONSES IN AN EUKARYOTIC CO-CULTURE

SYSTEM.

DISSERTATION

Presented in Partial Fulfillment of the Requirements for

the Degree Doctor of Philosophy in the Graduate School

of Texas Southern University

By

Folasade Adedoyin, B.Tech., M.S.

Texas Southern University

2021

Approved by

Dr. Jason A. Rosenzweig
Chairperson, Dissertation Committee

Dr. Gregory H. Maddox
Dean, The Graduate School

Approved By:

Dr. Jason A. Rosenzweig   04/29/2021
_____   _____
Chairperson, Dissertation Committee   Date

Dr. Maruthi Sridhar Balaji Bhaskar   04/29/2021
_____   _____
Committee Member   Date

Dr. Hyun-min Hwang   04/29/2021
_____   _____
Committee Member   Date

Dr. Daniel Vrinceanu   04/29/2021
_____   _____
Committee Member   Date

Dr. Jim Briggs   04/29/2021
_____   _____
Committee Member   Date

BACTERIAL ASSESSMENT OF SOIL SAMPLES IN HOUSTON AREA WATERSHEDS;

IMPACT OF HEAVY METAL, AND STRESS RESPONSES OF BACTERIA IN AN

EUKARYOTIC CO-CULTURE SYSTEM.

By

Folasade Adedoyin, Ph.D.

Texas Southern University, 2021

Professor Jason A. Rosenzweig, Advisor

Houston has a complex watershed in which bayous intersect one another making the city prone to flooding, as evidenced by the 2017 Hurricane Harvey flood. We sought to evaluate bacterial population dynamics in Houston watershed soils pre- and post-Hurricane Harvey; additionally, we evaluated population dynamics in neighboring, downstream bayous ~ 1 year later in the summer and winter of 2018. This study quantified bacterial loads for pre-Hurricane Harvey (June 2017) and post-hurricane Harvey (November 2017) soil samples, as well as competitive samples from one year later [summer (June 2018) and winter (November) 2018].

 Unexpectedly, bayous closer to Houston's densely populated urban core, including Buffalo, Halls, Mustang, and Horsepen Bayous, had significantly higher enteric bacterial loads during the winter than the summer. Perhaps this was due to water flow rate changes or proximity to wastewater treatment plants. Following bacterial load determination, isolated colonies were identified using biochemical tests and DNA sequencing of the 16S ribosomal DNA region.

Additionally, we employed next generation metagenomic sequencing of 16S rDNA, capturing both culturable and unculturable organisms. The phyla *Proteobacteria*, Actinobacteria, *Bacteriodetes* and *Firmicutes* were found to be dominant in our metagenomic analysis and are human gut bacteria. Some opportunistic bacterial *Proteobacteria* pathogens identified in our metabolomic analysis were *Serratia marcenscens, Pseudomonas mendocina, Pseudomonas fulva, and Pseudomonas putida.*

To investigate the effects of heavy metal exposures, an environmentally isolated *Serratia marsescens* and its reference strain were exposed to Pb, Zn and manganese and subsequent oxidative stress responses and biofilm production were measured. Additionally, heavy metal exposures were characterized in gut and lung cell co-culture models using CCD-841, HT29 and BEAS-2B cell lines. Additionally, MTT assays were performed to determine cell cytotoxicity in bacterial cultures containing 10, 50, and 100 μg/ml of Zn and Pb and 100, 500 and 1000 μg/ml of Mn. Interestingly, the environmentally isolated *S. marsescens* produced increased biofilm and was more resistant to oxidative stress in the presence of Zn and Pb than its reference strain. Perhaps this was due to environmental adaptations of the environmental isolate.

To our knowledge, this is the first study that compares Houston-area bacterial populations before and after a major flooding event. Taken together, Hurricane Harvey likely contributed to a redistribution of enteric bacteria, as there was a significant increase in the enteric population of Buffalo and Halls Bayous following the Hurricane Harvey flooding event. Similarly, our 2018 winter data set followed the same trend, as significant increases were seen in the enteric populations of Horsepen, Mustang, and Cypress Creek watershed soils. Further, the environmentally isolated *S. marcescens* was better able to withstand environmental stressors than the reference strain and the lung cell line was more susceptible to lead treatment by a decrease in

viability of about 2.0-fold when compared with the gut cell lines. Also, the cell co-culture infection with the environmental isolate in the presence of various metal toxicants respond differently to its environmental reference strain and a significant decrease ($p < 0.05$) in bacteria proliferation at various time points for the cell lines were observed.

TABLE OF CONTENTS

LIST OF TABLES

LIST OF FIGURES

LIST OF ABBREVIATIONS

μ: Micro

SME: *Serratia marcescens* environmental strain

SMS: *Serratia marcescens* reference strain

Pb: Lead

Mn: Manganese

H2O2: Hydrogen Peroxide

Zn: Zinc

Hr: hour

mg: milligram

Min: minute

mL: Milliliter

RNA: Ribonucleic Acid

PPM: parts per million

PCR: Polymerase chain reaction

CFU: Colony forming units

CCD-841: Normal Human Colon Epithelial Cells

BEAS-2B: Human Lung Epithelial Cells

HT-29: Adenocarcinoma Human Colorectal Epithelial Cells

EPA: Environmental and Protection Agency

TCEQ: Texas Commission for Environmental Quality

VITA

2010... B.Tech., Ladoke Akintola University

Oyo, Nigeria

2014-16..… Graduate Assistant

Department of Aviation

Texas Southern University

Houston, Texas

2016...… M.S. Texas Southern University

Houston, Texas

2017- 21……………………………... Graduate Teaching Assistant,

Biology, Texas Southern University

Houston, Texas

2018- 21……………………………... Tittle III Research Fellow and Research

Assistant, EIS, Texas Southern University

Houston, Texas

Major Field... Environmental Toxicology

ACKNOWLEDGEMENT

CHAPTER 1

INTRODUCTION

Houston is popularly known as the "Bayou City," and its watersheds serve as recreational areas for residents (Wooster 2010). Recreationalists are at increased risk for exposure to bacterial contamination as well industrial contaminants from construction sites and shipping channels (Pandey et al. 2014; Wooster 2010). Wastewater outflows and agricultural runoff increase the loads of microorganism in these various watersheds thereby posing a threat to human health (Arnone et al. 2007; Celebi et al. 2014). According to the US Environmental Protection Agency (USEPA), watersheds are prone to bacterial contamination from natural and anthropogenic sources and are enhanced by urbanization, thereby leading to increased microbial populations (USEPA 2000). As a result, increased bacterial loads increase water turbidity, produce foul odor, and decrease dissolved oxygen (USEPA. 2012a). The USEPA has set acceptable threshold limits of both *Escherichia coli* and *Enterococci* spp. at 235-575 cfu/100 ml and 104 – 575 cfu/100 ml, respectively (US. EPA. 2012a) for primary fresh- and salt-water contact. In the state of Texas, acceptable *Escherishia coli* and *Enterococci* spp. levels have been set more stringently for surface water primary contact at 399 cfu/100 ml and 78 cfu/100 ml, respectively for single sample while secondary contact to no contact is set at 165cfu/ml -540cfu/ml (TCEQ. 2018; 2020).

Previously, microbial loads in various water systems in Canada and the United States have been characterized (Ahmed et al. 2019; Wilkes et al. 2014). Further,

1

Escherichia coli loads increased in the Squaw Creek watershed in Iowa and Beltsville, Maryland watershed increased in the Grand River watershed following a heavy rain event during the summer season (Lee et al. 2014). Weather conditions play an important role in the variability of microbial population dynamics in urban watersheds in Massachusetts. Flow rate can also affect the microbial population as high flow rate has been associated have been with the winter season with bacterial loads variable and getting re-distributed from one location to another while low flow rate is associated with the summer season (Van loon et al. 2015). More specifically, a two-day intense storm (45mm/day) led to higher *E. coli* loads than a light rainfall (0-10mm/day) that lasted over a week in upper Blackstone River (Wu et al. 2011). Additionally, after a major flooding event in Thailand, increases in *Sulfuricurvum*, *Thiovirga*, and *Hydrogenophaga* bacterial loads were recorded (Jeamsripong et al. 2018; Wuttichai et al. 2015).

In Houston, Texas, urban watersheds like Dickinson, Buffalo, and White Oak Bayous, all near dense populations, tend to have elevated bacterial loads when compared to neighboring rural watersheds (Brinkmeyer et al. 2015; Desai et al. 2010). More specifically, urban watersheds in Houston were found to have higher bacterial concentrations of *E. coli* and *Enterococcus* spp., and those elevations were influenced by rainfall events (Desai et al. 2010). Reports evaluating Houston watershed bacterial loads (Quigg et al. 2009; Desai et al. 2010; Brinkmeyer et al. 2015) have been published; however, to our knowledge, there have been no reports of bacterial loads in Houston watershed soil directly following flooding events. Soil harbors enormously diverse bacterial populations, and communities can vary greatly in composition (Barberean et al. 2012; Goto et al. 2011; Fierer *et al*. 2006). Houston has recently experienced three significant flooding events in a three-year span from 2015- 2017 (i.e., the Memorial Day flooding, the Tax Day flooding, and Hurricane Harvey). Such unprecedented flooding events warrant microbiological assessment of

bacterial loads in Houston watersheds to predict future redistribution and determine whether heavy rainfall events over short periods of time cause modifications therein.

Environmental heavy metals can potentially be noxious to the surrounding biota, indirectly impact freshwater habitats, and impact microbiological communities. In this study, zinc (Zn) (55.5mg/kg), manganese (Mn) (863.4mg/kg) and lead (Pb) (17.5mg/kg) levels measured during fall of 2017, 2018, and 2019 revealed levels (15mg/kg Pb; 30mg/kg Zn and 500mg/kg Mn) higher environmental agencies threshold. Elevated concentrations of environmental heavy metals can pose human health threats, and there are persistent environmental pollutants that can be introduced into the environment via anthropogenic activities. Consequently, bacteria have developed a variety of resistance mechanisms to counteract heavy metal exposures (Teitzel et al. 2003). More specifically, bacteria may form or isolate heavy metal complexes, reduce metals to a less toxic state, or expel the metal from within the cell (Ahemad et al. 2019; Prabhakaran et al. 2016). Superfund sites are areas that require removal of hazardous materials released by local industry and often contain elevated levels of heavy metals which can negatively impact freshwater habitats and their microbiological communities (Gough et al. 2011). Heavy metals, like Zn, and Pb are expected to be found in high concentrations during metal analysis of superfund sites soil samples (Hussein et al. 2013). Heavy metals can also induce the production of reactive oxygen species which then causes an imbalance in cellular oxidative status of bacteria and interfere with protein synthesis and function (Behera et al. 2014; Shahid et al. 2014).

Human health consequences of heavy metal exposures include lung damage, skin rashes, high blood pressure, memory loss, etc. (Mahurpawar 2015; Reheman et al. 2018). Heavy metal exposure to bacteria can generate reactive oxygen species and can express enzymes to detoxify H_2O_2 and also repair damages (Faulkner et al. 2011). The gut is one tissue that responds to heavy

metal exposure. More specifically, cadmium-chloride was shown to promote inflammation in the mouse gut but did not subsequently influence *Salmonella* infectivity (Breton et al. 2016). With regards to microbiota, the gut has the highest concentration of microbial organisms in the human body (Tchaptchet et al. 2011). The microbial environment of the gut can promote dysbiosis and potentially lead to numerous diseases including: gastroenteritis, obesity, and inflammable bowel syndromes (Cao et al. 2014; Khan et al. 2014).

In that vein, this study quantified bacterial loads for pre-Hurricane Harvey (June 2017) and post-hurricane Harvey (November 2017) soil samples, as well as competitive samples from one year later [summer (June 2018) and winter (November) 2018]. We identified representative isolated colonies using ribotyping and biochemical analysis, assessed global bacterial population dynamics using meta-genomic sequence analysis, generated phylogenetic trees, and employed Geographic Information System (GIS) mapping of bacterial loads across various watershed. Furthermore, an environmentally isolated *Serratia marcescens*, opportunistic pathogen and member of the *Enterobacteriaceae* family, was exposed to metal toxicants found in Houston watersheds, and its various responses to abiotic and biotic stressors were evaluated. *S. marcescens* has been shown to cause both lung (González-Juarbe et al. 2015) and gut infections (Ochieng et al. 2014) in humans, and, as a result, is an opportunistic pathogen of concern. More specifically, we isolated *S. marcescens* from the Buffalo and Dickinson Bayous. Since elevated levels of zinc (Zn), lead (Pb), and manganese (Mn) were measured in our bayou samples, the metals were used to challenge both our environmentally isolated *S. marcescens* as well as reference strain that we commercially acquired. Following metal challenge, biofilm production, oxidative stress resistance, growth kinetics, and interactions with human lung and gut cell lines were observed to determine whether the environmental isolate exhibited any beneficial adaptations.

ATTACHMENT	GROWTH	MATURATION	DETACHMENT	RE-DEVELOPMENT
Bacteria attach to a variety of surfaces, from metal, to plastic, to skin tissue, using specialized tail-like structures.	The cells grow and divide, forming a dense matrixed structure, many layers thick. At this stage the biofilm is too thin to be seen.	When there are enough bacteria in the developing biofilm the bacteria secrete a slimy extracellular matrix of proteins and polysaccarides.	The slime protects the bacteria from the harsh environments, shielding them from many chemicals, antibiotics and immune systems.	As the colonies mature, the structures created weaken and cast off bacteria that look for new places to grow and prosper.

Figure 1: Formation of Biofilm in Bacteria. Adapted from Understanding biofilms in agriculture by Jessica Derks. (Source: center for innovation, university of Auckland, New Zealand; 2001). This shows the five stages of biofilm formation in a bacterial organism.

Research Questions

a. Do major flooding events alter bacterial population dynamics?

b. Does temperature change during seasonal fluctuation impact bacterial load?

c. Will an environmentally isolated bacteria respond differently than its reference strain to stressors?

Hypothesis

a. If a major flooding event or a seasonal fluctuation occurs, a long-term modification to soil bacteria population dynamics will be observed.

b. If an environmental isolate is challenged with toxicants, then it will be better able to withstand stress exposures than its reference strain.

c. If environmentally isolate opportunistic pathogen *is* co-cultured with eukaryotic cells, it will proliferate better than its reference strain.
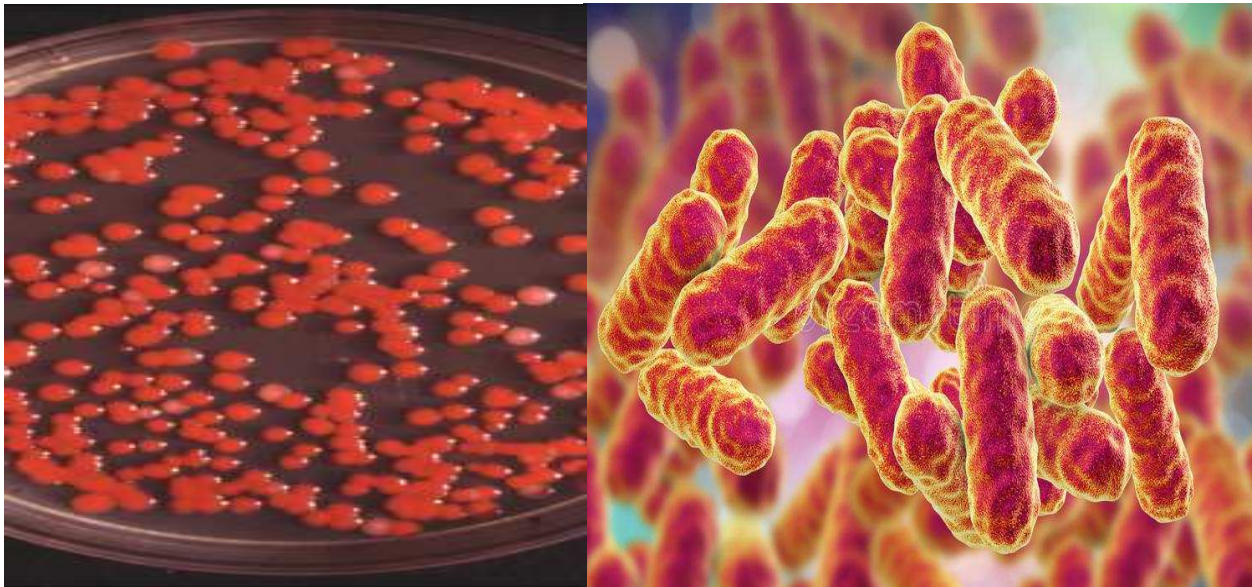
Figure 2: *Serratia marcescens* bacteria. This is a gram-negative bacterium; facultative anaerobe and it is rod shaped. It can also be classified as an opportunistic pathogen which is frequently related with hospital procured infections. This image was adapted from Kateryna Kon/science Photo Library which was uploaded on October 8th, 2019

Study Aims

AIM 1: To assess and quantify bacterial loads for summer and winter 2017, 2018 and 2019 Houston Bayou soil samples.

To determine whether Hurricane Harvey influenced total and enteric bacterial loads in watershed soils with high numbers of wastewater treatment facilities and superfund sites, we evaluated soil samples from 2017 (before and after Hurricane Harvey) and one year later in 2018. Over the course of our one-year study, we observed bayous fed by over 90 wastewater outflows such as Greens (2017), Dickinson (2018), Cypress Creek (2018) and Buffalo Bayous (2017) having increase in bacteria population. A total of 36 soil samples were collected from 12 locations spread over 5 watersheds during summer and winter 2017; while a total of 92 soil samples were collected from 14 locations spread over 5 watersheds during summer and winter 2018.

SAMPLING SITES

➤ A total of 36 soil samples were collected from 12 locations spread over 5 watersheds during summer and winter 2017; while a total of 92 soil samples were collected from 14 locations spread over 5 watersheds during summer and winter 2018.

➤ All the samples were collected in triplicate

Figure 3: Sampling sites. Approximately 128 soil samples were gotten over the period of 2017 and 2018.

To achieve the first aim, the following will be done.

    a.   Bacterial enumeration using different media.

The broad medium Luria Bertani (LB) agar (BD Difco™) was used to cultivate "total loads" while the selective and differential medium, MacConkey agar (Difco®), was used to enrich for enteric bacteria. The plates prepared were incubated, and the colonies were counted after 24hrs.

    b.   Identification of representative colonies using 16s rRNA sequencing, Biolog identification system and metagenomic analysis.

Identification at species level was performed by using Biolog GEN III micro plate (Biolog, Hayward, CA, USA) according to the manufacturer's instructions. The micro-plate was incubated at 30 °C or 35 °C depending upon the nature of the organism for 24 hours or more according to manufacturer's specification. Metagenomic identification and characterization was done at a taxonomical level.

    c.   Geographic data representation using information system.

The bayou flow lines, watershed boundary and the flood hazard layers were extracted from the National Flood Hazard Layer (NFHL) database (https://www.floodmaps.fema.gov/NFHL/status.shtml) and Houston-Galveston Area Council GIS datasets (http://www.h-gac.com/gis-applications-and-data/datasets.aspx). Soil sampling points of the study areas were imported into GIS as separate vector layer. The data were downloaded and processed using the ArcGIS Version 10.5 software (ESRI 2014).

AIM 2: To compare *Serratia marcescens* environmental strain type to its reference strain.

Concentrations of metal elements in soil samples were estimated by using inductively coupled plasma mass spectrometry (ICP-MS).

Figure 4: Impact of metals on the bacteria environment and on the health of human.

To achieve this aim, the following objectives would be carried out.

a. Evaluate growth kinetics, biofilm production, and oxidative stress responses in the presence of toxicants identified in the soil

b. Characterize *S. marcescens* strains when challenged with toxicants identified in the Houston bayou samples.

AIM 3: To evaluate the bacterial/cell co-culture as a model for exposure to metal toxicants

a. Assess the cytotoxic activity of eukaryotic cells exposed to trace metals using MTT assay

Compare S. *marcescens strains* growth in eukaryotic model infection system of both lung

and gut cells

CHAPTER 2

LITERARY REVIEW

<u>Watersheds</u>

From a long time, people made the choice to live near water, especially beside bayous, along rivers, coastlines, lakes and valleys. These attractions and recreational activities that water brings are numerous and diverse for human needs. The necessity of clean water is very crucial especially for numerous activities such as drinking, agricultural activities, industrial needs, transportation needs, fishing and so on. Apart from the enjoyment and positive impacts that water brings to people who live by them, there are also health impacts. People who live near these waterways play a significant role in impacting the quality of the water by using them to wash away and dilute society wastes and pollutants (Carpenter et al. 2013). Population increase comes with a high rate of production and consumption which makes the flushing down of wastes from upstream to downstream overwhelming for the natural cleansing capacities of earth waters. Increase in pollutants have also increased for the past decades which have resulted into the quality of water in rivers, lakes, valleys, streams, oceans etc. degrading (Carpenter et al. 2013).

This degradation can show up in the disturbance of normal aquatic ecosystems, and the subsequent loss of their component species as well as the services that these ecosystems once provided to society. Studies have evaluated the impact of microorganisms such as bacteria on different sources of water and soil. Assessing the water sheds area in Houston for the level of bacteria pathogen is very essential as it has been identified from previous research that there are

some water bodies prone to some species of water and soil bacteria which are dangerous to human and plants. The proximity of watersheds to farmlands, industries, construction sites, shipping channels etc. have increased the loads of microorganism especially bacteria pollutants which have continually been on the high side thereby leading to the deterioration in the quality of water in various water sheds (Carpenter et al. 2013).

Figure 5: Houston watershed study area. Soil samples for bacterial analysis were collected across the Greens, Halls, Hunting, White Oak, Buffalo, Cypress Creek, Dickinson Bayou, Horsepen and Mustang Bayou during the summer and fall of 2017 and 2018.

This deterioration disturbs the normal aquatic ecosystems and leads to loss of species and amenities that these natural water bodies once provided to the environment. These common microorganism pathogens found in watersheds can cause diseases therefore impacting the health of humans and that of plants as well. Some common genus of pathogens that have been identified to cause harmful diseases such as *Escherichia*; a gram-negative bacteria, *Staphylococcus*; a gram positive bacteria, *Enterococcus*; a gram positive bacteria, and *Pseudomonas*; which is a gram negative bacteria amongst a few.

Bacterial water quality standards

The bacterial indicator for fresh water is *E. coli* and *enterococcus* while marine water indicator is *enterococci*. Satisfactory levels are quantified in colony forming units (CFU) which usually include a 30 day mean or a single sample number. The bacteria water quality standard for fresh water and marine for different regulatory bodies are as follows:

TCEQ:

a. Freshwater: The standard set by TCEQ for *E. coli* geometric mean for primary contact recreation is 126cfu/100ml -206/100ml and for single sample is 399cfu/100ml. Secondary contact recreation is 630cfu/100ml - 1,030cfu/100ml. A non-contact recreation is set at 2,060cfu/100ml. *Enterococci* is measured for primary contact recreation at 33cfu/100ml for geometric mean, 78cfu/100ml for single sample. Secondary contact is 165cfu/100ml-270cfu/100ml while non-contact is 540cfu/100ml.

b. Marine water: *Enterococci* has a standard level of 35cfu/100ml geometric mean and 130cfu/ml single sample for primary contact. Secondary contact is set at 175cfu/100ml geometric mean while non-contact recreation is 350cfu/100ml.

c. Drinking water bacterial standard is set for 0 MCL (maximum contaminant level) or negative *E. coli* (TCEQ 2008; TCEQ 2018).

EPA:

a. Freshwater: *E. coli* has a geometric mean of 126cfu/100ml and a single sample number of 235cfu/100ml – 575cfu/100ml. *Enterococci* levels are set at 33cfu/100mL for a 30 day mean and 61 – 151cfu/100 mL for a single sample reading.

b. Marine water: *Enterococci* levels are set for 35cfu/100ml for a geometric mean and 104 – 501cfu/100mL for a single sample.

c. Drinking water bacterial standard is set for 0 MCL (maximum contaminant level) or negative *E. coli*. The maximum contaminant level was set at 0 because of disease outbreaks that occurs even at low levels of the indicator bacteria (EPA 212b)

WHO:

The estimated risk levels were done using the 95th percentile compliance level of the distribution of *enterococci*/100 ml as an indicator rather than the geometric mean. It was estimated that if this value is less than or the same as 40 *enterococci*/100ml, the risks of having gastro enteritis outbreaks and respiratory diseases will be below 1% and 0.3%, respectively. A higher 95th percentile value of 200/ml will result to risk higher of 1% - 5% and 0.3% - 1.9%. Water intended for drinking must have no detectable *E. coli* or indicator pathogen in a 100ml sample (WHO 2007).

Quality agency	Drinking water/100ml	Fresh water/100ml	Marine water/100ml
EPA	0 MCL	*E. coli: 126* *Enterococcus: 33*	*Enterococcus*:35
TCEQ	0 MCL	*E. coli: 126* *Enterococcus: 33*	*Enterococcus*: 35
WHO	Negative	Estimated *enterococci:* 40	Estimated: 40

Table 1: The bacterial water quality standards set by EPA, TCEQ and WHO for the drinking water, freshwater, and marine water recreation.

It is difficult to set the bacteria standards for soil quality because of its diversity and large accumulation of bacteria. Previous studies have reviewed the challenges of employing bacteria standards for soil quality assessment (Hussein 2013; Thiel-Bruhn et al. 2020). It was noted that characterizing soil bacteria in its natural state can be a challenging task due to its structural and functional diversity. They can also be influenced by their temporal and seasonal dynamics and fluctuation, spatial diversification, intrinsic characteristics etc. all which can limit the interpretation and validity of the data analysis obtained (kuffner et al. 2012; Regan et al. 2014; Surivavairun et al. 2019).

Microbial pathogens in watershed

Indicator organisms are bacteria such as non-specific coliforms, *Escherichia coli* and *Pseudomonas aeruginosa* that are very commonly found in the human or animal gut and which, if detected, may suggest the presence of sewage. Microbial pathogens which can be potentially present in different watersheds can be divided into three separate groups: viruses,

bacteria, and the protozoans (LeChevallier and Au, 2004). In this study, the primary focus will be based on the common bacteria pathogens found in the Houston water sheds. Watersheds are land areas that usually drain rainfall runoff or storm water to a general body of water. There are different types of water shed which are bayous, wastewater treatment facilities, basin etc.

According to previous research wastewater treatment facilities have become sin quo non in ensuring the discharges of high-quality wastewater effluents into receiving water bodies and consequence, a healthier environment. Increase in population all over the world has been predicted to result in a scarcity of ((Lauber et al. 2009)), and despite large advances in water and wastewater treatments, waterborne diseases still pose a major threat to public health worldwide. Several questions have been raised on the capacity of current wastewater treatment regimens to remove pathogens from wastewater with many waterborne diseases linked to supposedly treated water supplies. One of the major gaps in the knowledge of pathogenic microorganisms in wastewater is the lack of a thorough understanding of the survival and persistence of the different microbial types in different conditions and environments. This therefore brings the need for a thorough research into the movement and behavior of these microorganisms in wastewaters.

Several studies have also identified that soil can harbor a high load of bacteria pathogens. According to past research, soils harbor enormously diverse bacterial populations, and soil bacterial communities can vary greatly in composition across space (Lauber et al. 2009). However, our understanding of the specific changes in soil bacterial community structure that occur across larger spatial scales is limited because most previous work has focused on either surveying a relatively small number of soils in detail or analyzing a larger number of soils with techniques that provide little detail about the phylogenetic structure of the bacterial communities.

Plate count

The plate count technique depends on bacteria cultivating a colony on a nutrient medium so that the colony turn out to be visible to the naked eye and the quantity of colonies on a plate can be calculated. To be successful, the dilution of the previous sample must be assembled so that a standard between 30 and 300 colonies of the proposed bacterium are cultivated. Less than 30 colonies make the understanding statistically unsound whilst larger than 300 colonies regularly result in intersecting colonies and inaccuracy in the count. To guarantee that an appropriate number of colonies will be created, numerous dilutions are typically cultured. This methodology is widely used for the assessment of the usefulness of water treatment by the deactivation of representative microbial pollutants such as *E. coli* following ASTM D5465.

The laboratory process entails creating serial dilutions of the sample (1:10, 1:100, 1:1000, etc.) in sterilized water and growing these on nutrient agar in a plate that is wrapped and incubated. Normal media involve plate count agar for a common count or MacConkey agar to count Gram-negative bacteria such as *E. coli*. Usually, one set of the dish is incubated at 22 °C and for 24 hours and a second set at 37 °C for 24 hours. The makeup of the nutrient typically includes components that withstand the growth of non-target organisms and make the target organism easily detected, often by a color difference in the medium. Some recent techniques involve a fluorescent agent so that calculating of the colonies can be programmed. At the end of the incubation time the colonies are calculated by eye, a method that takes a few minutes and does not involve a microscope as the colonies are normally some millimeters across.

Biofilm

Bacteria take on a multicellular manner that enables survival in diverse environmental places, and this manner or alternative lifestyle is called biofilm. Single-cell organisms usually assume a temporary lifestyle like that of multicellular organisms that facilitates their survival in a harsh environment through biofilm formation (Kostakiosti et al. 2013; Flemming et al. 2010). This causes difficulty in their eradication and these characteristics are sometimes used to determine to an extent the effectiveness of antimicrobial treatments (Zuroff et al. 2014). Bacteria are enclosed in a state of an extracellular matrix of protein and DNA, which have factors that might impact the integrity of the biofilm formation. (Maden 2011; Branda et al. 2006; Curtis et al. 2007; Devaraj et al. 2015; Gallaher et al. 2006; Thomas et al. 2008). The effect of these factors on biofilm integrity is still undergoing research. However, it has been reported in different studies that the factors play an essential role in the resistance and sensitivity of the biofilm bacteria to antibiotics. (Drenkard 2003; Zuroff et al. 2014). Majority of infections are known to be caused by bacteria biofilm (Joo et al. 2012) and the lifecycle for biofilm is divided into Attachment, Maturation, and dispersal stages (Joo et al. 2012; O'Toole et al. 2000). The first stage, the attachment phase, is characterized by the expression of protein factors that allow adhesion to surface and the down-regulation of factors involved in motility. The maturation stage can be mediated by the increased expression of exopolysaccharides (EPS) in which the bacteria is embedded (O'Toole et al., 2000).

Finally, the dispersal stage involves the dispersal of biofilm-associated bacteria, presumably due to environmental signals (O'Toole et al. 2000). Although contentious, many studies have alluded to quorum sensing molecules' role in the dispersal phase of the biofilm lifecycle (O'Toole et al. 2000). Despite the unifying description described here and in many review articles, many studies suggest that biofilm physiology and molecular basis of regulation can vary

widely even among bacteria belonging to the same genus (O'Toole et al. 2000). This has searched a unifying regulator of biofilm formation, a widely researched topic (O'Toole et al. 2000).

There exist both *in vitro* and *in vivo* (examples are crystal violet biofilm assay, Confocal scanning laser microscopy, Electron microscopy, Resazurin assay, BioTimer, assay *C. elegans* viability assay, Mouse model biofilm assay, Pig model biofilm assay) methods for analyzing biofilms (Pantanella et al. 2013). A widely used biofilm assay method is the crystal violet biofilm assay. This method is often criticized for its inability to differentiate exopolysaccharide produced by live cells involved in biofilm from dead cells. Many studies have countered this fact by attempting to normalize the biofilm values either based on quantity of live cells present within biofilm or on overall planktonic growth. However, the crystal violet biofilm assay is useful because it can convey both qualitative and quantitative information about biofilm formed.

Oxidative Stress

Oxidative stress knows how to bring about the damage of mutually the spine and core of nucleic acids, together with free and absorbed dissolved amino acids, and also as cofactors of proteins. To relieve the harm of oxidative stress on the biology of cell, separate stress reaction factors are stimulated in bacteria, based on the type of stressor (Imlay. 2015; Imlay. 2019).

Opportunistic Pathogens in the Gut

The human body is populated by a highly diverse microbes' group in a mutual relationship with their host. Some of these are intestinal commensals which perform homeostatic mucosal immune responses and fulfill physiologic functions that benefit the host. The gut encompasses the esophagus, the stomach, and the small and large intestines. In each of these organs, an established microbial flora has been shown to exist. The gut also contains the highest density of microbial

organisms in the human body (Tchaptchet and Hansen 2011). The microbial population is usually introduced from the environment to the vaginal tract almost after birth and then grows till adulthood (Fanaro et al. 2003).

The gut microbiome contains both opportunistic and commensal pathogens. They can also serve as a barrier to the colonization of the gut by pathogens, aid in food digestion, and prime the immune system (Robles Alonso and Guarner 2013). The gut flora is also involved in the extensive interactions with other systems (Dinan and Cryan 2012; Tchaptchet and Hansen 2011). Take, for instance, communication with the brain extensively, thereby promoting standard neuronal functionality (Dinan and Cryan 2012). Microbes have overwhelming benefits within the gut, but they also promote pathologies (Penders et al. 2013; Tchaptchet and Hansen 2011).
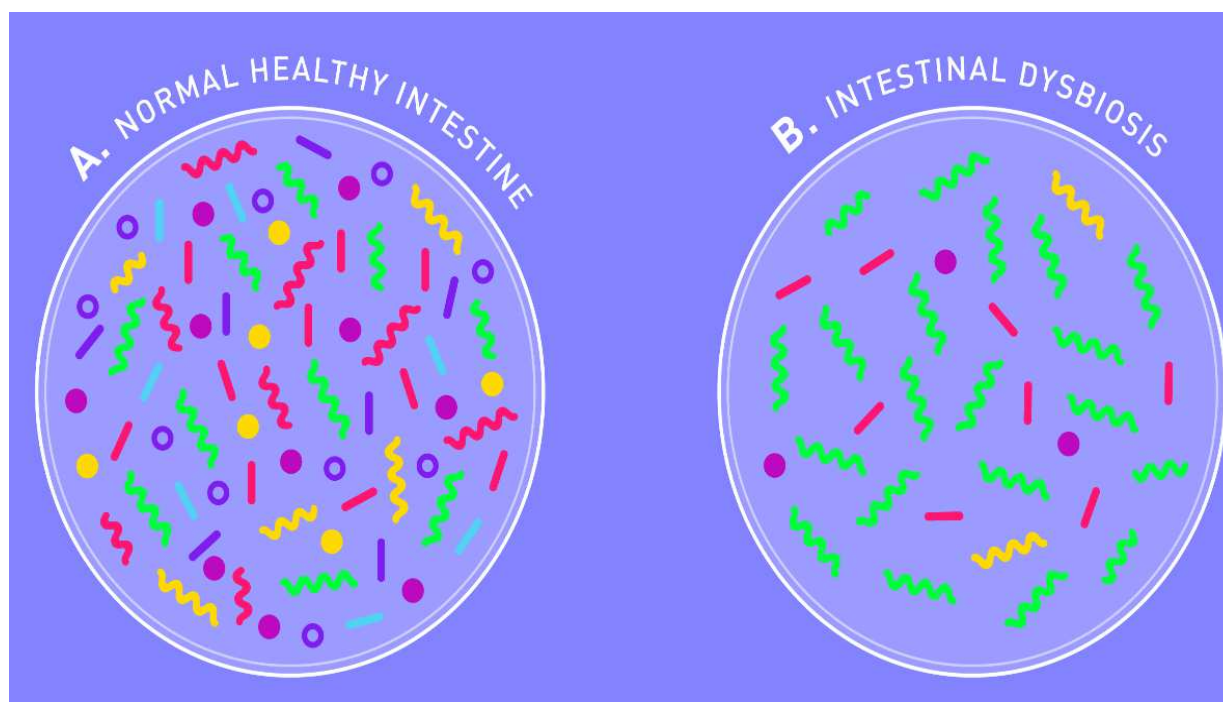
Figure 6: Opportunistic pathogen in the gut. Figure adapted from Dysbiosis: The Facts On Gut Dysbiosis And How To Heal Your Gut (atlasbiomed.com)

Once in the gut microenvironment, some specific conditions are created, allowing opportunistic pathogens to go rogue leading to a dysbiosis (remodeled gut environment). This condition has been linked to a wide array of diseases like gastroenteritis, neonatal flesh eating disease, obesity, and inflammable bowel syndromes (Cao et al. 2014; Ferreira et al. 2014; Geuking et al. 2014; Khan et al. 2014; Kotzampassi et al. 2014; Robles Alonso and Guarner 2013). In this study, opportunistic pathogen *Serratia marcescens* was exposed to toxicants found in watershed to evaluate its response to stressors

Opportunistic pathogens in lung

Anaerobic bacteria have been found to be the most common opportunistic pathogen in the lung due to them causing aspiration by lung abscesses. Examples of these anerobic bacteria are the Bacteroides, Prevotella, Fusobacterium amongst few. Despite the high risk of opportunistic infection pneumonias related to the more conventional bacterial pathogens are still more prevalent in immunocompetent individuals, with fever, respiratory symptoms, focal consolidation, and rapid rises in inflammatory markers. These are particularly common post-viral illness. The major risk factors are neutropenia, antibody deficiencies and high-dose corticosteroids. The organisms involved are more diverse than in conventional pneumonia and more likely to be resistant to first-line antibiotics. These include both Gram-positive (*Streptococcus pneumoniae*, *Staphylococcus aureus*) and Gram-negative (e.g., *Pseudomonas aeruginosa*, *Proteus* species, *Escherichia coli*, other enteric pathogens) organisms. Reactivation of latent tuberculosis also occurs; *Mycobacterium tuberculosis* cultures and polymerase chain reaction (PCR) must therefore be performed on respiratory samples from immunocompromised individuals with pulmonary infiltrates, particularly in high-prevalence areas.

Serratia marcescens

Serratia marcescens is an opportunistic gram-negative bacterium pathogen and member of the *Enterobacteriaceae* family, was also prevalent in some of the watersheds we sampled like Buffalo bayou and Dickinson bayou. *Serratia marcescens* is a gram-negative bacillus that occurs naturally mainly in soil and water. *S. marcescens* produces a very bright red pigment when grown at room temperature. This microorganism is associated with several infections such as urinary tract infection, septicemia, hospital-related infections, respiratory tract infections, endocarditis, eye infections, meningitis, and wound infections. Transmission is usually by direct contact. Hospital cases usually occur when droplets of *S. marcescens* are seen growing on catheters and supposedly sterile solutions. There are reported cases of outbreaks in Taiwan, such as contaminated intravenous fluids for pain control being the major cause of the outbreak in a hospital (Chiang et al. 2013). This study aimed at investigating the effect of heavy metal such as zinc, lead and manganese on *Serratia marcescens* environmental and surrogate strains when exposed to stressors such as biofilm production, oxidative stress, and growth. One of the purposes of this study was to compare the reactions of different strains of *Serratia marcescens* with heavy metal treatment and their co-culture in the BEAS-2B, CCD-841, and HT29 cell lines. Majority of bacteria exist in communities called biofilms which makes them more resistant to antibiotics and phagocytosis (Hoiby et al. 2010; Sadowska et al. 2013).

Heavy metal toxicants

The presence of high concentrations of heavy metals in our environment can be very harmful to the health of life surrounding polluted area. They are persistent environmental pollutants that can be introduced through anthropogenic activities into the environment. Bacteria have developed a variety of resistance mechanisms to counteract heavy metal stress (Teitzel et al. 2003). The developed mechanisms can be a formation or isolation of heavy metal complexes, a reduction of the metal to a less toxic component, and a discharge or removal of the metal from the bacterial cell. Superfund sites are also known contaminants of heavy metal which can indirectly impact the freshwater habitats and alter the microbiological communities (Gough et al. 2011). Heavy metals like Zinc and lead are expected to be found in high concentrations during metal analysis of soil samples (Hussein et al. 2013). Heavy metals can also induce the production of reactive oxygen species which then causes an imbalance in cellular oxidative status of bacteria and interfere with protein synthesis and function (Behera et al. 2014; Shahid et al. 2014). Some of the consequences of heavy metal exposures to man are known to include lung damage, skin rashes, high blood pressure, memory loss etc. organisms exposed to heavy metal stress also undergo vulnerability to the toxic conditions caused by reactive oxygen species.

Why should we care?

a) Is there a change in bacteria population following a major flooding event?

b) Does seasonal temperature impact the bacteria load?

c) People use these water sheds as recreational centers which make them prone to contamination.

d) These watersheds range from suburban and rural areas watershed with some closer to farm lands.

e) The bay of Galveston is also impacted by the water flow in these watersheds including bacteria and industrial runoff.

What can be done?

There are a few factors to be considered ranging from the watershed quality parameters to its use as recreational activities with the former been very key. Assuming a need to develop a standard to assess the water quality of Houston Bayou and the beaches of Galveston Bay arises, a wide range of water quality parameters besides the microbial parameters should be considered which will be monitored within the bayou. These parameters are dissolved oxygen, pH, alkalinity, salinity, turbidity, nutrients (total nitrogen and total phosphorus), chlorophyll etc. before setting the standard for bacterial indicators. This is because the presence of pathogens in a watershed can cause cloudy water, unpleasant odors, and decreased levels of dissolved oxygen. Adequate care and restriction should be taken in terms of recreational events to maintain the quality of watersheds. To propose the bacterial standards and keeping in mind the above parameters to help determine the source of the watershed (fresh, salt or brackish) and its recreational functions, regulatory bodies should propose more indicator bacteria apart from *E.coli* and *enterococci* for fresh water and marine water. To test the presence of bacteria levels, the total maximum daily load should still be used. It determines the level of pollutant the bayou can support and at the same time still support other recreational uses. Additionally, there should be the use of the colony forming unit per 100 milliliters using the membrane filtration method to determine the thresholds of this bacteria indicators. The threshold

should be revised and reduced for both fresh water and salt water (the current standard is

0/100ml for drinking water, 35/100ml for fresh water and 35/100ml for saltwater taking

into consideration proposals of other regulatory bodies). Taken together, routine bacterial

surveillance of local watersheds is warranted and should be aimed at characterizing

increased antibiotic resistance and virulence potential of environmentally isolated

bacterial pathogens.

CHAPTER 3

DESIGN OF STUDY

Materials and methods

Study Areas

The Halls Bayou begins in the northern part of Houston, Texas and flows for a 32 km

length. It empties into Greens Bayou and serves as recreational site for fishing for locals (H-

GAC. 2008). The Buffalo Bayou flows for approximately 85 km, through Houston, and

eventually into Galveston Bay and the Gulf of Mexico. It is a heavily urbanized watershed

surrounded by ~ 440,000 people and has several tributary bayous (White Oaks, Greens, and

Brays Bayous) flowing into it (Sipes et al. 2012; Oliveria et al. 2007; HCFCD 2020). Hunting

Bayou originates in the northeast of Houston and flows into the Buffalo Bayou. From the 2010

U.S. Census, the probable population of the Hunting Bayou watershed is 75,908 and is extremely

built-up with a mixture of residential, business, and industrial developments. Greens Bayou

originates in northwest Houston and flows into the Buffalo Bayou. The watershed encompasses

about 549 km^2 and involves numerous primary streams. There are about 495 km of open streams,

involving primary streams and tributary channels (HCFCD 2020). From the 2010 U.S. Census,

the projected population of the Greens Bayou watershed is 528,720. The White Oak Bayou

flows from the southeast to its convergence with the Buffalo Bayou in downtown Houston. It has

234 km of open watercourses, and from the data on the 2010 U.S. Census, the expected

population of the White Oak Bayou watershed is 433,250.

Mustang Bayou originates in the northern part of Houston and is surrounded by mostly rural homesteads. It is serviced by a municipal collection system and wastewater treatment facility (HGAC 2015; HCFCD 2015; HCFCD 2020). Dickinson Bayou is a 33 km-long, slow-moving, coastal stream that drains into Dickinson Bay, a subunit of the Galveston Bay system. Horsepen Bayou runs north of Clear Lake, Texas and east of Armand Bayou. It has a wastewater treatment plant located adjacent to it (HGAC 2002; TCWP 2008; Rifai 2007; HGAC 2008).
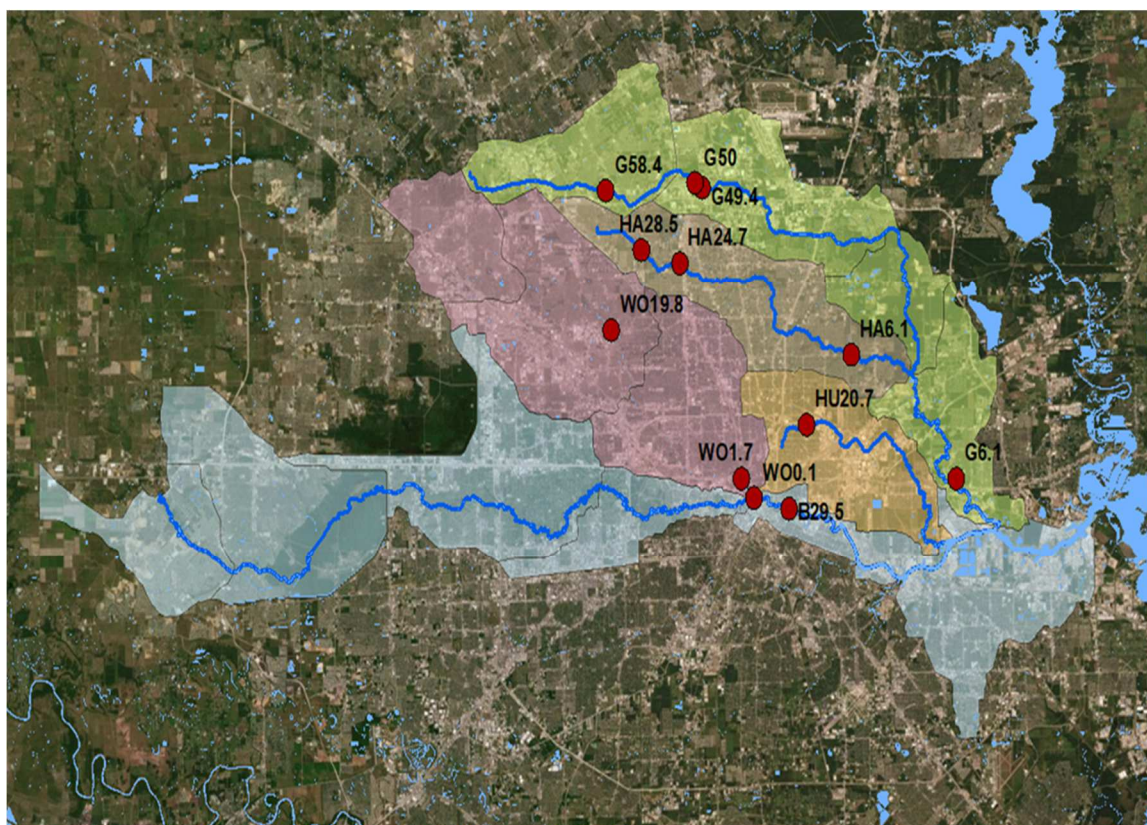
Figure 7: Map of the 2017 study sites was created using the arc map 10.3 by Esiri.

Soil samples for bacterial analysis were collected across the Greens, Halls, Hunting, White Oak, and Buffalo bayous during the summer and fall of 2017. Location of soil samples, G6.1, G49.4, G50, and G58.4 along Greens Bayou; HA6.1, HA24.7, and HA28.5 along Halls Bayou; HU15.1 and HU20.7 along Hunting Bayou; WO0.1, WO1.7, and WO19.8 along the White Oak Bayou and

B29.5 and B32.5 along Buffalo Bayou are shown in the image. All the samples were collected in triplicate.
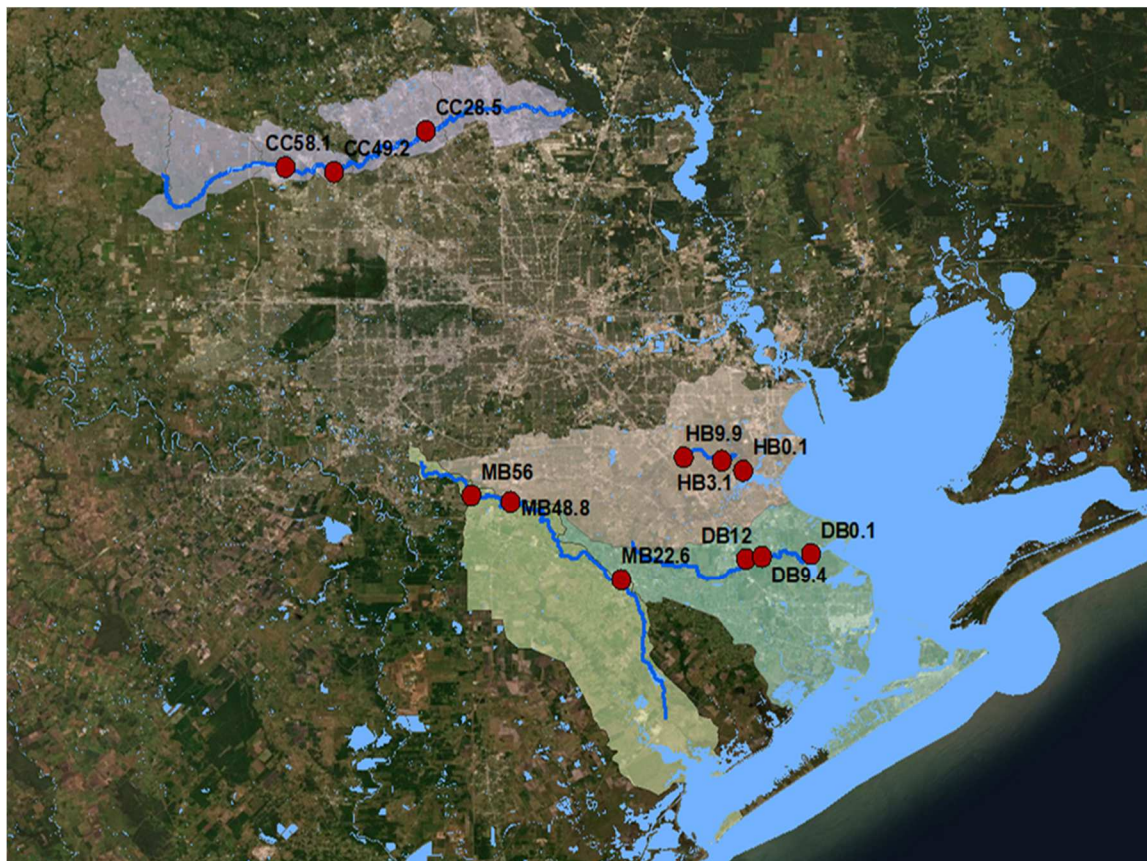
Figure 8: Maps of the 2018 study sites was created using the arc map 10.3 by Esiri.

Soil samples for bacterial analysis were collected across the Cypress Creek, Dickinson Bayou, and Mustang Bayou during the summer and fall of 2018. Location of soil samples, CC28.5, CC49.2, and CC58.1 along Cypress Creek; DB0.1, DB9.4, and DB12 along Dickinson Bayou, MB22.6, MB48.8, and MB56 along Mustang Bayou; HB0.1, HB3.1 and HB9.9 along Horsepen Bayou are shown in the image. All the samples were collected in triplicate.

Finally, Cypress Creek Bayou drains into an area of 495 km^2 and lies in the northern part of Houston surrounded by rural farmland (Chellam et al. 2008; Teague et al. 2013). It is a major

source of drinking water and a contributor of pollutant and urban runoff into Lake Houston (Sneck-Fahrer et al. 2005; Chellam et al. 2008).

Sample collection and processing

Identification of rural and suburban watershed area with accessible locations using the GPS and GIS map was done to get samples of soil. The following watersheds were sampled in summer and fall 2017 and 2018 (Fig. 7 and Fig. 8). Rural and suburban watershed areas with accessible soil sampling locations were identified using the Geographic Information Systems (GIS) (Arc map 10.3, ESRI Inc.). Watershed soil was sampled in the summer and fall of 2017 (Fig. 2) and 2018 (Fig. 3). In short, 0-10 cm of surface soil along the bayou flood plain was collected from all watersheds in this study using a trowel and a probe. An amount of 100 g samples was placed in zip lock bags and refrigerated within 6 hours. A total of 36 surface soil samples were collected from 12 locations spread over five watersheds during the summer (June 29.40C) and winter (November 13.80C) of 2017, while a total of 92 surface soil samples were collected from 14 locations spread over five watersheds during summer (June 28.30C) and winter (November 12.20C) of 2018. All samples were collected in triplicate. The soil samples were collected from G58.4, G50, and G49.4 and G6.1 location along Greens Bayou, B29.5 along Buffalo Bayou, HU20.7 along Hunting Bayou, HA28.5, HA24.7, and HA6.1 along Halls Bayou, W019.8, WO1.7, W00.1 along White Oak Bayou was collected during 2017, and CC58.1, CC49.2 and CC28.5 along Cypress Creek, MB56, MB48.8, and MB22.6 along Mustang Bayou, DKB 12, DKB9.4 and DKB0.1 along Dickinson Bayou, HB9.9, HB3.1 and HB0.1 along Horsepen Bayou were collected during 2018. The sample locations were named with a letter followed by a number as suffix where the letters stand for the name of the Bayou and the number represents the distance of the sample site in km from the mouth of the Bayou. For example, G58.4 represents the sample site located at

58.4 km from the mouth of the Greens Bayou. Soil samples were dried at room temperature for 16 hr. An amount of 1 g of dry soil was suspended in 10 mL of deionized water and was vigorously agitated to disrupt soil aggregates; agitation periods varied from 10 min to 1 hr. depending on need and different soil types. 10-fold serial dilutions were prepared in 1 mL volumes ranging from 10^0-10^{-7}(Thomas et al. 2015).

Media Preparation

Nutrient conditions were modelled using broad based medium and selective and differential medium respectively with Luria Bertani agar (BD Difco™ Dehydrated Culture Media: LB Agar, Lennox) and Mackonkey agar (Difco®). Nutrient Agar plates were prepared using 35g of dehydrated Luria Bertani medium (LB) in 1L of distilled water (Table 1). The solution was then autoclaved using Ward's science 16L autoclave at 121 °C for 30 minutes. It can cool, and then poured into fisher brand petri dishes to solidify and then inverted after 1hr to allow plates to dry at room temperature. Mackonkey agar medium was prepared using 50g of dehydrated agar in 1L of distilled water then autoclaved at 121 °C for 30 minutes to sterilize (Fig 4).

Figure 9: Flow chart for media preparation

LB	MACKONKEY
Tryptone 10g/L	Pancreatic digest of Gelatin 17g/L
Yeast extract 5g/L	Peptones (meat and Casein) 3g/L
Sodium Chloride 5g/L	Sodium Chloride 5g/L
Agar 15g/L	Agar 13.5g/L
Lactose N/A	Lactose 10g/L
Neutral red N/A	Neutral red 0.03g/L
Crystal violet N/A	Crystal Violet 1mg/L

Table 2: Components of the media used in this study. The composition of the selective or differential nutrient usually includes reagents that resist the growth of non-target organisms and make the target organism easily identified, often by a color change or indicator in the medium.

Bacterial Enumeration

The broad medium Luria Bertani (LB) agar (BD Difco™) was used to cultivate "total loads" while the selective and differential medium, MacConkey agar (Difco®), was used to enrich for enteric bacteria. Media was prepared (per manufacturer's specification) and were then autoclave- sterilized at 121°C for 30 minutes. Either 100 µl or 33 µl of soil suspension dilutions (described above) were aseptically plated in triplicate and spread on both MacConkey and LB media and incubated at either 32°C or 37°C for 18 hr. Colonies were then enumerated by plate counting. To compare the enterococci threshold levels, cfu/100ml is equivalent to cfu/100g. cfu/100g is 100cfu/g.
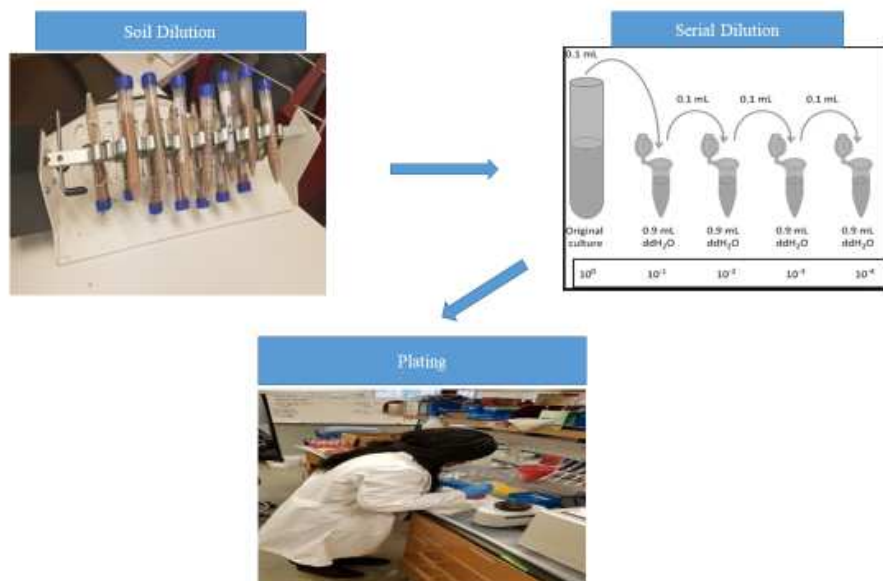
Figure 10: Flow chart of sample preparation

Bacterial Enumeration

The broad medium Luria Bertani (LB) agar (BD Difco™) was used to cultivate "total loads" while the selective and differential medium, MacConkey agar (Difco®), was used to enrich for enteric bacteria. Media was prepared (per manufacturer's specification) and were then autoclave- sterilized at 121°C for 30 minutes. Either 100 μl or 33 μl of soil suspension dilutions (described above) was aseptically plated in triplicate and spread on both MacConkey and LB media and incubated at either 32°C or 37°C for 18 hr. Colonies were then enumerated by plate counting. To compare the enterococci threshold levels, cfu/100ml is equivalent to cfu/100g. cfu/100g is 100cfu/g.

Bacterial isolation and characterization

Twelve representative down-selected colonies from both LB and MacConkey plates were isolated and subjected to Gram-staining, catalase, and oxidase tests. For Gram-staining, smears of

isolates were prepared on glass slides, heat fixed, and flooded with crystal violet for 1 min, Gram's iodine for 1 min, decolorizer for 15 sec, and then the counter-stained with safranin for 1 min. For the catalase test, a drop of 3% hydrogen peroxide was added to bacterial smears, and positive results were indicated by gaseous O_2 bubble formation. Oxidase tests employed a colorless oxidase reagent (BD oxidase reagent dropper catalog #261181), and positive results were scored by a purple color gain.
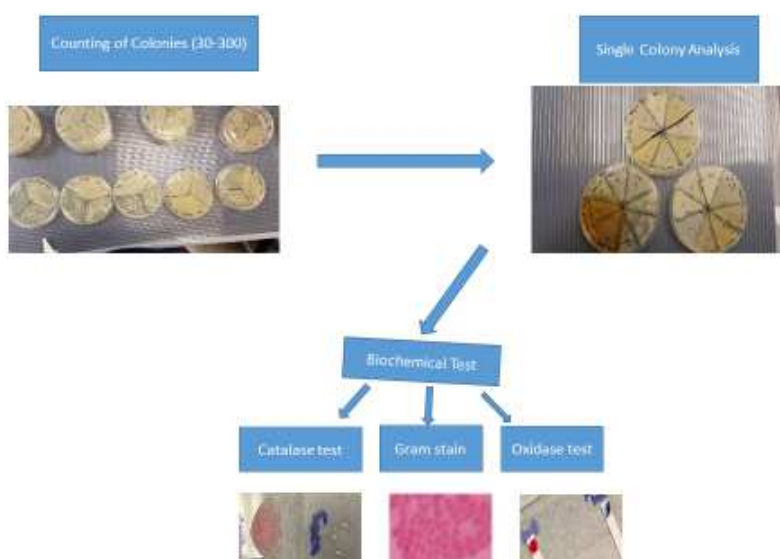
Figure 11: Flow chart of Bacteria Enumeration, Isolation and Biochemical Test

Biolog Identification

Identification at species level was performed by using Biolog GEN III micro plate (Biolog, Hayward, CA, USA) according to the manufacturer's instructions. The micro-plate was incubated at 30 °C or 35 °C depending upon the nature of the organism for 24 hours or more according to manufacturer's specification. Protocol A according to the manufacturer's handbook was employed. The procedure in brief is growing pure culture of the bacterium on a broad-based

medium (LB) agar plate. A single colony of bacteria from the fresh culture was swabbed with a sterile applicator from the surface of the LB agar plate and suspended in inoculating fluid (IF-A GEN III Cat #:72401) to a specified density. 100 microliters of the bacterial suspension were pipetted into each well of the micro-plate. The micro-plate was then incubated at the appropriate temperature that suits the nature of the organism for a minimum of 24 hours. The micro-plate was then read with the Biolog Micro Station TM system and compared to the database for the purpose of organism specie level identification.

Figure 12: Flow chart of Biolog protocol

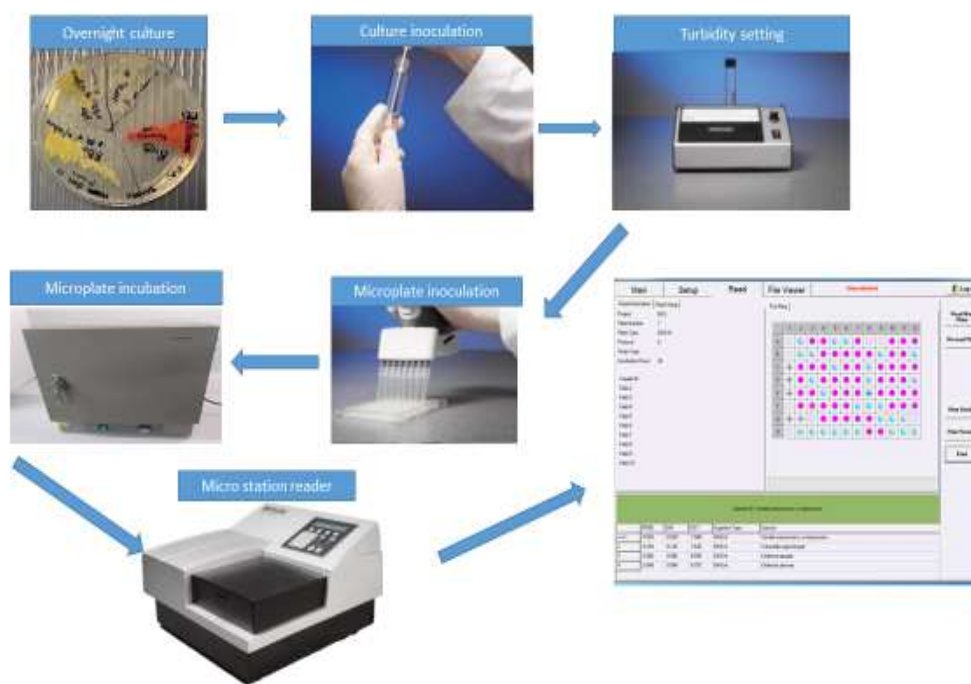**Dirty colony PCR Sequencing**

It is done using a Bio-Rad T100 thermal cycler. This analysis is a cell free DNA replication carried out in a test tube. This was done by amplifying the DNA samples and sequencing the reaction using Sanquer sequencing which targets the 16s ribosomal DNA. The procedure is a modified Rozenzweig et al. 2014. The PCR reaction is done by adding 12.5μl of a 2x concentrated Taq master mix (New England Biolabs cat #: M0270L) that contained the necessary dNTPs (at 0.2 mM each) as well as Taq polymerase. Pure isolated single colony bacteria were cultured on agar plates at the required temperature and time. A single colony of the cultured bacteria sample was mixed with 1μl of desired forward and of reverse primers each. This primer set consists of 27F (AGAGTTTGATCCTGGCTCAG) and 1387R (GGGCGGGTGTACAAGGC) which can amplify a product of approximately 1360 nucleotides (Ferris et al., 2007). 10.5μl of nuclease free water was also added to the mixture to give a total final volume of 25μl reaction in the micro-centrifuge tube. The samples were then placed on a thermocycler which can be programmed to alter the temperature of the PCR reaction in different steps and cycles for few minutes to allow the denaturing and synthesis of DNA. The steps are 30–35 cycles of the following temperatures for the indicated periods: 95°C for 5 minutes (DNA denaturation step), 95°C for 1 minute (DNA melting/denaturation step), 55°C for 1 minute (primer annealing step), and 72°C for 1minute/kilo-base (1000 nucleotides) of DNA (primer extension/elongation step). Steps 2-4 is repeated for 35 cycles before the final extension for 5 minutes at 72°C. At the conclusion of a successful reaction, one original molecule of template DNA will have been amplified more than 108-fold (Rosenzweig et al. 2014). (The thermocycler is described in Figure 8). The PCR products were then run on a 0.7% agarose gel using electrophoresis.

UNIVERSAL PRIMERS	BINDING AND SEQUENCE
FORWARD 27F	AGAGTTTGATCCTGGCTCAG
REVERSE 1387R	GGGCGGGTGTACAAGGC

Table 3: Primers used in this study with their binding and sequence

16s Sanger Sequencing

The PCR reactions generated were labelled appropriately, stored in ice and sent to lone star lab Houston for 16s ribosomal DNA sequencing. This targets the 16s r RNA of the amplified DNA samples. The data is then blasted on a NCBI software to give the name of the organism and the specific specie.

Agarose gel analysis

The procedure is a modified Rozenzweig et al. 2014. The PCR reaction is done by adding 12.5µl of a 2x concentrated Taq master mix (New England Biolabs cat #: M0270L). Pure isolated single colony bacteria were cultured on agar plates at the required temperature and time. A single colony of the cultured bacteria sample was mixed with 1µl of desired forward and of reverse primers each. This primer set consists of 27F (AGAGTTTGATCCTGGCTCAG) and 1387R (GGGCGGGTGTACAAGGC) which can amplify a product of approximately 1360 nucleotides (Ferris et al., 2007). 10.5µl of nuclease free water was also added to the mixture to give a total final volume of 25µl reaction in the micro-centrifuge tube. Amplified samples were run on a 0.7% agarose gel containing SYBR safe (Invitrogen; cat#S33102).
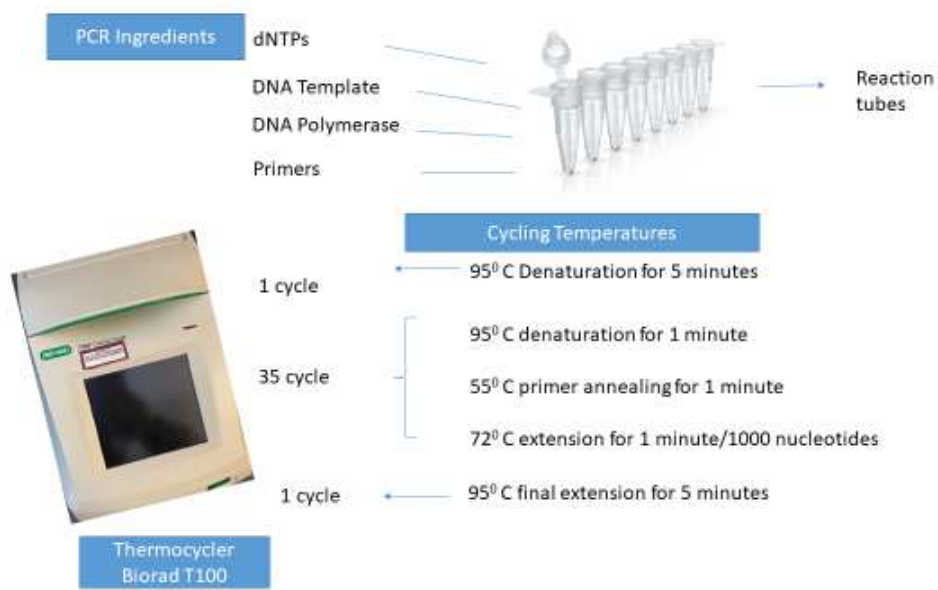
Figure 13: Polymerase Chain Reaction (PCR) of selected samples

Metagenomics Analysis

5g of soil from several representative watersheds was shipped to MR DNA (Shallowater, Texas) where DNA extractions, purifications were carried out. DNA was extracted using the DNeasy PowerSoil Kit (Qiagen). 250 mg solid samples were used to extract the DNA. Pellets were resuspended in 100 □l water and used for extraction. DNA quantity and quality was determined using NanoDrop2000 (Thermo Scientific). Samples were then used to quantify the bacterial concentrations by qPCR using Bacteria2F and Bacteria2R primers. 1 □l of the template DNA was used to perform the qPCR reactions using 2X Universal Taqman PCR Mastermix (Applied Biosystems) in StepOnePlus Real-Time PCR System (Applied Biosystems). Three replications were used for each sample. DNA from E. coli was used as standard. More specifically, 16S rRNA gene V4 variable region PCR primers 515/806 (barcoded on the forward primer) were used in a 30 cycle PCR using the HotStarTaq Plus Master Mix Kit (Qiagen, USA) using the following conditions: 94°C for 3 min, followed by 30 cycles of 94°C for 30 sec, 53°C for 40 sec and 72°C

for 1 min, proceeded by a final elongation at 72°C for 5 min. Following amplification, PCR products were evaluated in 2% agarose gel for quality control and to determine relative band intensities. Multiple samples were pooled together and purified with Ampure XP beads (e.g., 100 samples) in equal proportions based on their molecular weight and DNA concentrations. Pooled and purified PCR products were then used to prepare Illumina DNA libraries. Sequencing was also performed at MR DNA (Shallowater, TX, USA) on a MiSeq (Illunima Inc.) following the manufacturer's guidelines. Sequence data were processed using MR DNA analysis pipeline and Qiime. In summary, sequences were joined and depleted of barcodes and primers. Then, sequences <150bp were removed, and sequences with ambiguous base calls were removed. Operational taxonomic units (OTUs) were defined by clustering at 3% divergence (97% similarity) while controlling for chimeras. Final OTUs were taxonomically classified using BLASTn against RDPII and NCBI databases ([http://www.ncbi.nlm.nih.gov, http://rdp.cme.msu.edu).

Molecular CFU Counts

DNA was extracted using the DNeasy PowerSoil Kit (Qiagen). 250 mg solid samples were used to extract the DNA. Pellets were reuspended in 100 □l water and used for extraction. DNA quantity and quality was determined using NanoDrop2000 (Thermo Scientific). Samples were then used to quantify the bacteria concentrations by qPCR using Bacteria2F and Bacteria2R primers. 1ul of the template DNA was used to perform the qPCR reaction using 2XUniversal Taqman PCR Mastermix (Applied Biosystems) in StepOnePlus Real-Time PCR System (Applied Biosystems). Three replications were used for each sample. DNA from E. coli was used as standard.

Geography Information System (GIS) mapping

The bayou flow lines, watershed boundary and the flood hazard layers were extracted from the National Flood Hazard Layer (NFHL) database (https://www.floodmaps.fema.gov/NFHL/status.shtml) and Houston-Galveston Area Council GIS datasets (http://www.h-gac.com/gis-applications-and-data/datasets.aspx). Soil sampling points of the study areas were imported into GIS as separate vector layer. The data were downloaded and processed using the ArcGIS Version 10.5 software (ESRI 2014).

Bacteria strains, metals and media

S. marsescens (Carolina item #: 155455), and wild type *S. marsescens ss marsescens* (Biolog identified 2019) were the bacterial strains used in this study. Nutrient conditions were modelled with Luria Luria Bertani broth (BD Difco™) media. For all experiments LB medium was used to grow bacterial strains with agitation (250 rpm) at 37 °C. All absorbance readings were taken using a BioTek™ Elx™800 microplate reader. Metals (Pb, Zn and Mn) were purchased from Carolina.

Eukaryotic cell lines

BEAS-2B (ATCC CRL-9609), CCD 841 (ATCC CRL-1790) and HT-29 cells (ATCC HTB38) were cultured as previously described (Petiot et al. 2000) with some minor modifications. Dulbecco's modified eagles' medium (DMEM) (ATCC 30-2002) and Eagle's minimal essential medium (EMEM) (ATCC 30-2003) supplemented with 10% FBS (Thermo Fisher 16140071) and 5% pen-strep (Thermo Fisher 15140122) was used. Cells were incubated at 37 °C with 5% CO_2. Flask medium was changed every 3 days.
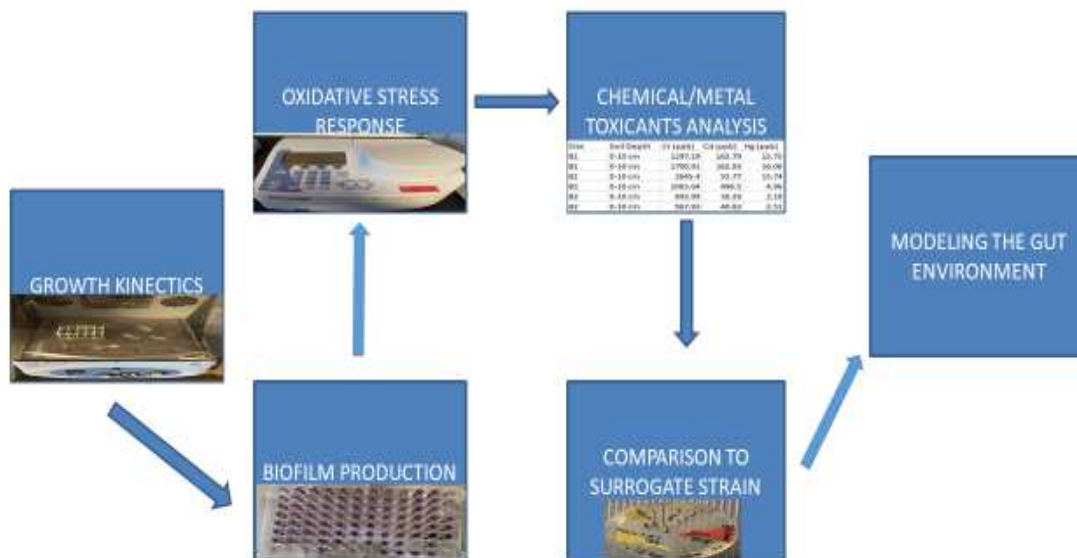
Figure 14: Experimental design for heavy metal toxicants analysis

Measurements of Metals

Concentrations of metal elements in soil samples were estimated by using inductively coupled plasma mass spectrometry (ICP-MS). Following treatment of 0.5g of soil with 10 ml nitric acid (HNO_3), samples were placed into Mars 6 microwave vessels. Subsequently, they were digested using the EPA 3015a method (Dirk et al. 1999). Digested samples were then further digested for another 24 h. Finally, 0.2 μl of supernatant was diluted in water and analyzed by ICP-MS following calibrations with appropriate standards, and samples were statistically analyzed using MINITAB software (MINITAB Inc., State College, PA, USA).

Growth kinetic analysis

Previously described methods (Suraju et al. 2015) with slight modifications was employed. Briefly, Lead, Zinc and Manganese were diluted in sterile distilled water at concentrations of 10μg/mL, 50μg/mL, and 100μg/ml. Saturated cultures of *S. marsescens* surrogate and wild type grown in LB broth were then diluted to a starting optical density of 0.2 in corresponding broth-

type in a 96-well plate to make a final volume of 200µl. Only media was added to the controls. Growth was monitored every 30 minutes for 12hours at a wavelength of 595$_{nm}$. All growth assays were conducted in triplicate.

Oxidative stress assay

Previously described methods (Suraju et al. 2015) with slight modifications was employed. Briefly, Lead, Zinc and Manganese were diluted in sterile distilled water at concentrations of 10µg/mL, 50µg/mL, and 100µg/ml. Saturated cultures of *S. marsescens* surrogate and wild type grown in LB broth were then diluted to a starting optical density of 0.2 in corresponding broth-type in a 96-well plate to make a final volume of 200µl. Only media was added to the controls. At the 1-hour time point, oxidative stress with hydrogen peroxide was introduced at concentrations of 20 and 50mM. Oxidative stress sensitivity was monitored for 6hrs at a wavelength of 600nm. All experiments were carried out in triplicate.

Crystal violet biofilm assay

For our biofilm formation assay, we employed our previously described methods (Suraju et al. 2015) with slight modifications. Briefly, saturated cultures of *S. marsescens* surrogate and wild type grown in LB broth, were diluted to an optical density (595 nm) of 0.2 in a 96-well plate (final volume, 200 µL/well). Microtiter plates were incubated for 24 h with agitation (~ 100 rpm) at 37 °C, after which optical densities at 595 nm were measured. Wells were washed with water and and incubated with 0.1% (vol/vol) crystal violet (total vol – 125µl/well) for 1 hour at room temperature. Nonspecifically bound crystal violet was removed by washing with water, and the wells could dry overnight. Biofilm bound crystal violet was dissolved in 250ul of 30% acetic acid. Optical densities of solubilized crystal violet were measured at a wavelength of 570$_{nm}$. Biofilm formed was normalized based on relative biomass (optical densities of biofilm formed/ optical

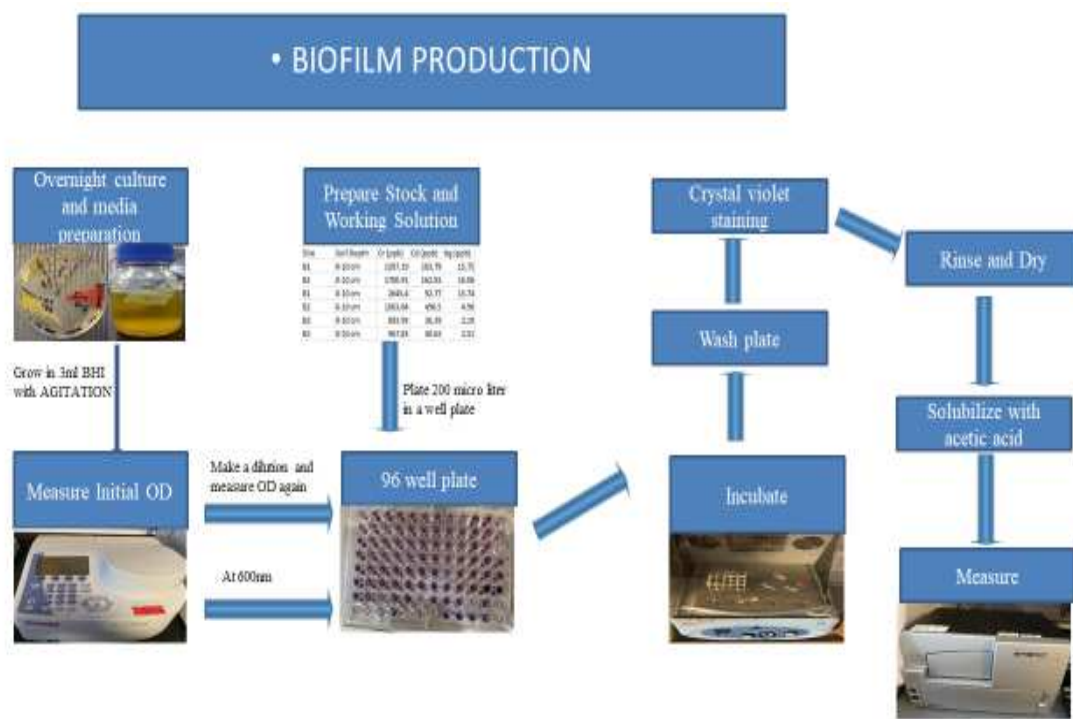density of terminal bacterial growth). All experiments were carried out in triplicate or quadruplicate.

Figure 15: Flow chart of Biofilm protocol

MTT (3-(4, 5-dimethylthiazol-2-yl) -2, 5-diphenyltetrazolium bromide) assay

Previously described methods (Bado et al. 2017) with slight modifications was employed. Briefly, BEAS-2B and HT29 cells were seeded in a 96-well plate at a density of 5000 cells/well while CCD-841 cells were seeded at 2500 cells/well ~ 24 h preceding the experiment. The following day, treatment of designated wells using 10, 50, and 100 μg/mL of Pb, Zn, and Mn occurred for 0, 3, 6, 8, 12 or 24h. Twenty microliters of 5 mg/mL MTT was added to each well, followed by incubation at 37 °C with 5% CO_2. After 4 h, medium was gently removed from each

well and replaced with 100 µL of DMSO. Cells were agitated on an orbital shaker for 5 to 10 min, and absorbencies were read at 570 nm with a reference filter of 630 nm.

Bacterial co-culture with eukaryotic cells

Previously described methods (Bado et al. 2017) with slight modifications was employed. Briefly, BEAS-2B, CCD-841, and HT29 cells were seeded into 24-well plates at densities of ~ 1 × 10^5/well, 24 h prior to bacterial infection. At this seeding density, monolayers were sub confluent (~ 60–80% confluency) at the time of the experiment. Bacteria were grown to saturation in LB broth at 37°C with agitation (~ 250 rpm), washed with 1X PBS, and diluted to optical densities (600 nm) of 1.0 in DMEM + 10% FBS. Diluted cultures of *S. marsescens* was further diluted (as necessary) to achieve multiplicities of infection of 10. Following a 1hr attachment period, each well was washed with PBS, and DMEM containing 10, 50 and 100 µg/mL of either Pb, Zn, Mn was added to each well. Viable colony plate counts were enumerated for both the 0- and 6-h end points, and fold increases over that time period were calculated. All plates were incubated for 24 h at 37 °C.

Statistical analyses*:*

All experiments were carried out in triplicate and averaged. Statistical analysis of the data was done using Microsoft Excel. The student's two tailed, unequal variance T-test was used to derive p-values. To be considered statistically significant, p-values less than or equal to 0.01 representing two asterisks and p-values less than or equal to 0.05 representing one asterisk and a difference of 20% or more between averages had to be observed.
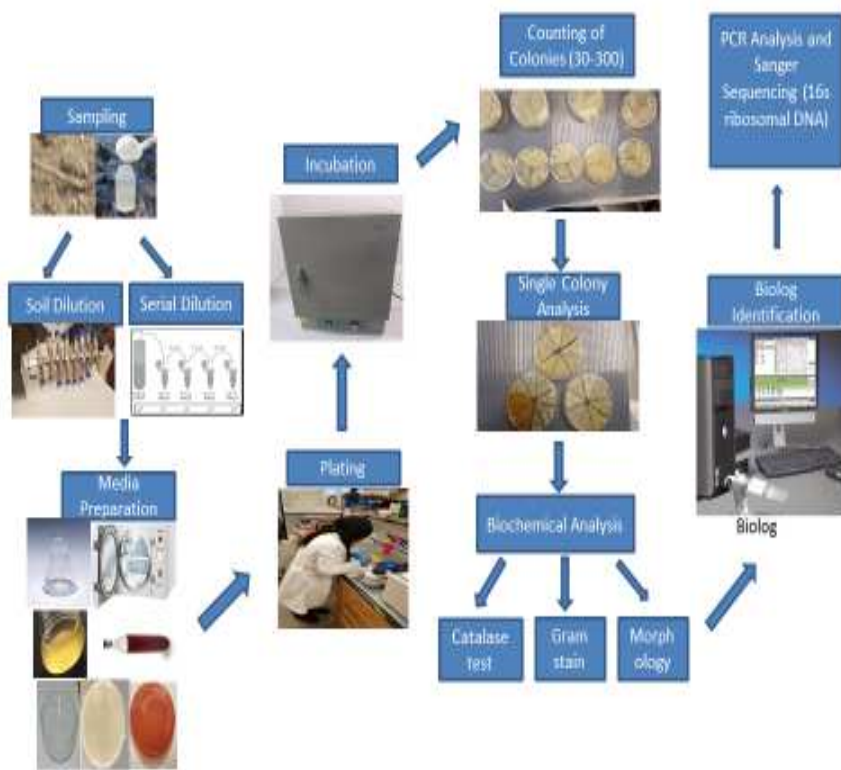
Figure 16: Overall Experimental Design

.

CHAPTER 4

RESULTS AND DISCUSSION

To determine whether Hurricane Harvey influenced total and enteric bacterial loads in watershed soils with high numbers of wastewater treatment facilities and superfund sites, we evaluated soil samples from 2017 (before and after Hurricane Harvey) (Fig. 7) and one year later in 2018 (Fig. 8). Over the course of our one-year study, we observed bayous fed by over 90 wastewater outflows such as Greens (2017), Dickinson (2018), Cypress Creek (2018) and Buffalo Bayous (2017) (Table 4; Figs. 2-3, 12-14).

In 2017, we observed significantly higher total bacterial populations in 3 out of our 4 Greens Bayou locations ($p < 0.01$), 1 out of our 3 Halls Bayou locations ($p < 0.01$), and our one Buffalo Bayou location ($p < 0.001$) when comparing pre-Hurricane Harvey (summer) to post-Hurricane Harvey (winter) (Fig. 17A). Surprisingly, 1 of 4 Greens Bayou locations, G49.4 conversely reported 1.4-fold significantly lower ($p < 0.01$) total pre-Harvey (summer) bacterial loads (2.5×10^6 cfu/g) relative to post-Harvey (winter) loads (3.5×10^6 cfu/g) (Fig. 17A) for reasons unexplained.

Watershed	Soil type	Wastewater discharge	Pollution sources
Greens	Clay and silt, locally sandy	300	Wastewater outfall. Municipal solid waste sites, superfund sites
White oaks	clay loam, sandy clay, silty clay	49	Wastewater outfall, construction, agriculture, industrial/commercial. Mining, golf courses and waterways
Buffalo	Clay	183	Wastewater outfall. Municipal solid waste sites, superfund sites, recreational activities
Dickinson	silty clay loam, sandy clay	92	Wastewater outfall. Municipal solid waste sites, superfund sites, recreational activities
Mustang	Sandy and loamy	43	Wastewater outfall. Municipal solid waste sites, superfund sites
Halls	Silt, sandy and clay	47	Wastewater outfall, sanitary sewer outflow, sewage facilities
Hunting	Mixture of clay and loamy	9	Wastewater outfall, pets, sanitary sewer outflows, storm water.
Horsepen	Clay loam	NR	Storm water, human and pets discharge, construction sites
Cypress creek	Silty, clay loamy	99	Wastewater outfall. Municipal solid waste sites

Table 4: Pollution sources in Houston area watershed soil samples. The soil types in all the watershed include clay, sandy, and loamy. The highest wastewater discharge is seen in Buffalo Bayou followed by Cypress Creek. No superfund site is seen in Cypress Creek watershed in addition to the lowest enteric counts recorded in this watershed.
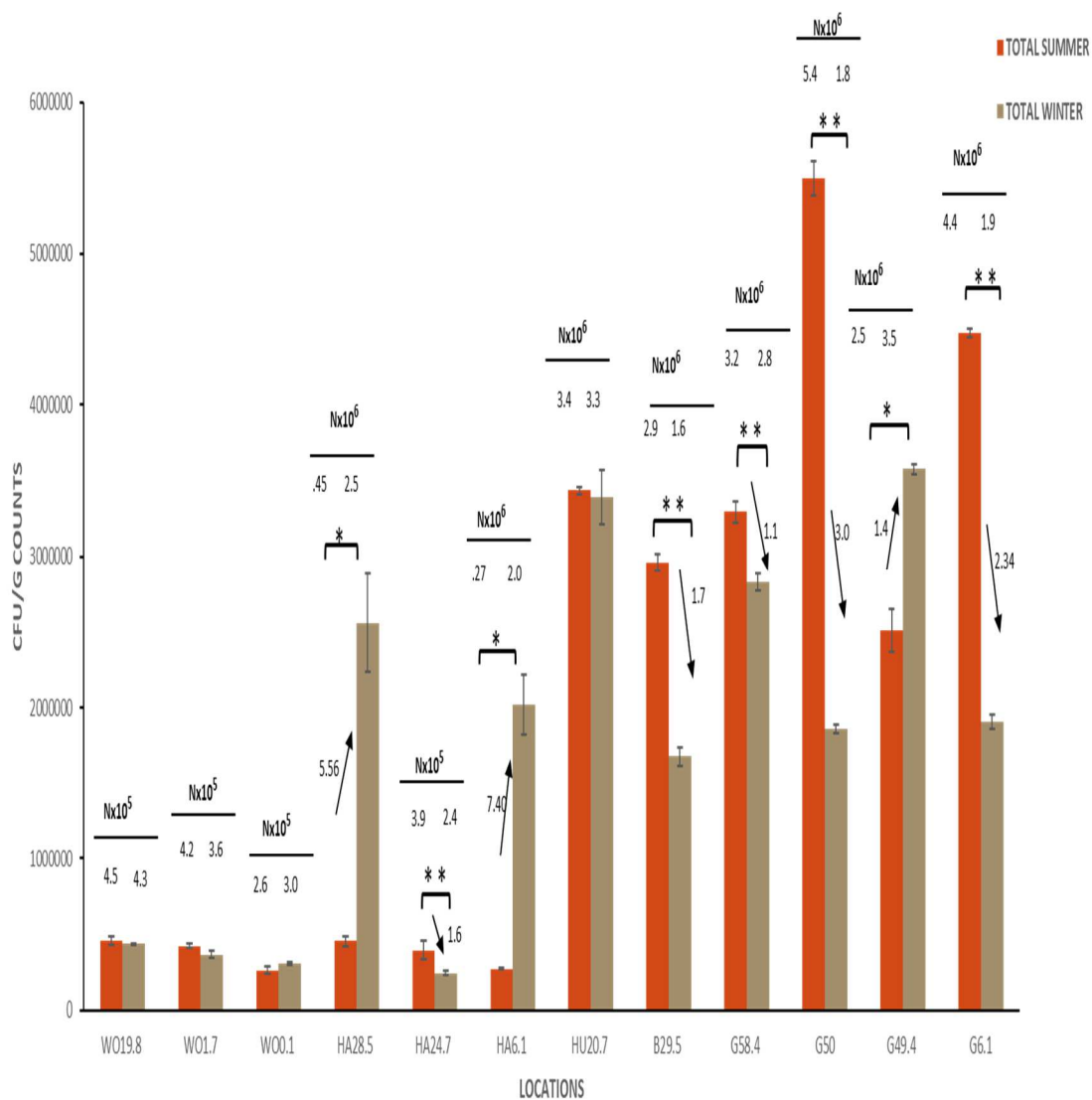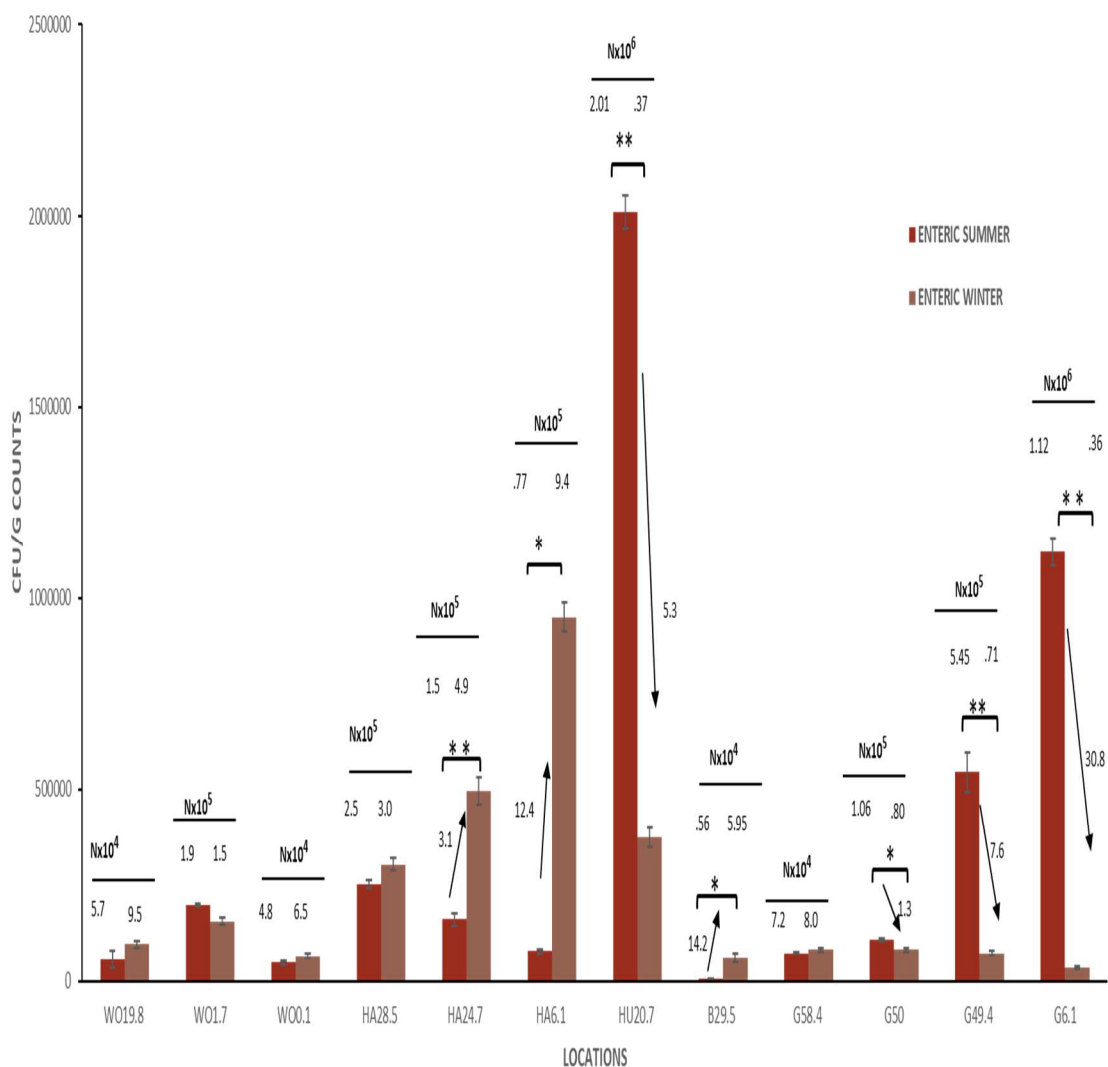
Figure 17A: Total bacterial counts for the 2017 study sites. The five watersheds sampled in 2017 summer (A) and winter (B) were Greens, Halls, Hunting, Buffalo, and White Oaks Bayous. This experiment was run in triplicate and statistical analysis was determined using the Student's T-test, with $p < 0.05$ denoted by one asterisk and $p < 0.01$ denoted by two asterisks.

Fig

17B: Enteric bacterial counts for the 2017 study sites. The five watersheds sampled in 2017 summer (A) and winter (B) were Greens, Halls, Hunting, Buffalo, and White Oaks Bayous. This experiment was run in triplicate and statistical analysis was determined using the Student's T-test, with $p < 0.05$ denoted by one asterisk and $p < 0.01$ denoted by two asterisks.

In that same vein, 2 of 3 Halls Bayou locations similarly had bacterial loads that were significantly lower (5.5- and 7.4-fold, respectively) during pre-Harvey (summer) when compared to post-Harvey (winter) (Fig. 17A). Overall, significant differences (higher or lower) were observed in 3 of 4 bayou soil samples being evaluated (Fig. 2) when comparing total loads pre-Harvey (summer) to post-Harvey (winter). The sole exception was White Oak Bayou, for which no significant differences were observed when comparing pre-Harvey (summer) to post-Harvey (winter) total bacterial loads at any of the 3 locations evaluated (Fig. 17A).

Beyond evaluating total bacterial loads, we sought to determine whether changes in enteric bacterial loads were prompted by the Hurricane Harvey flooding event, on account of many enteric bacteria being either opportunistic or bona fide pathogens. Mirroring what we observed for total bacterial loads (Fig. 17A), none of the three White Oaks Bayou soil samples exhibited statistically significant difference in summer enteric loads relative to winter enteric loads (Fig. 17B). Of the three Halls Bayou sites examined, only 2 of 3 sites (HA24.7 and HA28.5) exhibited 3.1- and 12.4-fold significantly lower, respectively, pre-Harvey summer enteric loads (1.5×10^5 cfu/g and 7.7×10^4 cfu/g) compared to the post-Harvey winter enteric load (4.9×10^5 cfu/g and 9.4×10^5 cfu/g) (Fig. 12B). We observed that our enteric bacterial values were above the EPA and Texas Commission on Environmental Quality (TCEQ) thresholds (104 – 575 cfu/100 ml). Despite our one Buffalo Bayou soil sample site having significantly higher total bacteria pre-Harvey (summer) relative to post-Harvey (winter) (Fig. 17A), in sharp contrast, the enteric bacterial load was 14.2-fold significantly lower ($p<0.05$) when comparing those same two time points (Fig. 17B). More specifically, the pre-Harvey enteric load for our Buffalo Bayou soil sample was 5.6×10^3 cfu/g (below the EPA threshold) compared to 6.0×10^4 cfu/g post-Harvey winter enteric loads, exceeding the EPA threshold (Fig. 17B). Largely in agreement with what we observed for total

bacterial loads (Fig. 17A), 3 of 4 Greens Bayou (G49.4, G50 and G58.4) enteric loads were 1.3-, 7.6-, and 31-fold significantly higher in pre-Harvey (summer) samples relative to post-Harvey (winter) samples (Fig. 17B). More specifically, Greens Bayou G49.4, G50 and G58.4 summer enteric loads were 1.1×10^5 cfu/g, 5.5×10^5 cfu/g, 1.1×10^6 cfu/g compared to 8.1×10^4 cfu/g, 7.2×10^4 cfu/g, and 3.6×10^5 cfu/g winter loads respectively (Fig. 17B). The post-Harvey Green's Bayou soil loads all exceeded EPA and/or TCEQ threshold water limits.

When evaluating bayou soil samples for both total and enteric bacterial loads one year following the Hurricane Harvey flooding event, we chose to evaluate sites that were either in a less dense region of Greater Houston (Cypress Creek Bayou) or further south of Houston (Horsepen, Mustang and Dickinson Bayous) to where bacteria may have been redistributed following the flood (Fig. 8). With regards to total bacterial loads, 2 of the 3 Horsepen Bayous evaluated were 1.9- and 1.2-fold significantly higher post-Harvey relative to pre-Harvey measures (Fig. 18A). Only 1 of the 3 Dickinson Bayou samples (DB9.4) exhibited a 2.59-fold significantly higher summer load relative to winter (Fig. 18A).
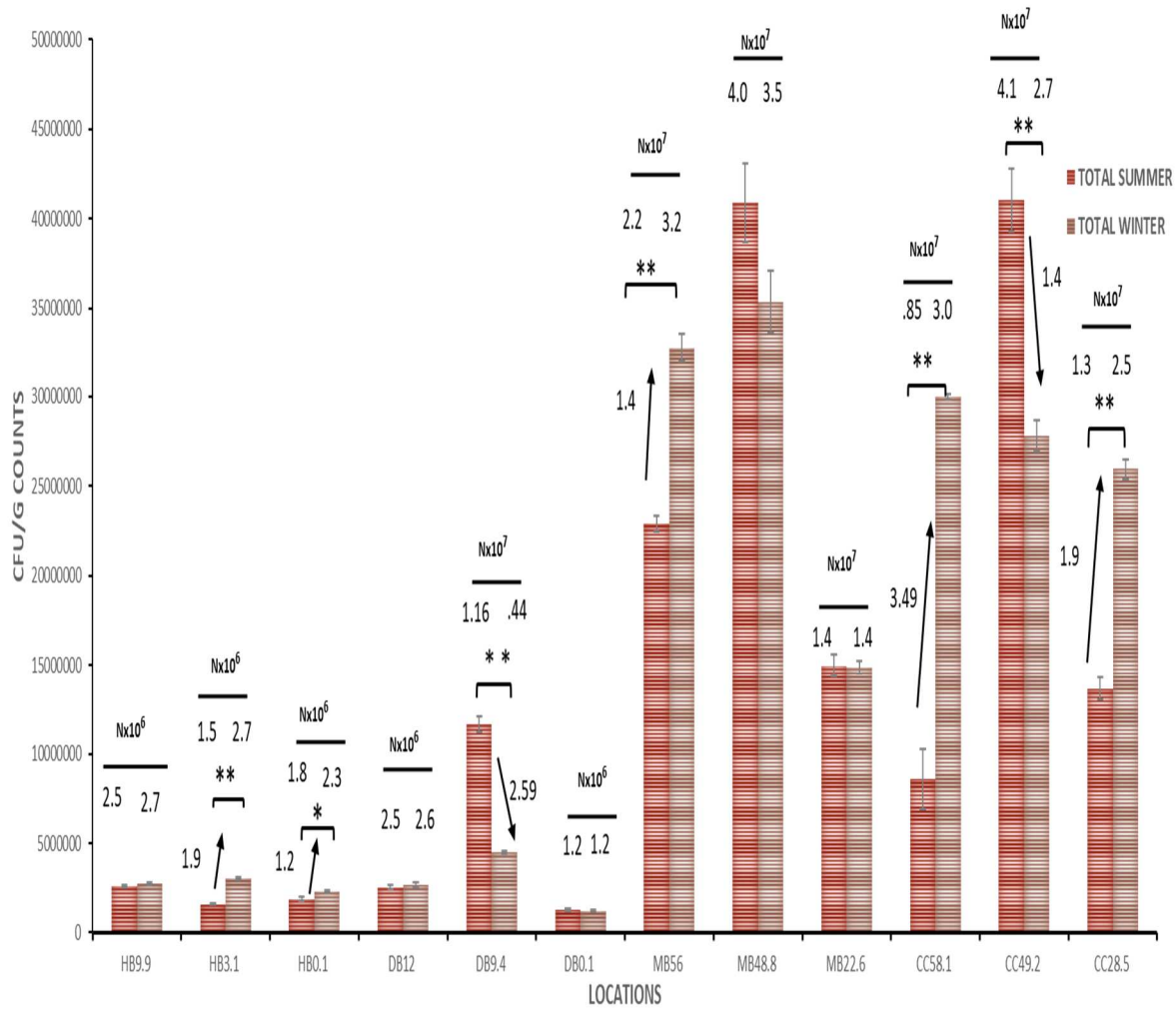
Figure 18A: Total bacterial counts for the 2018 study sites. The four watersheds sampled in 2018 summer (A) and winter (B) were Horsepen, Dickinson, Mustang, and Cypress Creek Bayous. This experiment was run in triplicate and statistical analysis was determined using the Student's T-test, with p < 0.05 denoted by one asterisk and p < 0.01 denoted by two asterisks.
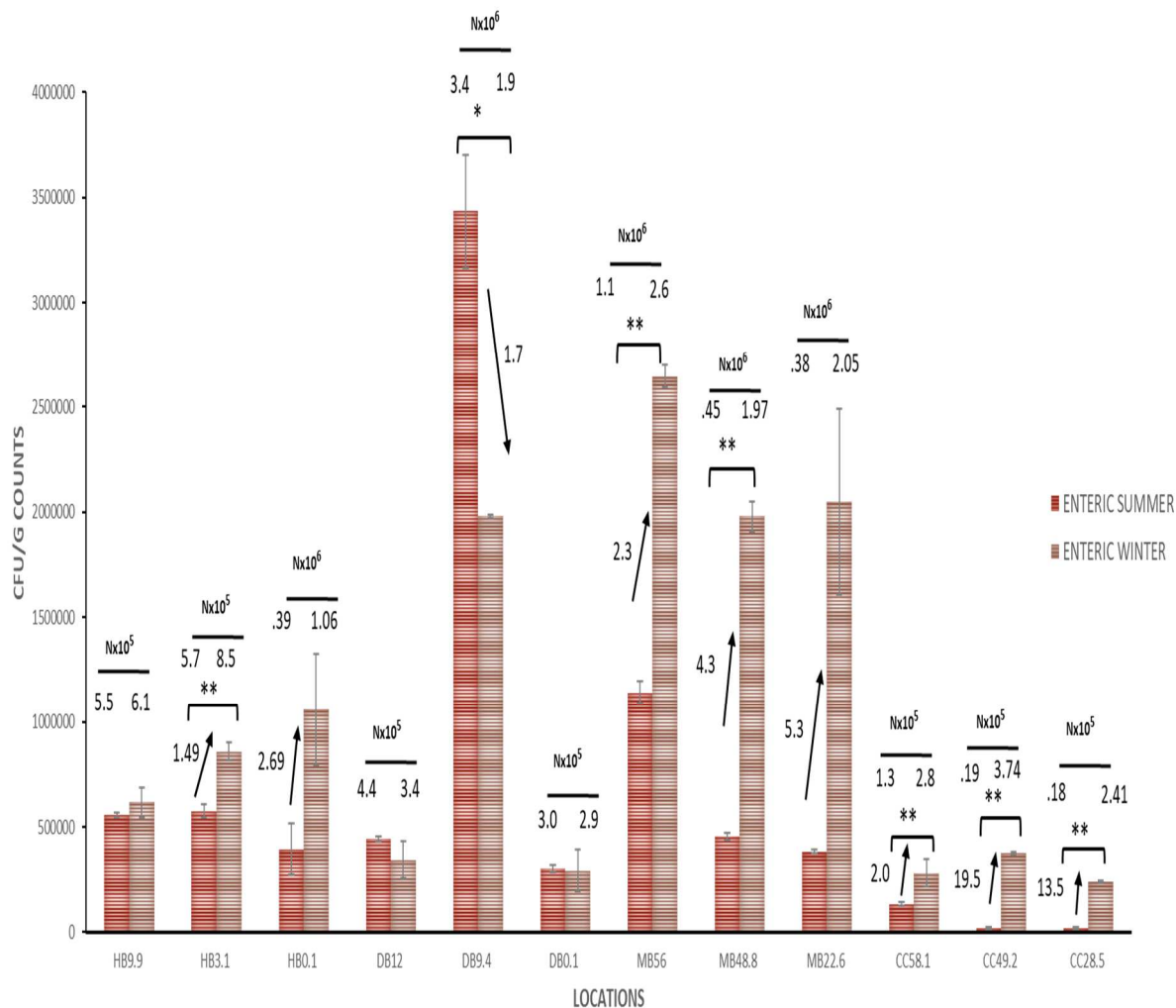
Figure 18B: Enteric bacterial counts for the 2018 study sites. The four watersheds sampled in 2018 summer (A) and winter (B) were Horsepen, Dickinson, Mustang, and Cypress Creek Bayous. This experiment was run in triplicate and statistical analysis was determined using the Student's T-test, with $p < 0.05$ denoted by one asterisk and $p < 0.01$ denoted by two asterisks.

Similarly, only 1 of our 3 Mustang Bayou (MB56) sample sites revealed a significant difference in total bacterial load; however, the 1.4-fold significantly higher difference was in post-Harvey total load compared to its pre-Harvey counterpart (Fig. 13A). Unlike the above-mentioned bayous evaluated in 2018, the Cypress Creek Bayou revealed significant differences, although not entirely consistent, in all three of our sample sites. More specifically, 2 of the 3 (CC58.1 and CC28.5) revealed 3.49- and 1.9-fold significantly higher total bacterial loads in the winter compared to the summer (Fig. 13A). Interestingly, CC49.2 exhibited a 1.4-fold significantly higher total summer load (4.1×10^7 cfu/g) compared to the corresponding winter load (2.7×10^7 cfu/g) (Fig. 13A).

Buffalo bayou watershed was sampled in 2019 and half of the locations showed significantly higher loads during the winter as compared to the summer for both total and enteric bacteria loads (Fig 19). This answers our question if the trend remained the same for the 2017 locations after 2 years. We saw that the trend remained the same and a redistribution after rainfall or seasonal change had occurred especially for Buffalo bayou locations. Buffalo bayou was chosen because majority of the watershed in the 2017 samples flows or joins this bayou before flowing to Galveston bay.
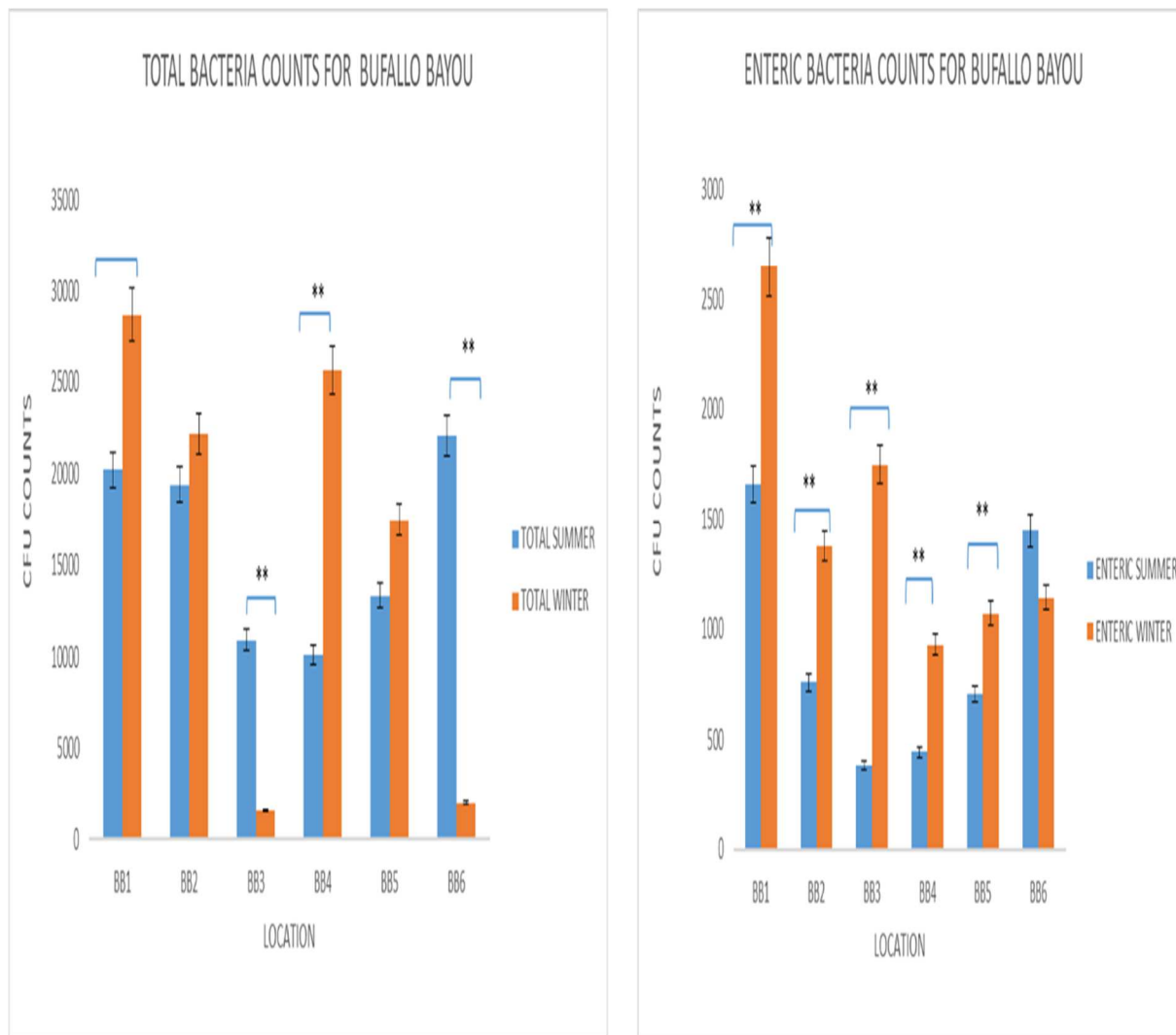
Figure 19: Total and enteric bacterial counts for the 2019 Buffalo bayou study site. 2-years sampling was done to ascertain if the trend remained the same and to answer the question of seasonal distribution. Samples were gotten from the Buffalo bayou 2017 locations. Buffalo bayou watershed was sampled in 2019 and half of the locations showed significantly higher loads during the winter as compared to the summer for both total and enteric bacteria loads

Colony/Morphology	Environmental source	Medium	Gram test	Oxidase test	Catalase test	Biolog identification
UK1/Red	Buffalo Bayou	M	-	-	+	Serratia marcescens
UK2/Cream	Dickinson Bayou	LB	-	-	+	Raoutella planticola
UK3/Yellow	Buffalo Bayou	LB	-	-	+	Pseudomonas fulva
UK4/Yellow	Halls Bayou	LB	-	-	+	Pseudomonas putida
UK5/Orange	Greens Bayou	LB	+	+	-	Bacillus cibi
UK6/Cream	White oaks Bayou	M	-	-	+	Pseudomonas pertucinogena
UK7/Orange	White oaks Bayou	LB	+	+	+	Sporosarcina aquimarina
UK8/Cream	Horsepen watershed	M	-	-	+	Pseudomonas mendocina
UK9/Cream	Horsepen watershed	LB	-	-	+	Pseudomonas taetrolens
UK10/pale yellow	Horsepen watershed	M	-	-	+	Acinetobacter soli
UK11/Pink	Hunting watershed	M	-	-	+	Shewanella algae
UK12/White	Cypress creek watershed	LB	-	+	+	Delftia tsuruhatensis

Table 5: Morphology and Biochemical test of isolated unknowns. Environmental isolates were identified through Gram staining, biochemical reactions, and the Biolog Micro station. *Serratia marcescens*, *Routella planticola*, *Pseudomonas fulva*, *Pseudomnas putida*, *Pseudomonas pertucinogena*, *Bacillus cibi* and *Sporosarcina aquimarina* are few of the identified species using the Biolog reader.

Similarly, only 1 of our 3 Mustang Bayou (MB56) sample sites revealed a significant difference in total bacterial load; however, the 1.4-fold significantly higher difference was in post-Harvey total load compared to its pre-Harvey counterpart (Fig. 13A). Unlike the above-mentioned bayous evaluated in 2018, the Cypress Creek Bayou revealed significant differences, although not entirely consistent, in all three of our sample sites. More specifically, 2 of the 3 (CC58.1 and CC28.5) revealed 3.49- and 1.9-fold significantly higher total bacterial loads in the winter compared to the summer (Fig. 13A). Interestingly, CC49.2 exhibited a 1.4-fold significantly higher total summer load (4.1 X 10^7 cfu/g) compared to the corresponding winter load (2.7 X 10^7 cfu/g) (Fig. 13A).

When we evaluated enteric bacterial loads at our 2018 sites, only one of the Horsepen Bayou samples (HB3.1) had a 1.49-fold significantly higher winter load compared to summer (Fig. 13B). Similarly, only one of the three Dickinson Bayou samples (DB9.4) exhibited a 5.3-fold significantly higher summer load (3.4 X 10^6 cfu/g) compared to winter (1.9 X 10^6 cfu/g) (Fig. 13B). All 3 of the Mustang Bayou samples similarly had 2.3-, 4.3-, and 5.3-fold significantly higher winter enteric loads compared to their summer counterparts (Fig. 13B). Finally, mirroring the Mustang Bayou enteric load data, All 3 of the Cypress Creek Bayou samples similarly had 2.0-, 19.5-, and 13.5-fold significantly higher winter enteric loads compared to their summer counterparts (Fig. 13B), all above EPA and TCEQ threshold water limits. Soil levels tend to be higher because of accumulation.

Sample	Bacteria identification (16S ribosomal RNA)	Watershed	Pathogenesis
1	Aeromonas hydrophila strain I-N-5-1 16S ribosomal RNA gene, partial sequence Sequence ID: KU570299.1 Length: 1418 Number of Matches: 1	Buffalo	Meningitis
2	Rhizobium vitis strain 4-3-blue 16S ribosomal RNA gene, partial sequence Sequence ID: JX083378.1 Length: 1335 Number of Matches: 1	Cypress creek	Lung disease Acute meningitis
3	Pseudomonas fluorescens strain psf6 16S ribosomal RNA gene, partial sequence Sequence ID: MN256392.1 Length: 1436 Number of Matches: 1	Buffalo	Blood transfusion related septicemia Catheter related bacteremia
4	Enterobacter aerogenes strain KNUC5006 16S ribosomal RNA gene, partial sequence Sequence ID: JQ682636.1 Length: 1466 Number of Matches: 1	Horsepen	Bacteremia Urinary tract infection
5	Raoutella planticola strain N4 16S ribosomal RNA gene, partial sequence Sequence ID: KC189899.1 Length: 1414 Number of Matches: 1	White oaks	Pneumonia
6	Pseudomonas putida. JP-2014-A18 partial 16S rRNA gene, isolate A18 Sequence ID: HG934404.1 Length: 419 Number of Matches: 1	Halls	Urinary tract infection Respiratory infection
7	Aeromonadales bacterium F2V20G05 partial 16S rRNA gene, isolate F2V20G05 Sequence ID: HG322905.1 Length: 891 Number of Matches: 1	Dickinson	gastroenteritis
8	Leclercia adecarboxylata strain 10_Lec 16S ribosomal RNA gene, partial sequence Sequence ID: KX267844.1 Length: 644 Number of Matches: 1	Buffalo	Acute myeloid leukemia
9	Vibro cholera: KC189899.1 Length: 1414 Number of Matches: 1	Dickinson	Food poisoining

Table 6: Identification of down selected colonies using Sanger sequencing. A dirty colony PCR was done on some down selected samples and confirmed through gel electrophoresis. Samples were cleaned up for PCR sequencing and sequences were blasted on the National Center for Biotechnology Information (NCBI) website to get the species identification. The table above shows some of the identified species that Sanger sequencing was been done on.

From our total and enteric loads, 12 down-selected representative colonies were selected for further characterization and identification (Table 5). Using the BIOLOG Microstation, we identified 10 Gram-negative bacteria on both broad and selective media including: *Serratia marcescens*, *Routella planticola*, *Pseudomonas fulva*, *Pseudomnas putida*, *Pseudomonas pertucinogena*, *Pseudomonas mendocina*, *Pseudomonas taetrolens*, *Acinetobacter soil*, *Shewanella algae*, and *Delftia tsuruhatensis* as well as 2 Gram-positive organisms: *Bacillus cibi* and *Sporosarcina aquimarina* (Table 5).

We also identified some down selected colonies through Sanger sequencing. After performing a dirty colony PCR and gel electrophoresis, the samples were cleaned up and sent to the lab for PCR sequencing. The sequence was blasted on the National Center for Biotechnology Information (NCBI) website to get the species identification. Some of the species identified were, *Aeromonas Hydrophilia, Rhizobium vitis, Pseudomonas florescens, Enterobacter aerogenes, Serratia marcescens, Pseudomonas putida and Vibrio cholera* (Table 6).
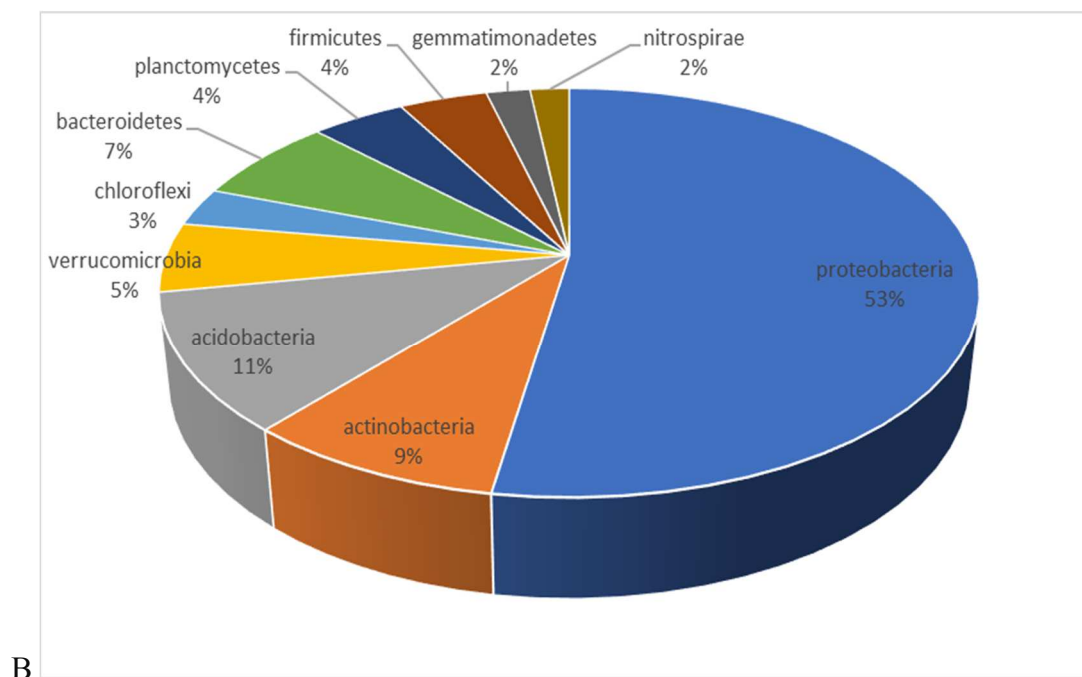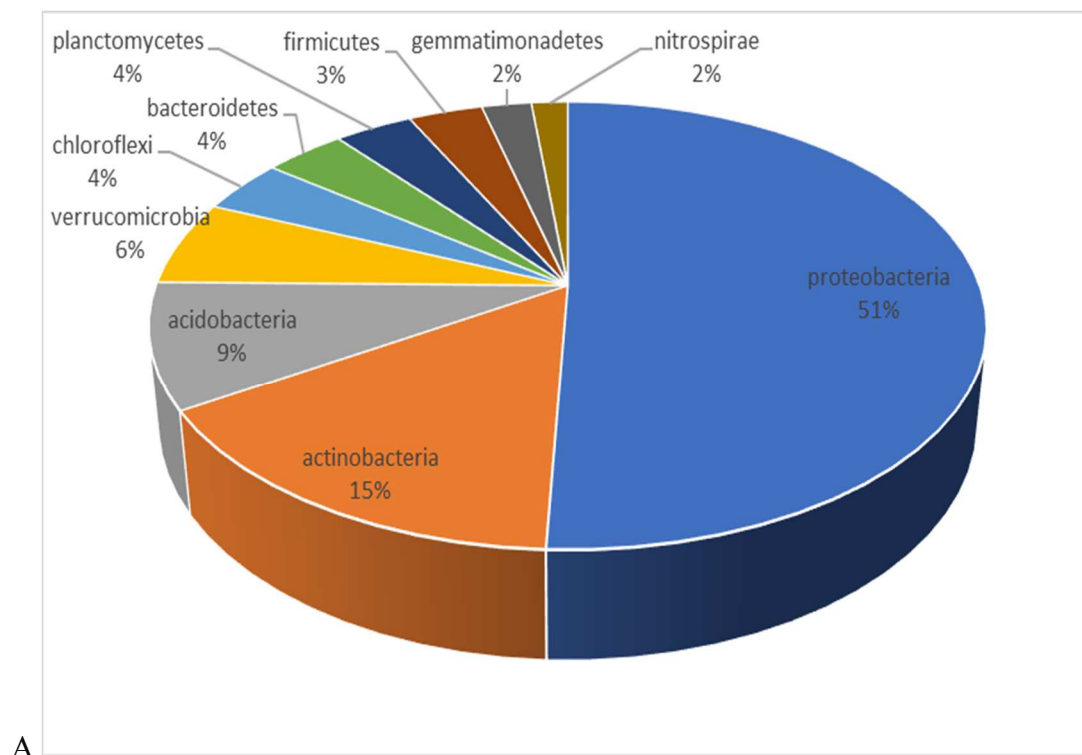
Figure 20: Operational Taxonomical Unit (OTU) percentage distribution of phyla from Halls Bayou soil samples during the summer (A) and winter (B) in 2017. The four predominant phyla are *Proteobacteria, Actinobacteria,* Acidobacteria, and *Firmicutes*.

In efforts of achieving a more comprehensive assessment of bacterial population dynamics and diversity in our soil samples, we undertook a global metagenomic approach to compare population dynamics of our Halls Bayou summer (Fig. 20A) and winter (Fig. 20B) 2017 pooled samples. In both the summer and winter of 2017, the *Proteobacteria* (which include several pathogenic and non-pathogenic Gram-negative bacteria) represented the largest percentage operational taxonomic unit phylum, 53% and 51%, respectively (Fig. 20). This is in agreement with the 10 of 12 Gram-negative bacteria that we isolated from the multiple Bayous we examined, including Halls Bayou (Fig. 17). In fact, the majority of Gram-negative isolates (Table 5) were pseudomonads which all fall under the phylum Proteobacteria. The remaining 9 phyla, including the Firmicutes and their large number of Gram-positive bacteria, compared had very similar percent distribution of operational taxonomic units in the summer and winter of 2017 (Fig. 20). These data suggest that despite an unprecedented flooding event, the population dynamics at the phyla level did not change much within Halls Bayou (Fig. 20). When examining sequence counts the species level from our metagenomic data, we compared summer to winter counts of 24 species including the pathogenic *Burkholderia* spp., in which there was an observed 2.69-fold increase in winter sequence counts (Fig. 21). Similarly, we observed a 2.0–fold increase in *Pseudomonas* spp. in the winter counts as well. Taken together, these data suggest that although population dynamics at the phyla-level may not change dramatically following a flooding event (Fig.20), changes could occur at the species-level (Fig. 21) promoting the expansion of disease-causing pathogens.
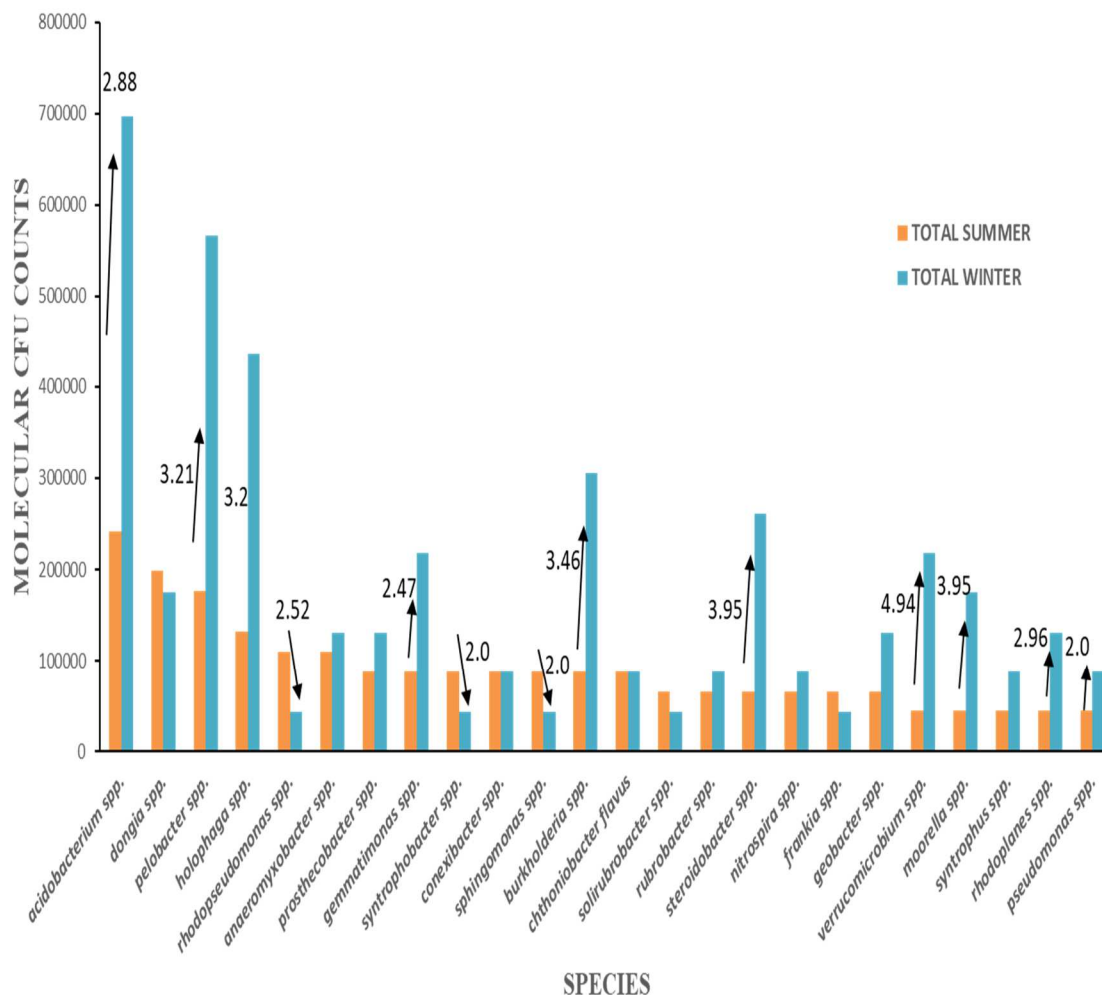
Figure 21A: Molecular CFU counts. Using our metagenomic data, we semi-quantitatively compared the 2017 summer and fall numbers of 24 bacterial species from Halls Bayou. Summer counts are denoted by dark black while winter counts are denoted by light black. Fold-differences are shown for both sequence counts (A) and derived molecular cfu counts (B).
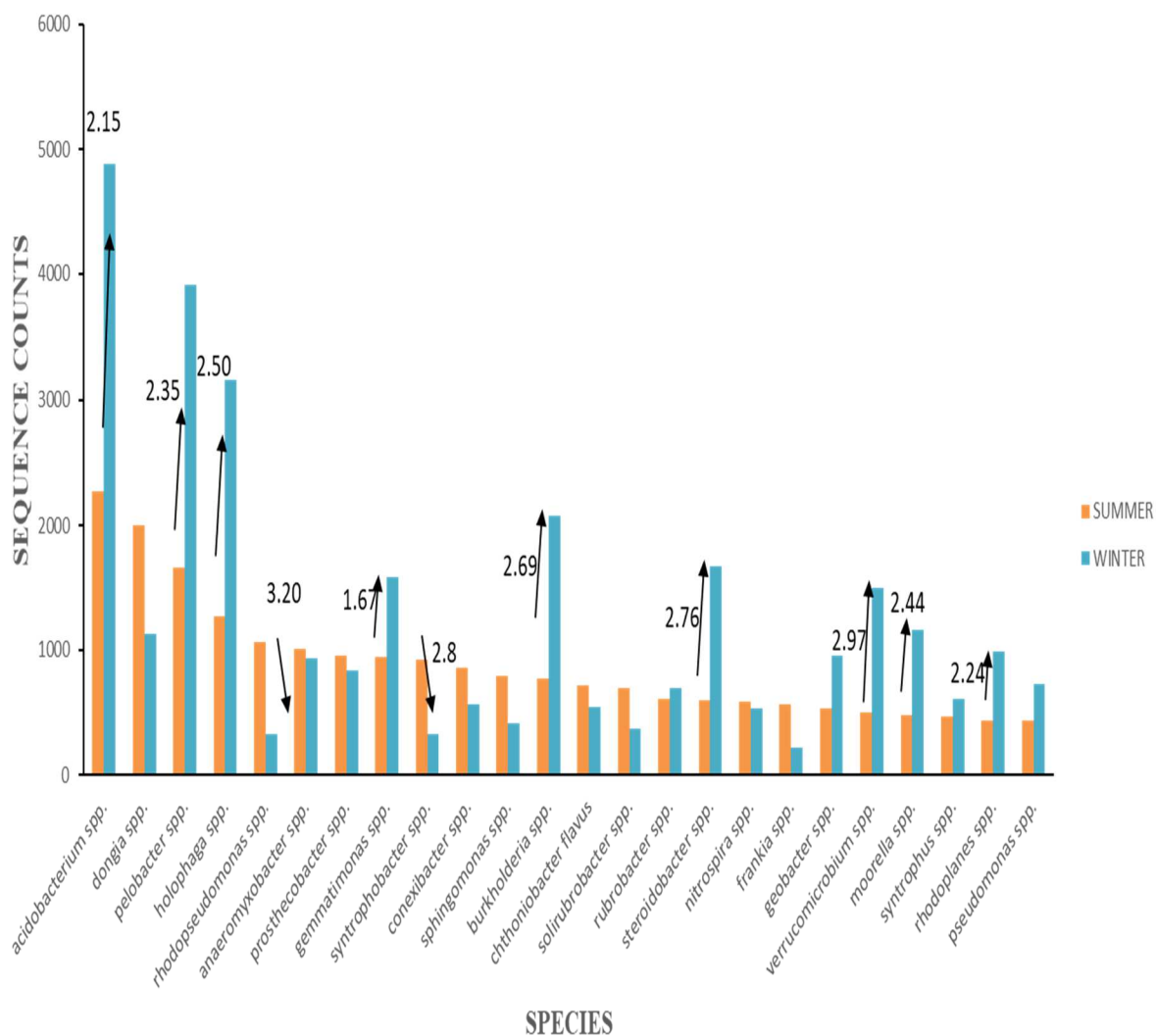
Figure 21B: Sequence counts. Using our metagenomic data, we semi-quantitatively compared the 2017 summer and fall numbers of 24 bacterial species from Halls Bayou. Summer counts are denoted by dark black while winter counts are denoted by light black. Fold-differences are shown for both sequence counts (A) and derived molecular cfu counts (B).

A   B
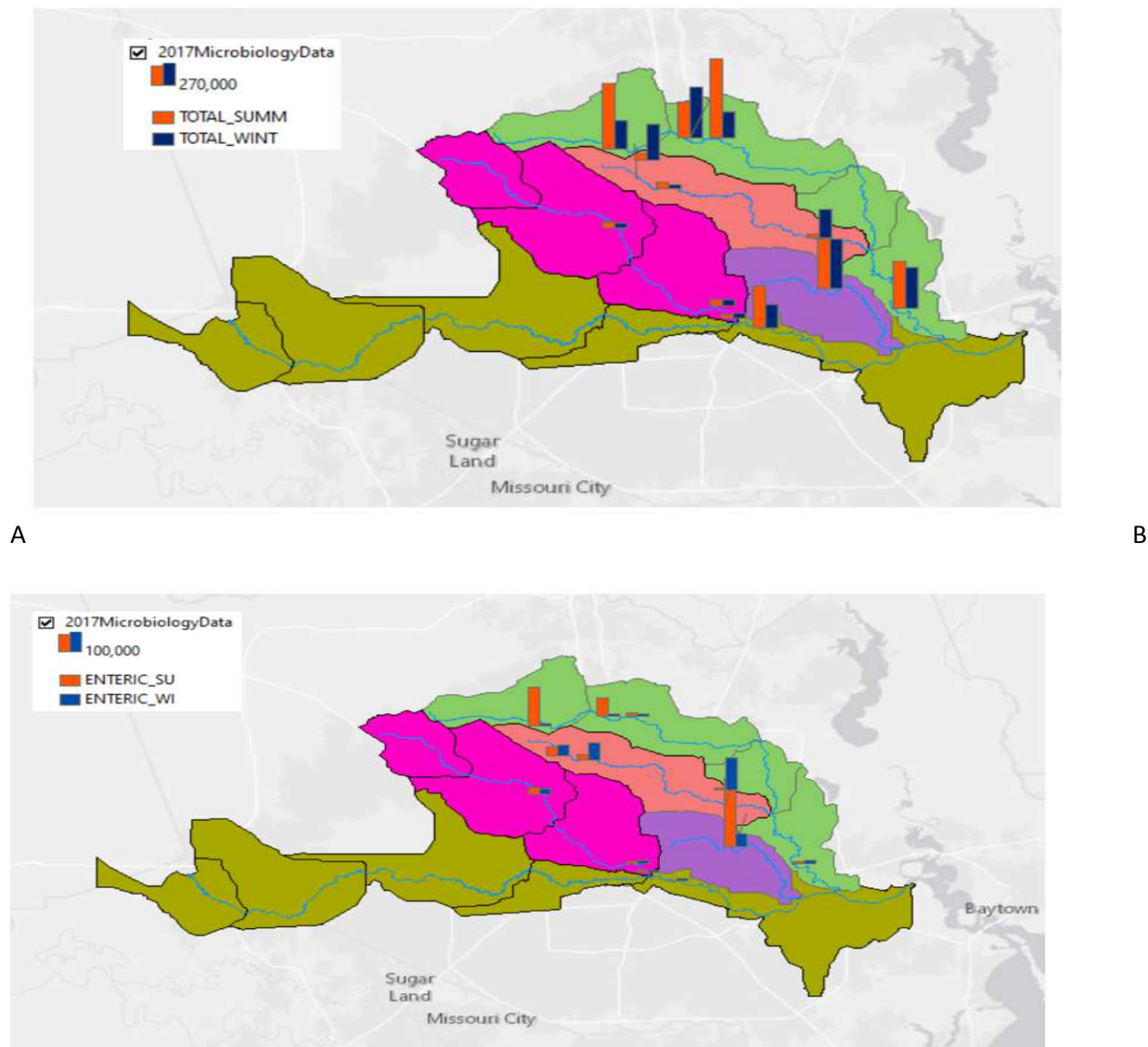
Fig 22: GIS Mapping of 2017 (A) total and 2017 (B) enteric bacteria population across watershed. The bayou flow lines, watershed boundary and the flood hazard layers were extracted from the National Flood Hazard Layer (NFHL) database. (https://www.floodmaps.fema.gov/NFHL/status.shtml) and Houston-Galveston Area Council GIS datasets (http://www.h-gac.com/gis-applications-and-data/datasets.aspx). Soil sampling points of the study areas were imported into GIS as separate vector layer. The data were downloaded and processed using the ArcGIS Version 10.5 software (ESRI 2014)
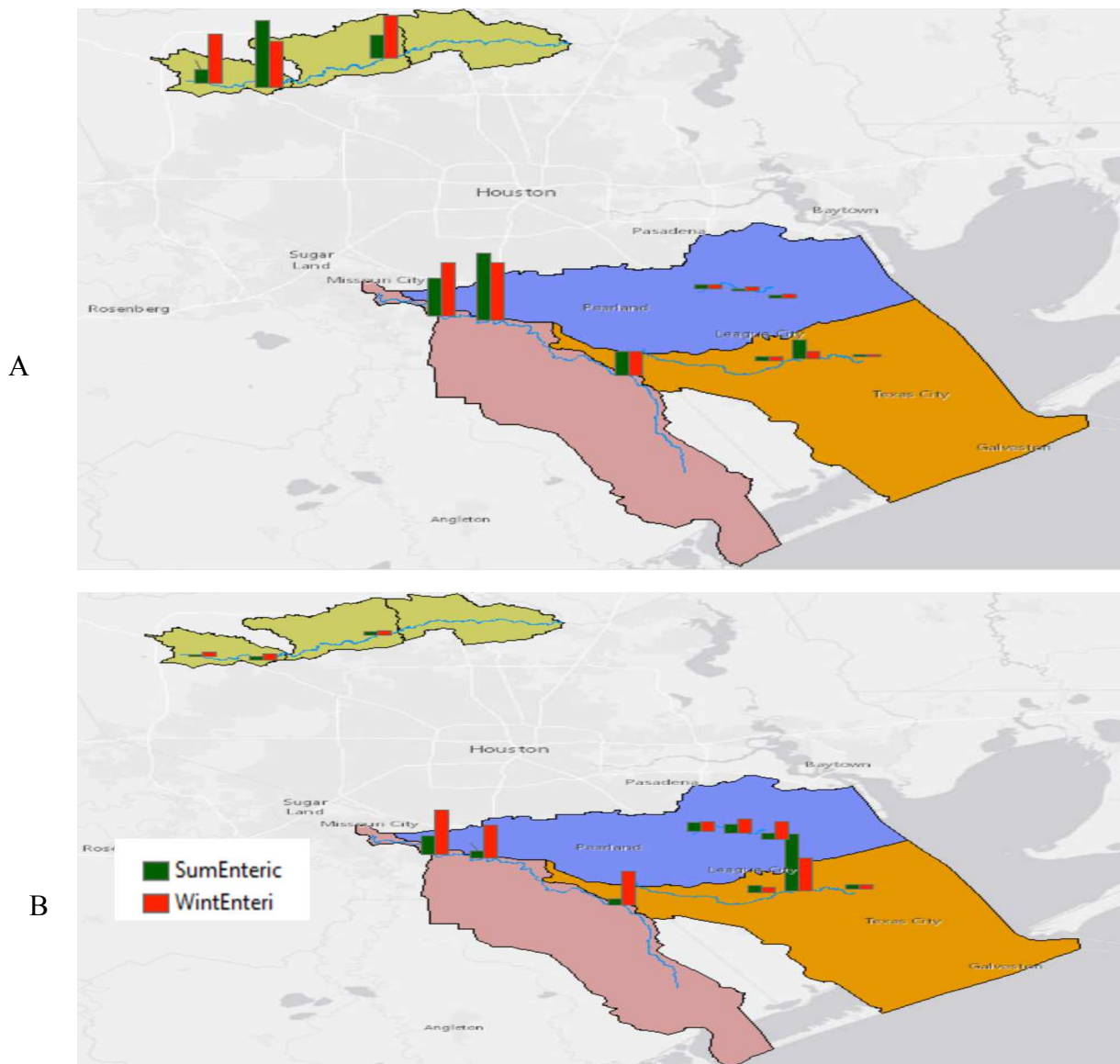
Figure 23: GIS Mapping of 2018 (A) total and 2018 (B) enteric bacteria population across watershed. The bayou flow lines, watershed boundary and the flood hazard layers were extracted from the National Flood Hazard Layer (NFHL) database. (https://www.floodmaps.fema.gov/NFHL/status.shtml) and Houston-Galveston Area Council GIS datasets (http://www.h-gac.com/gis-applications-and-data/datasets.aspx).
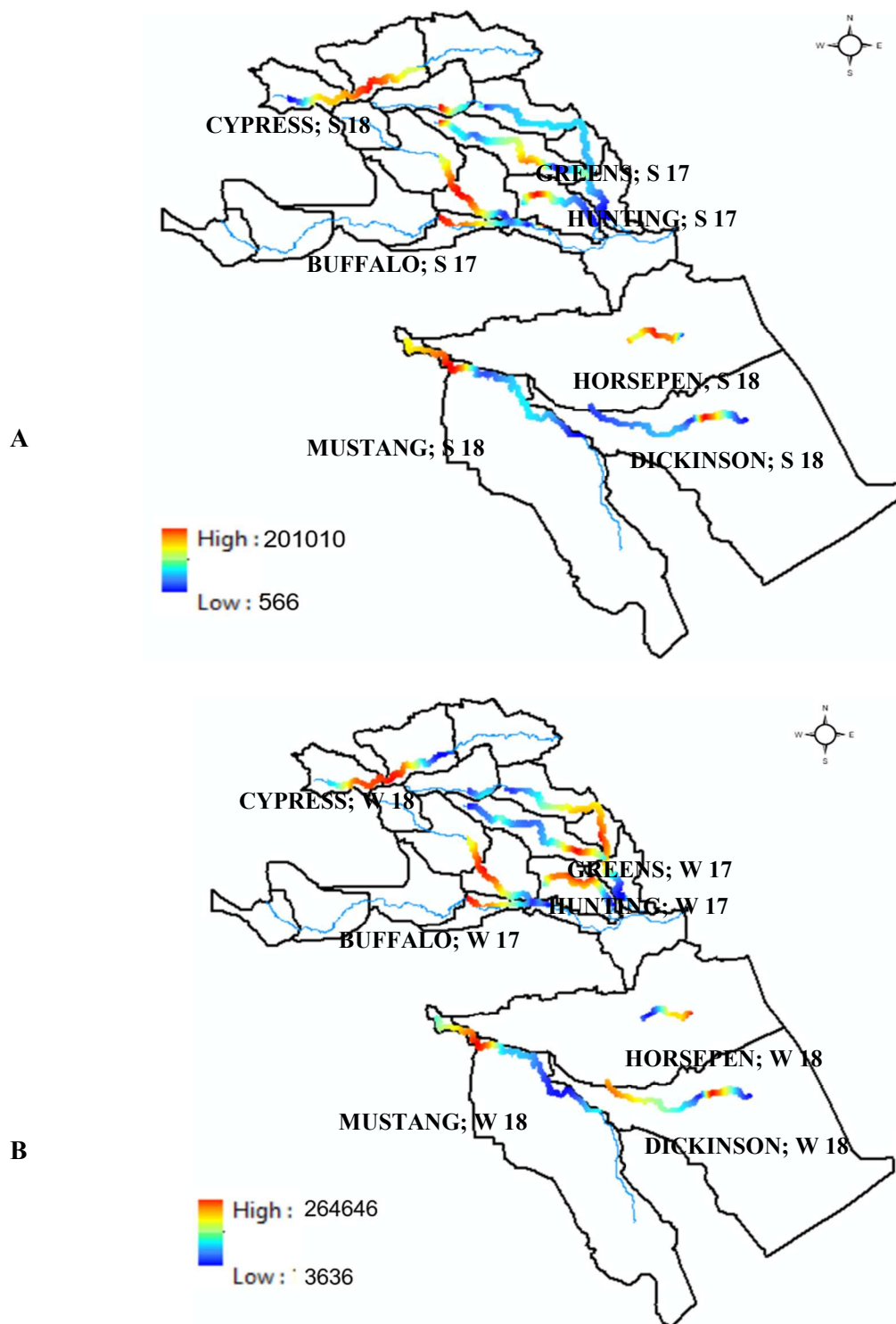
Figure 24: Interpolation map showing the enteric bacteria population over time for (A) summer 2017 and 2018.; enteric bacteria population over time for (B) winter 2017 and 2018.

The bayou flow lines, watershed boundary and the flood hazard layers were extracted from the National Flood Hazard Layer (NFHL) database

(https://www.floodmaps.fema.gov/NFHL/status.shtml) and Houston-Galveston Area Council GIS datasets (http://www.h-gac.com/gis-applications-and-data/datasets.aspx). Soil sampling points of the study areas were imported into GIS as separate vector layer. The data were downloaded and processed using the ArcGIS Version 10.5 software (ESRI 2014).

In efforts of determining metal contaminant levels in Houston watershed soils, like Buffalo Bayou, we found that Pb (17.5 ppm), Zn (55.5 ppm), and Mn (836.5 ppm) were all elevated and exceeded Texas Commission on Environmental Quality (TCEQ) threshold levels (15, 30, and 500 ppm, respectively). We observed similarly elevated levels of the three-aforementioned heavy metals exceeding both TCEQ and Environmental Protection Agency thresholds in several other Houston Watershed Soils. Previously, we sought to evaluate bacterial loads in Houston watershed soil samples following flooding events and isolated the opportunistic pathogen *S. marsescens* from G58.4, G50, and G49.4 and G6.1 location along Greens Bayou, B29.5 along Buffalo Bayou, HU20.7 along Hunting Bayou, HA28.5, HA24.7, and HA6.1 along Halls Bayou, W019.8, WO1.7, W00.1 along White Oak Bayou was collected during 2017, and CC58.1, CC49.2 and CC28.5 along Cypress Creek, MB56, MB48.8, and MB22.6 along Mustang Bayou, DKB 12, DKB9.4 and DKB0.1 along Dickinson Bayou, HB9.9, HB3.1 and HB0.1 along Horsepen Bayou were collected during 2018. The sample locations were named with a letter followed by a number as suffix where the letters stand for the name of the Bayou and the number represents the distance of the sample site in km from the mouth of the Bayou. For example, G58.4 represents the sample site located at 58.4 km from the mouth of the Greens Bayou (Adedoyin et al. 2021). To determine whether, the environmentally isolated *S. marsescens* had adapted to increased metal exposure levels, we compared its growth to that of a commercially acquired reference strain.

10µg/ml, 50µg/ml and 100µg/ml of zinc affected the growth rate of both *Serratia marsescens* environmental isolate (SME) and *Serratia marsescens* surrogate strain (SMS). However, 100µg/ml of zinc significantly decreased the growth of both strains ($p < 0.01$), when compared to 50µg/ml and 100µg/ml of zinc (Fig 25a and 25b). When comparing both strains, 100µg/ml of zinc significantly affected the growth phase of SMS as it maintained a lag phase with an inhibition in growth throughout the time point when compared to SMS (Fig 25a and 25b). 10µg/ml, 50µg/ml and 100µg/ml of lead did not significantly affect the growth rate of SME. However, the growth kinetics of SMS was significantly inhibited ($p < 0.05$) for all concentrations of treatment with lead (Fig. 25a and 25b). Hence, we hypothesize that the observed differences between the effect of lead in both SME and SMS on growth might be as a result of their different ability to withstand environmental stressors.

Metals	EPA standard	TCEQ standard	Halls	Buffalo	Greens	White Oak	Hunting
Arsenic	4.54	5.9	0.86	1.44	2.23	1.62	2.78
Copper	20.3	15	19.97	7.67	29.98	7.66	853
Chromium	43.2	30	15.56	3.75	7.75	5.90	46.46
Lead	32.6	15	26.47	17.51	25.04	22.85	407
Mercury	0.13	0.04	0.05	0.02	0.07	0.01	0.08
Zinc	43.1	30	155	55.57	127	93.89	1061
Cadmium	1.74	8.75	0.32	0.50	1.21	0.97	3.16
Manganese	N/R	500	745	863	2011	2500	838

Table 7: The soil background concentrations for heavy metals according to environmental agencies. The highest heavy metals recorded for the isolated watershed were lead (Pb), Zinc (Zn), and Manganese (Mn). They were above the set threshold for heavy metals in watersheds.

When grown in the presence of 10, 50 or 100 µg/ml (ppm) of Zn, the environmental *S. marsescens* isolate had significantly enhanced (p< 0.01) biomass at multiple time points (particularly between the 3-8 h time points) during a 9.5 h growth curve experiment than the reference strain. Similarly, when challenged with 50 or 100 µg/ml (ppm) Zn, the environmental isolate had significantly greater biomass than the reference strain. Interestingly, however, unlike the diminished but continued growth following 100 µg/ml (ppm) of Pb treatment, 100 µg/ml (ppm) of Zn treatment completely arrested the reference strain's growth while only diminishing the isolate strain's growth (compare Fig. 24 panels A to B). With regards to Mn treatment, the environmental isolate had significantly greater biomass than the reference strain when challenged with either 100 or 500 µg/ml (ppm). However, for reasons unexplained, the highest concentration challenge [1000 µg/ml (ppm)] yielded no difference between the environmental and reference strains' biomasses.

At 1000µg/ml of manganese, there was no significant difference in the growth rate of both treated SME and SMS when compared to the non-treated bacterial strains. We also observed that at 500µg/ml and 100µg/ml of manganese, there was no significant difference in growth for SME but on the other hand, at the same concentrations, growth was significantly inhibited for SMS (Fig. 19). In line with this hypothesis is the observation that SME can withstand environmental stressors than SMS which resulted in growth inhibition for SMS.
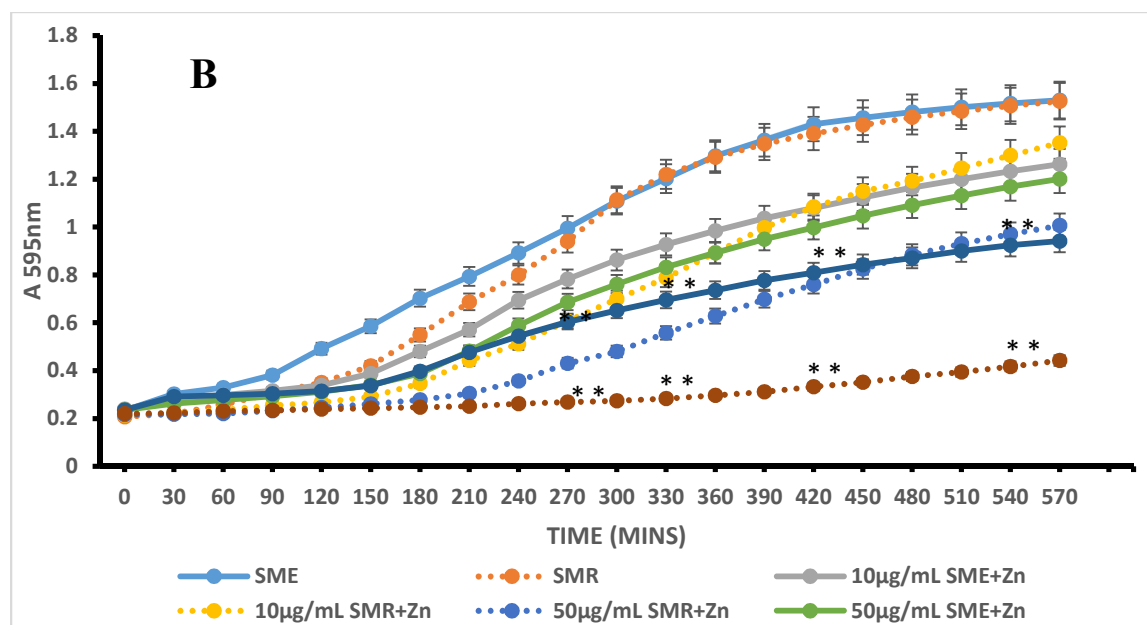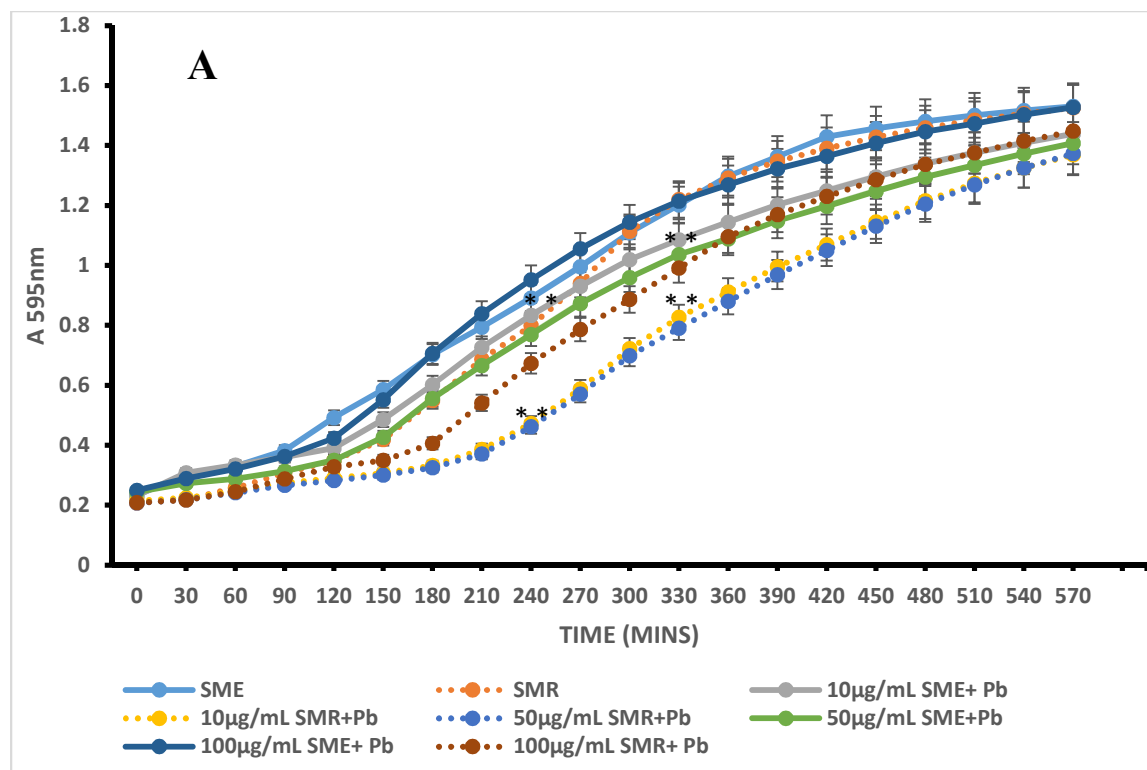
Figure 25a: Growth response of *Serratia marcescen*s strains to heavy metal exposure.
The growth curve of *Serratia marcescen*s environmental isolate (SME) and *Serratia marcescen*s surrogate strain (SMS) in response to (A) zinc and (B) lead and (C) manganese exposure.
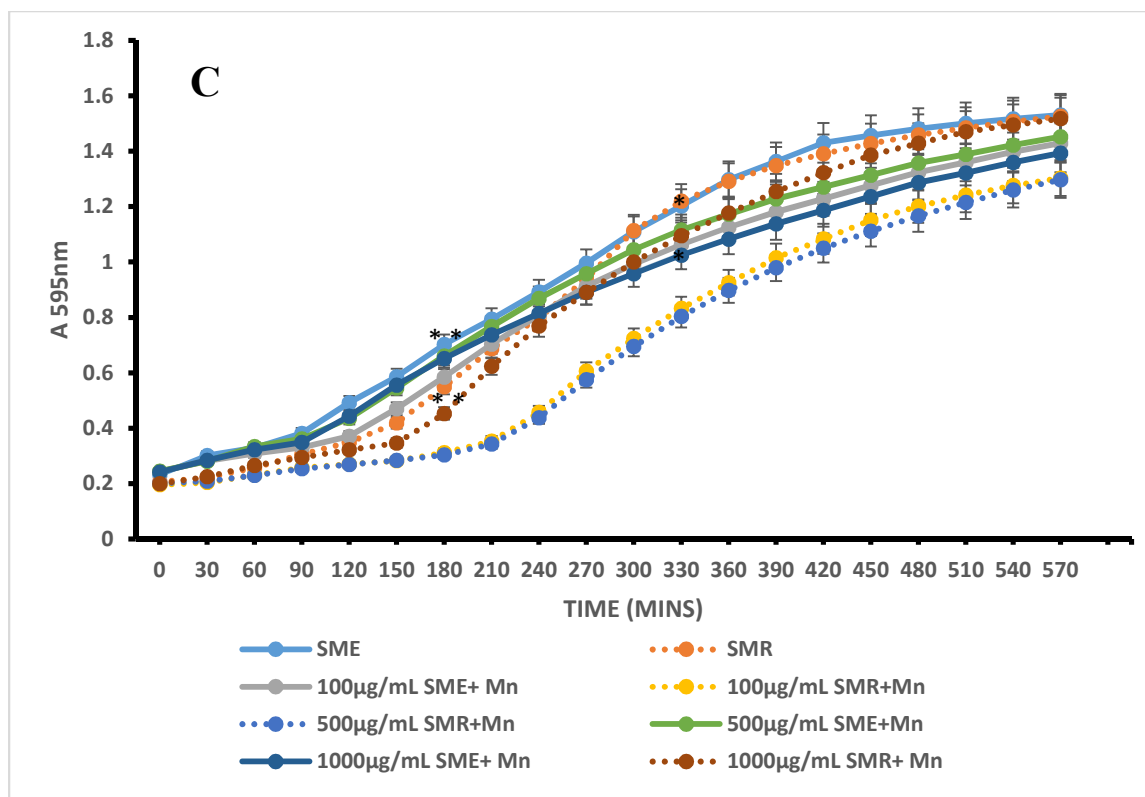
Figure 25b: Growth response of *Serratia marcescen*s strains to heavy metal exposure.

The growth curve of *Serratia marcescen* environmental isolate (SME) and *Serratia marcescen*s surrogate strain (SMS) in response to (C) manganese exposure. This experiment was run in triplicate and statistical analysis was determined using the Student's T-test, with p < 0.05 denoted by one asterisk and p < 0.01 denoted by two asterisks.

Following characterization of growth curves, we next sought to determine whether the environmental isolate was better able to resist oxidative stress via H_2O_2 challenge, a stress commonly encountered when facing immune cells. In the same way that the environmental isolate grew significantly better than did the reference strain in the presence of metals, the environmental isolate grew significantly better than did the reference strain when challenged with 50mM H_2O_2. Moreover, the environmental isolate's significantly greater (than the reference strain's) oxidative stress resistance to 50mM H_2O_2 was maintained even during 10 μg/ml (ppm) Zn (Fig. 26), 10 μg/ml (ppm) Pb (Fig. 26), and 100 μg/ml (ppm) Mn (Fig. 26) exposures. These data suggest that environmental adaptations had occurred in the *S. marsescens* environmental isolate.

100μg/ml of zinc significantly reduced ($p < 0.01$) the sensitivity of SME and SMS to oxidative stress, while 10μg/ml of zinc did not significantly affect the sensitivity of both strains to oxidative stress (Fig. 20) Since 10μg/ml and 50μg/ml of zinc affected the growth rate the same way and 100μg/ml significantly inhibited the growth of both strains, we investigated whether sensitivity to oxidative stress was increased in both 10μg/ml and 100μg/ml of zinc. At 10μg/ml of zinc, neither SME nor SMS demonstrated significantly increased sensitivity to hydrogen peroxide induced oxidative stress at both 20Mm and 50mM (Fig 26-27).

We observed that both 20mM hydrogen peroxide and 50mM hydrogen peroxide induced significantly increased sensitivities ($p < 0.01$) in both SME and SMS in the absence of zinc (Fig. 20) when compared with treated controls (Fig 21).
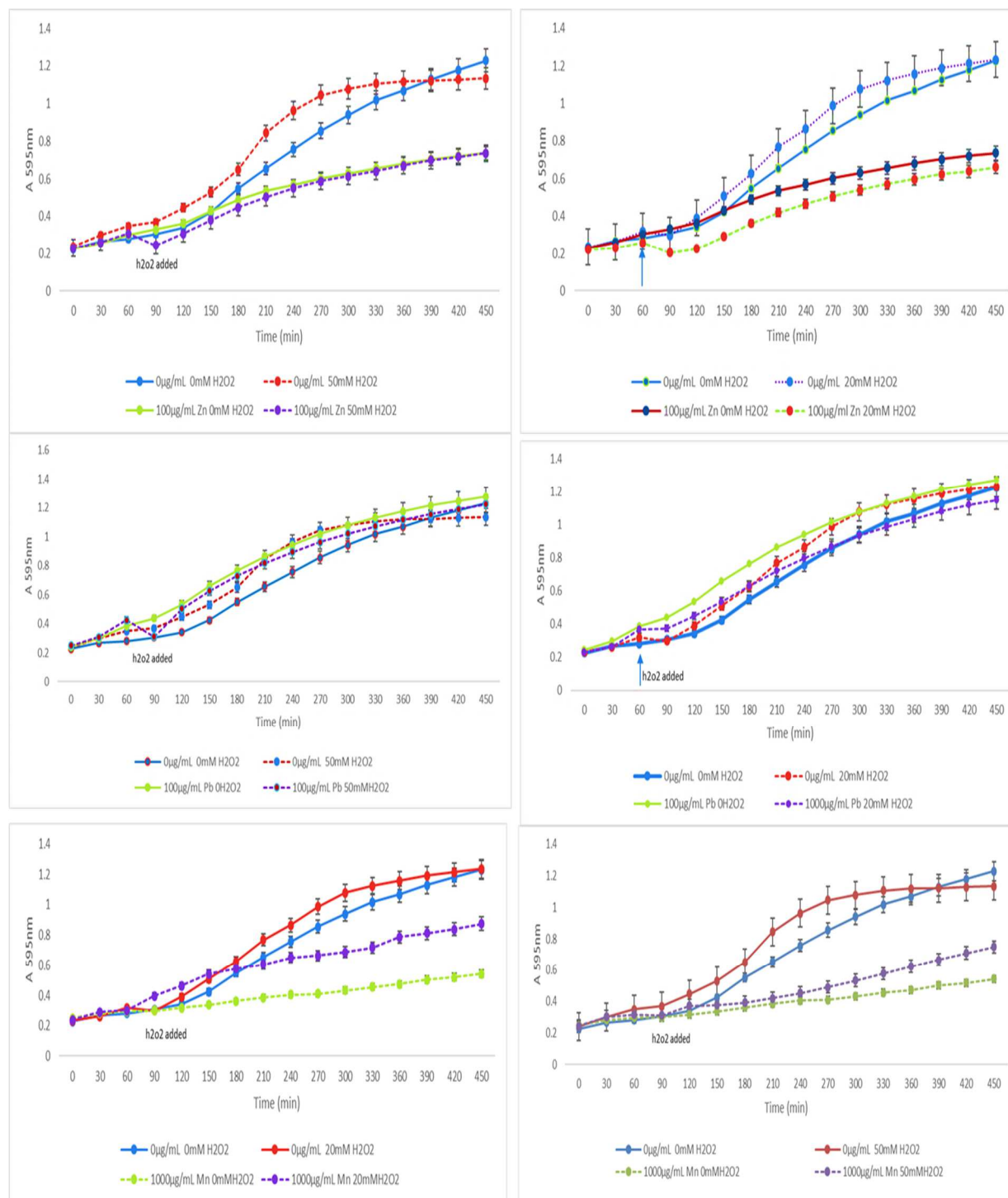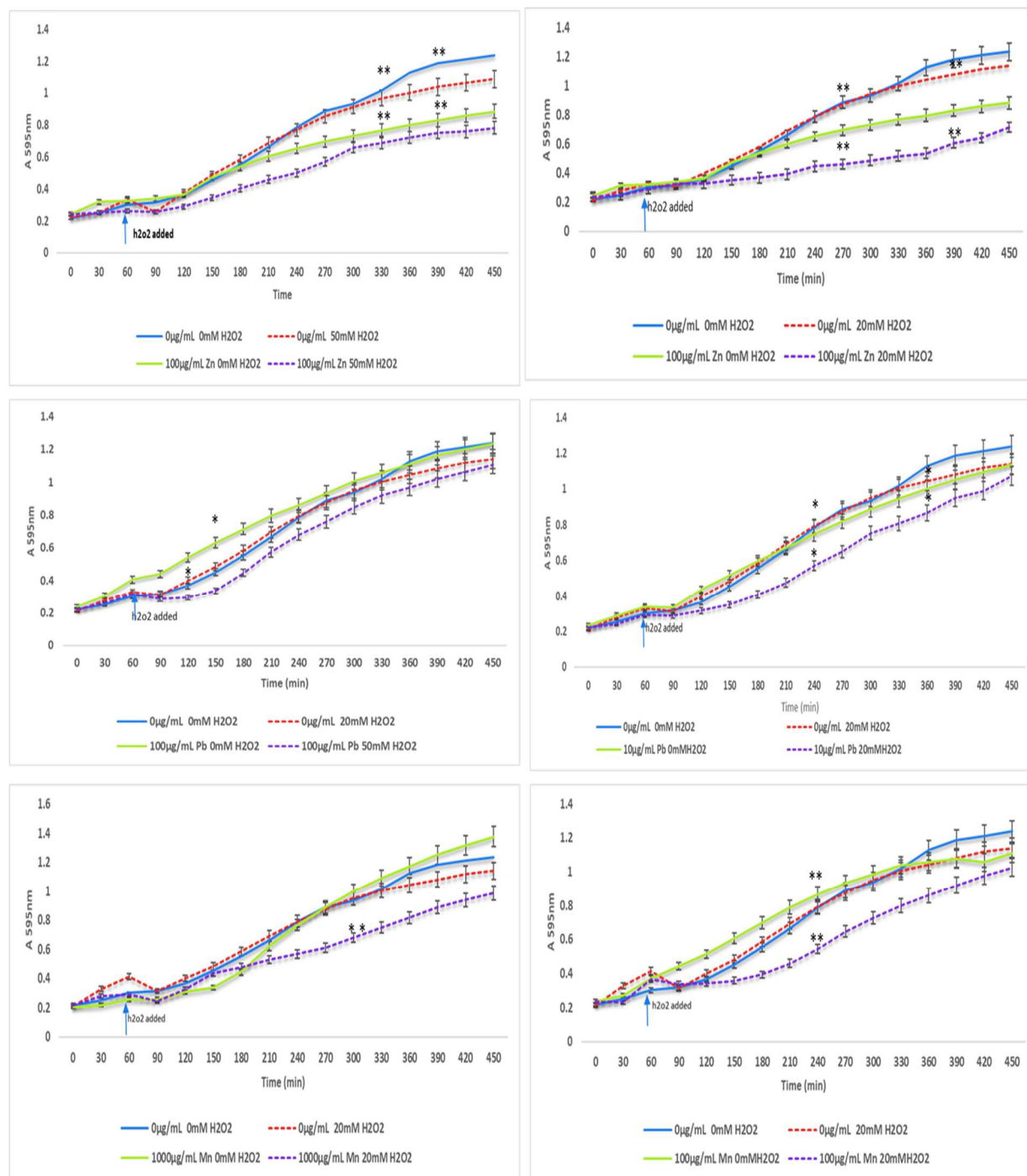
Figure 26: Oxidative stress sensitivity of *Serratia marcescen*s (SME) to heavy metal exposure. *Serratia marcescen*s environmental isolate (SME) and *Serratia marcescen*s surrogate strain (SMS) were exposed to 0, 20, and 50mM H_2O_2 with and without 10 μg/ml, 50 μg/ml and 100 μg/ml of zinc, lead and 100 μg/ml, 500 μg/ml and 1000 μg/ml manganese.

Figure 27: Oxidative stress sensitivity of Serratia marcescens (SMS) to heavy metal exposure. Serratia marcescens environmental isolate (SME) and Serratia marcescens surrogate strain (SMS) were exposed to 0, 20, and 50mM H2O2 with and without 10 μg/ml, 50 μg/ml and 100 μg/ml of zinc, lead and 100 μg/ml, 500 μg/ml and 1000 μg/ml manganese. This experiment was run in triplicate and statistical analysis was determined using the Student's T-test, with $p < 0.05$ denoted by one asterisk and $p < 0.01$ denoted by two asterisks.

We observed that both 20mM hydrogen peroxide and 50mM hydrogen peroxide induced significantly increased sensitivities ($p < 0.01$) in both SME and SMS in the absence of zinc (Fig. 27) when compared with treated controls (Fig. 26).

In the presence of lead, there was no significant effect in oxidative sensitivity of SME in both 10µg/ml and 100µg/ml but when compared to SMS, there was a significant reduction ($p < 0.01$) in oxidative sensitivity of both 10µg/ml zinc treated SMS (Fig. 27). We also observed that 1000µg/ml of manganese significantly inhibited ($p < 0.01$) the oxidative sensitivity of both SME and SMS at 20Mm and 50Mm hydrogen peroxide (Fig. 26-27). However, SME was not significantly affected by 10µg/ml manganese but both 20mM hydrogen peroxide and 50mM hydrogen peroxide significantly increased oxidative sensitivities ($p < 0.01$) in both SME and SMS in the absence of manganese (Fig. 26-27).

In addition to oxidative stress resistance, another important virulence associated factor is biofilm production. Motivated by that understanding, we sought to determine whether the environmental isolate, enhanced for oxidative stress–resistance (Fig. 28), was similarly able to produce more biofilm. Not only did the environmental isolate produce ~ 1.3-fold significantly more biofilm than the reference strain in the absence of metal exposures (Fig. 28) but also was able to produce significantly more biofilm than the reference strain when challenged with 2 of our 3 metals at the lowest challenge concentration. More specifically, when challenged with either 10 µg/ml (ppm) of Zn or Pb, significantly higher 1.3- and 1.2-fold, respectively, greater biofilm production was produced by the environmental strain vs. the reference strain (Fig. 32). Interestingly, challenge with the lowest concentration of Mn (100 µg/ml (ppm) Pb) resulted in a 1.4-fold significantly reduced biofilm production in the environmental strain vs. the reference strain (Fig. 28) for reasons that remain unclear. However, when evaluating 500 µg/ml (ppm) and

the highest 1000 µg/ml (ppm) Mn challenge concentrations, the environmental isolate had no significantly different biofilm production (Fig. 28) and significantly greater 1.17-fold increased biofilm production (Fig. 28), respectively. With regards to Zn and Pb challenges, the environmental isolate exhibited greater biofilm production than did the reference strain when challenged with intermediate [50 µg/ml (ppm)] or high [100 µg/ml (ppm)] (Fig. 28 panels B and C).

SME and SMS both exhibited significantly increased biofilm production when exposed to manganese by a two-fold or more (Fig. 28). Of the concentrations of metal treatment in SMS, only 10µg/mL and 1000µg/mL manganese exposure significantly enhanced biofilm production. The greatest fold increase in biofilm formed induced by SME when exposed to zinc was observed at 10µg/mL (2.00 fold; Fig. 28), while SMS had the greatest fold increase in biofilm formation when exposed to 100µg/mL manganese (2.34 fold; Fig. 28).
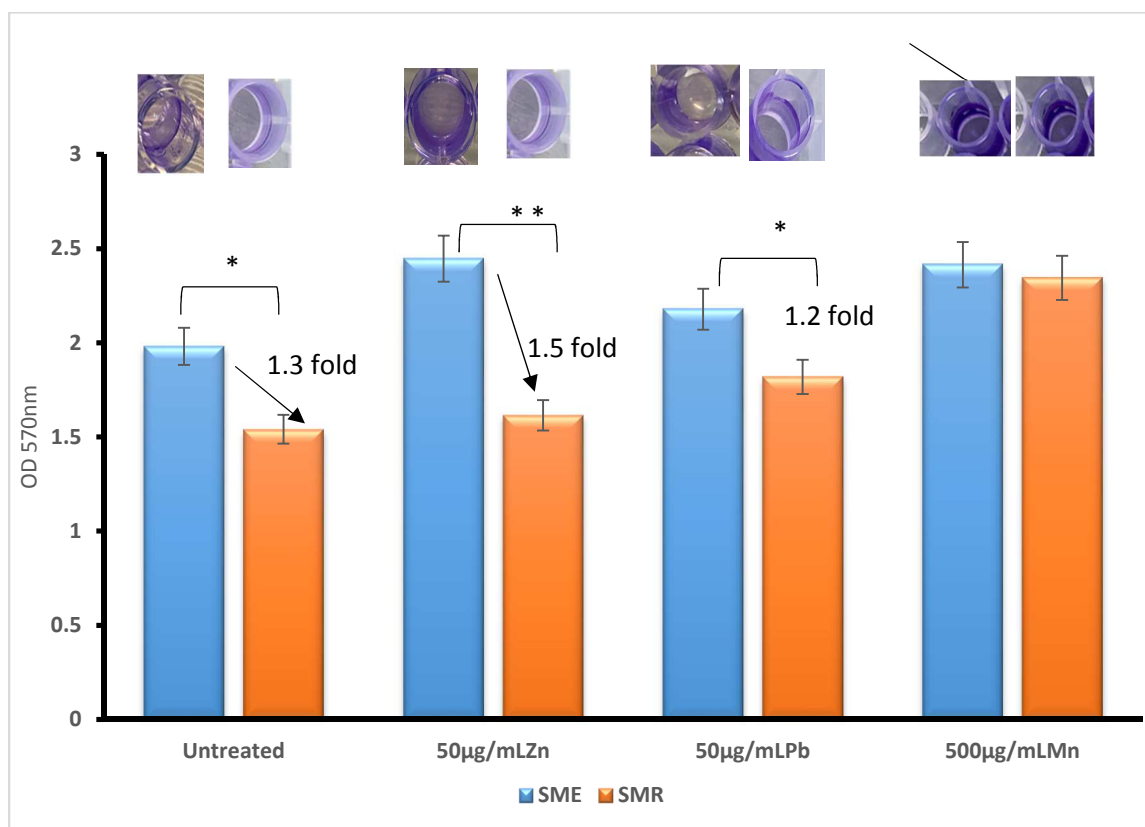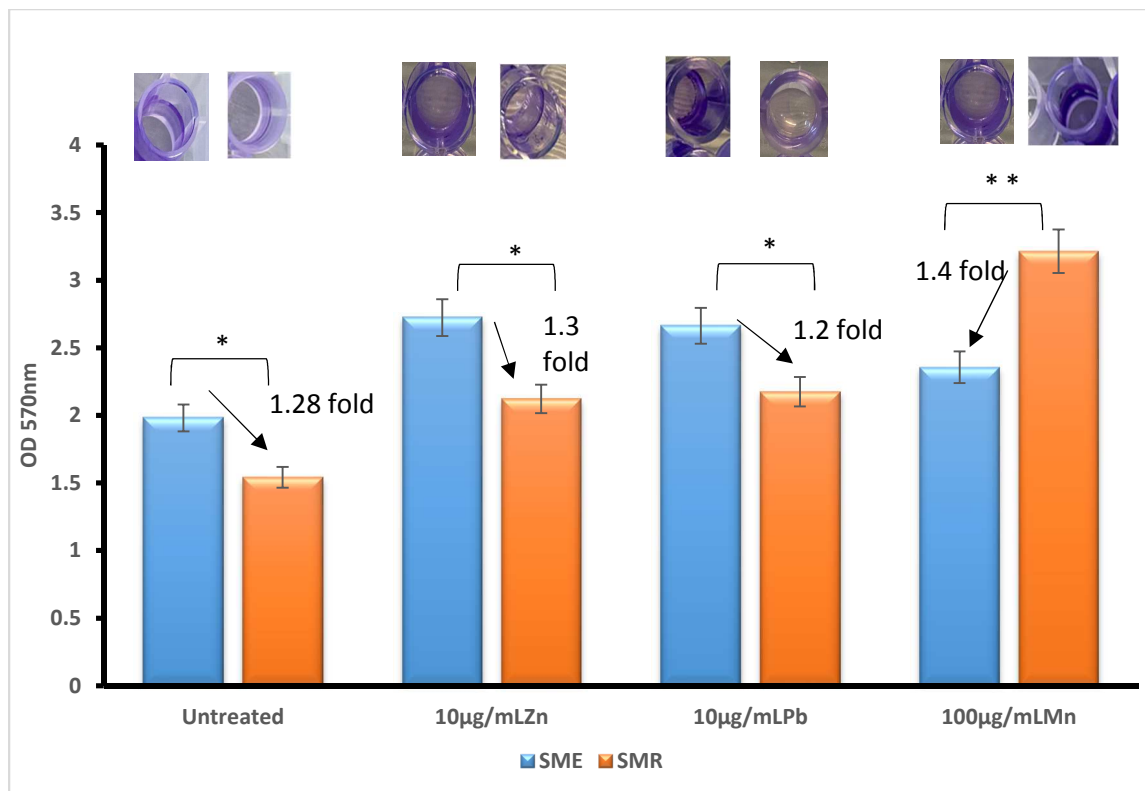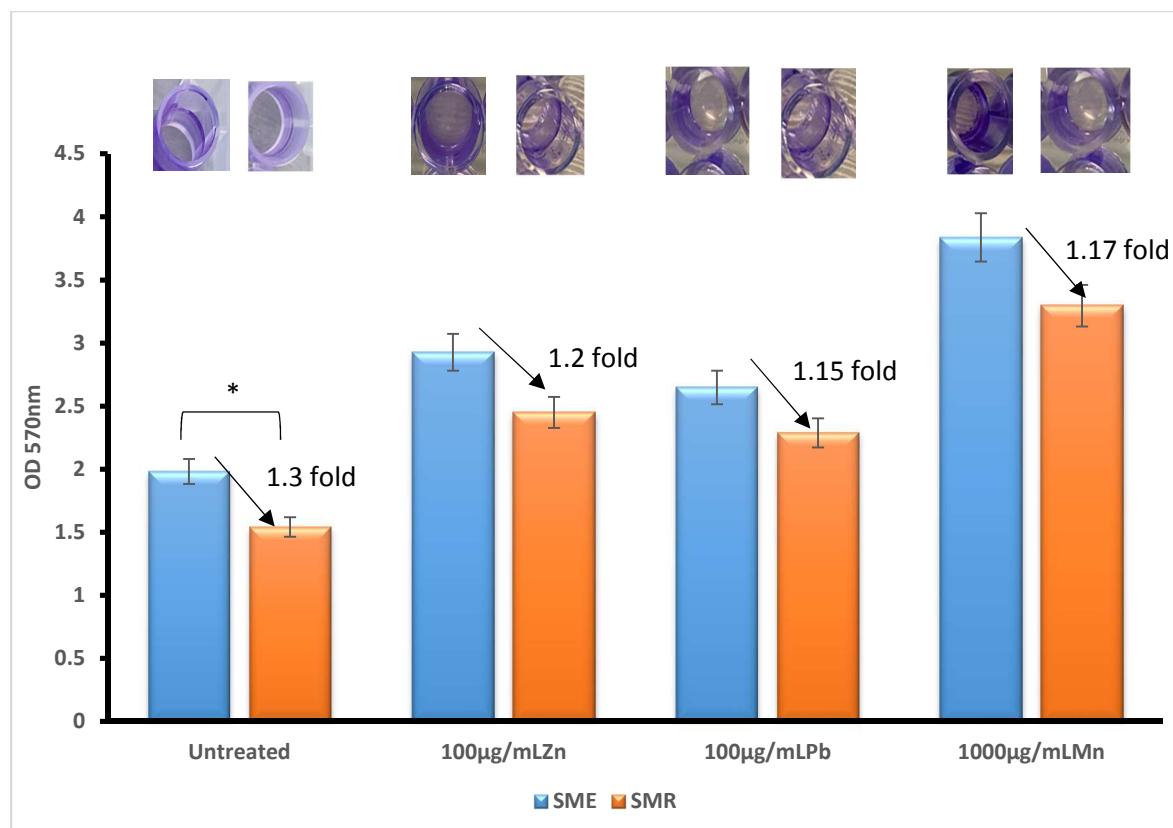
Figure 28: Biofilm production of *Serratia marcescen*s strains to heavy metal exposure. *Serratia marcescen*s environmental isolate (SME) and *Serratia marcescen*s surrogate strain (SMS) was exposed to 10 µg/ml, 50 µg/ml and 100 µg/ml of zinc, lead and 100 µg/ml, 500 µg/ml and 1000 µg/ml manganese. This experiment was run in triplicate and statistical analysis was determined using the Student's T-test, with $p < 0.05$ denoted by one asterisk and $p < 0.01$ denoted by two asterisks.

We observed that 10µg/ml, 50µg/ml and 100µg/ml of zinc and lead did not significantly increase the biofilm production of SMS when treated with the metals. However, there was a significant increase ($p< 0.05$) in the biofilm formation for all concentrations of manganese for SME (Fig. 28). Overall, both SME and SMS induced the largest-fold increase in biofilm formed in non-treatment conditions (7.13 fold, SME; 9.17 fold SMS).

Since the environmental strain appeared to be armed with enhanced virulence associated properties, namely increased oxidative stress resistance and biofilm production, we sought to determine whether the environmental isolate was able to better colonize both lung and gut models. However, prior to characterizing co-culture models, we first had to determine whether metal exposures were toxic to the eukaryotic cell lines, to be used, in pure culture. Of all 3 metals evaluated, Pb induced the greatest cytotoxicity in BAES 2B lung epithelial cells (Fig. 29). More specifically, the lowest challenge dose of Zn [10 µg/ml (ppm)] was the least cytotoxic to BAES 2B cells resulting in 68-56 % viability over 6 h; viability dropped to 43% at 12 h at the lowest dose challenge while the highest dose challenge [10 µg/ml (ppm)] resulted in ~ 95% cytotoxicity (Fig. 29). As indicated earlier, Pb was the most toxic metal to BAES 2B cells, and the lowest challenge dose of [10 µg/ml (ppm)] resulted in 25-20 % viability over a 12 h period (Fig. 29). Mn, of the 3 test metals, was the least toxic to BAES 2B cells; the lowest test concentration of 100 µg/ml (ppm) induced little cytoxicity resulting in 93-85% viability over a 12 h period.

In HT29 gut epithelial cells, Zn was the most toxic metal (Fig. 30), in sharp contrast with the BAES 2B cells, where Pb was the most toxic metal (Fig. 29). More specifically, at the lowest Zn challenge concentration [10 µg/ml (ppm)], 31% cell viability was observed following a 3 h challenge compared to 51% and 58% viability following 3 h lowest concentrations challenges of Pb [10 µg/ml (ppm)] and Mn [100 µg/ml (ppm)], respectively (Fig. 31 compare panels A to B and

C). Interestingly, unlike the BAES 2B cells with declining cell numbers (Fig. 29), HT29 cells proliferated over 3, 6, and 12 h time points when challenged with 10 and 50 µg/ml (ppm) of Zn and all test concentrations of Pb, and Mn (Fig. 31).

Environmental isolate in the untreated environment (1.16-fold) and Zn challenge [10 µg/ml (ppm)] environment (Fig. 32). Interestingly, those significantly enhanced differences were not maintained following a 6 h infection period; rather, significantly enhanced proliferation was only observed in the Pb challenge [10 µg/ml (ppm)] and Mn challenge [100 µg/ml (ppm)] environment, evidenced by 1.24-fold and 1.19-fold differences (Fig. 32). Taken together, depending on the infection period-length, the *S. marsescens* environmental isolate is enhanced in its proliferative capability in both lung and gut tissues.
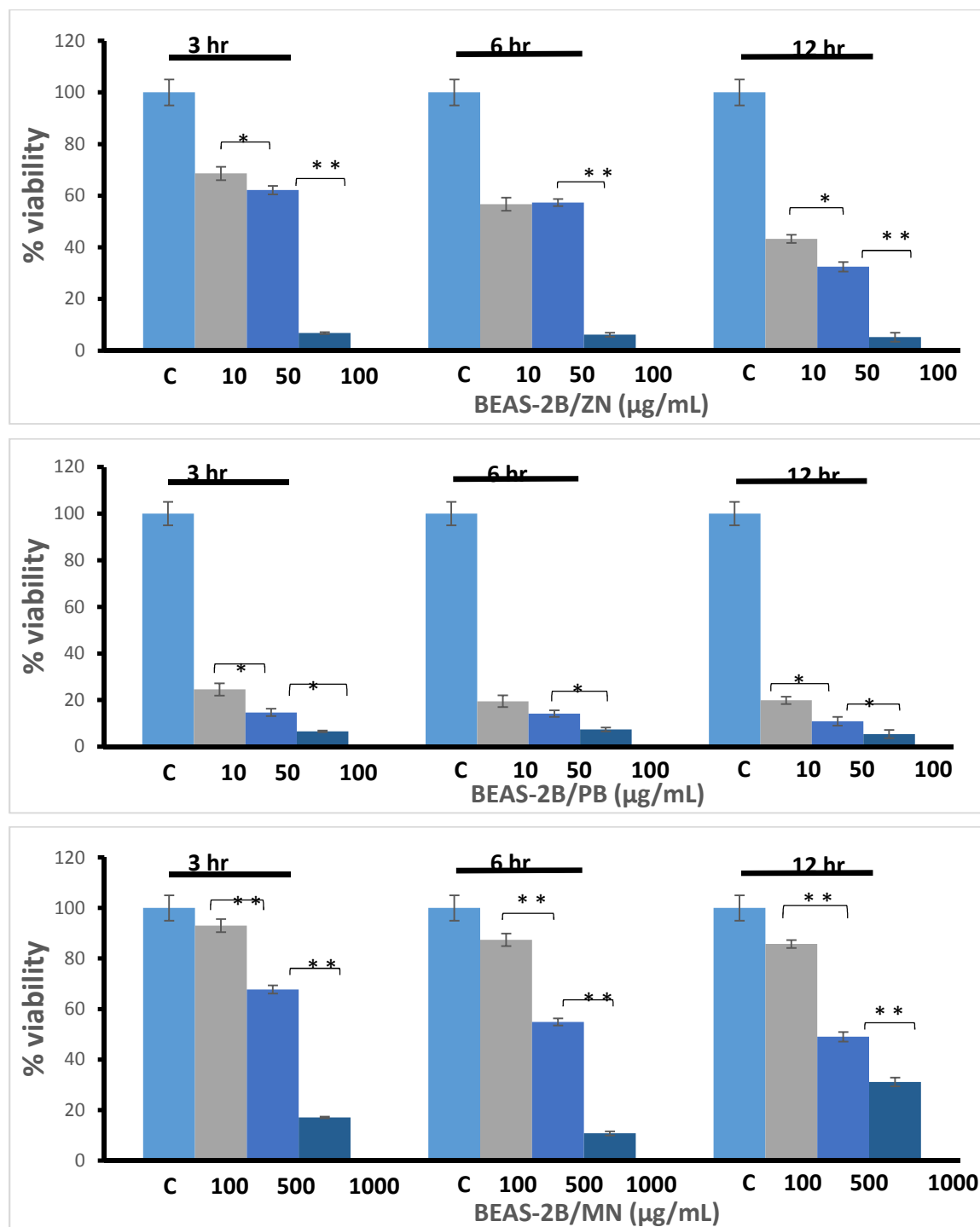
Figure 29: Heavy metal exposure on human lung epithelial BEAS-2B cells. Viability assays were performed to determine cytotoxicity of 10, 50, and 100 μg/ml of Zn, Pb and 100, 500, and 100 μg/ml on human BEAS-2B cells. This experiment was run in triplicate and statistical analysis was determined using the Student's T-test, with $p < 0.05$ denoted by one asterisk and $p < 0.01$ denoted by two asterisks.

We determined if there will be any significant changes in BEAS-2B normal lung epithelial cell, CCD-841 normal gut epithelial cell and HT29 cancer gut epithelial cell co-culture with *Serratia marsescens* infections (Fig. 23-25). We also determined if these changes were as a result of the bacterial responses to the heavy metals only and not due to an influence on the cells viability, a proliferation assay using MTT was performed on the cells alone without the co-culture of SME and SMS. We also gauged the cytotoxicity of the cells after treatment with different concentration of zinc, lead and manganese.

To determine this, 10, 50, and 100 µg/ml of zinc and lead and 100, 500 and 1000µg/ml of manganese were added to seeded BEAS-2B, CCD-841 and HT29 cells to for 0, 3, 6, and 12h.
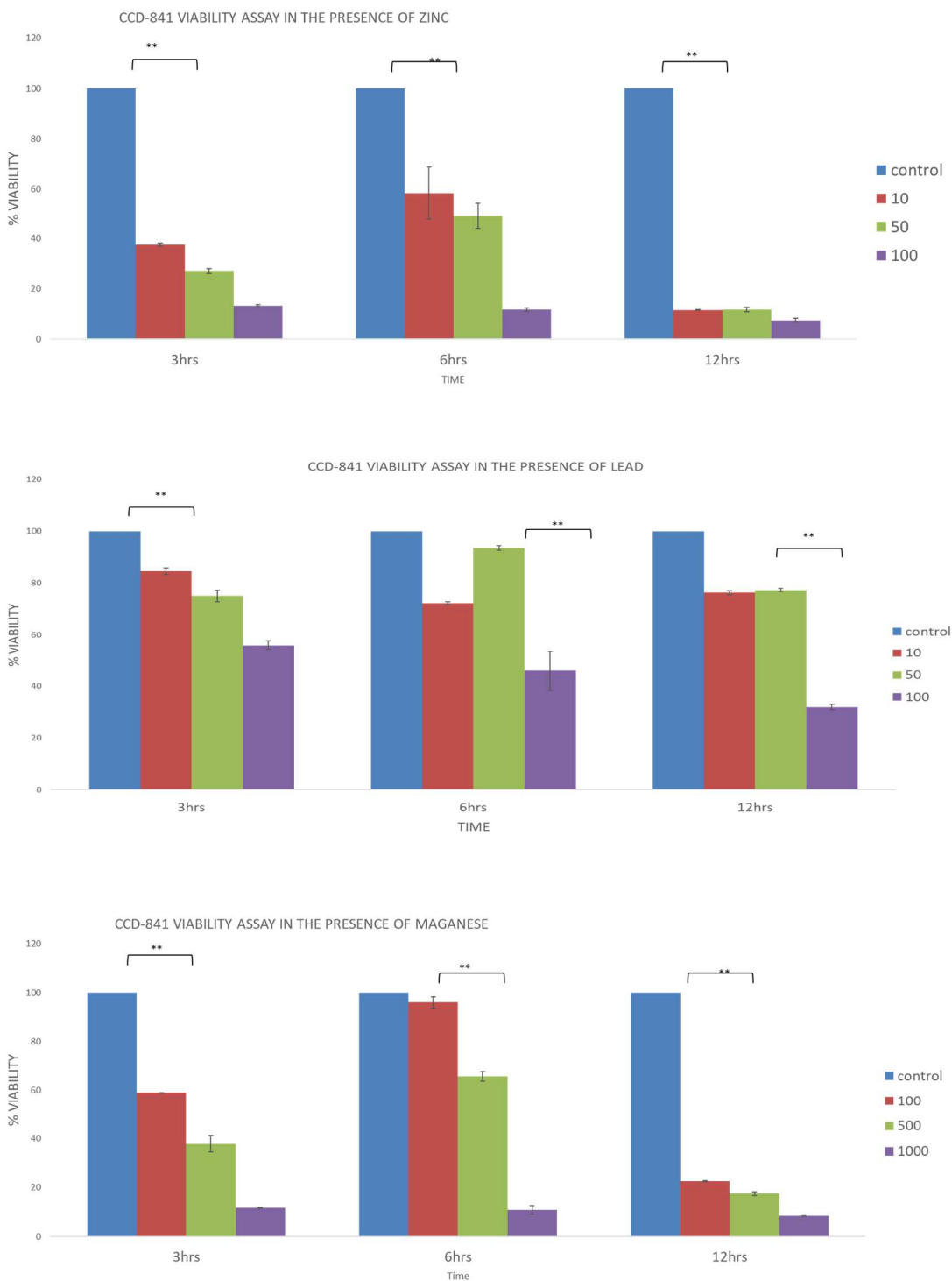
Figure 30: Heavy metal exposure on human lung epithelial CCD-841 cells. Viability assays were performed to determine cytotoxicity of 10, 50, and 100 µg/ml of Zn, Pb and 100, 500, and 100 µg/ml on human CCD-841 cells. This experiment was run in triplicate
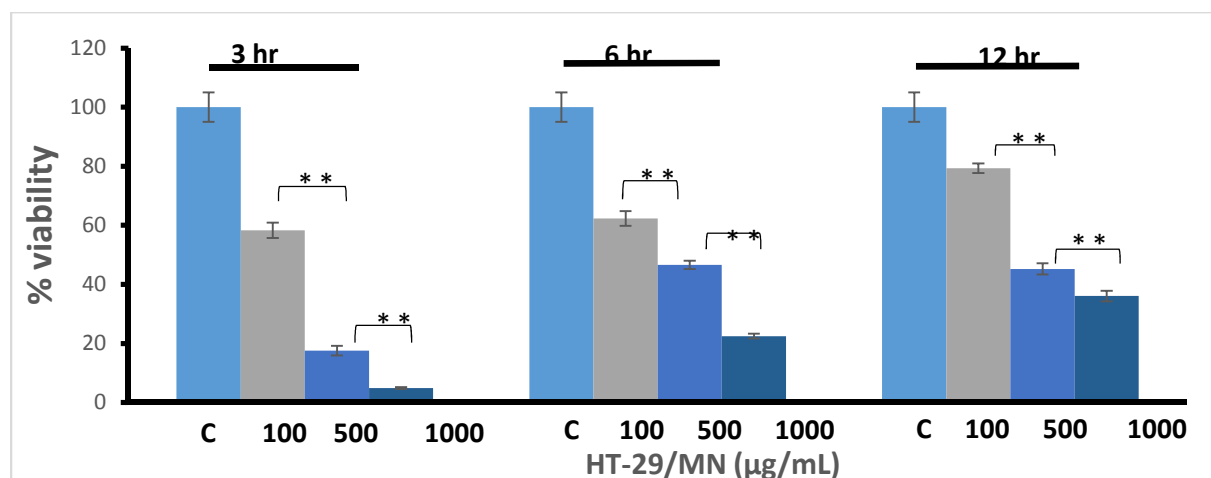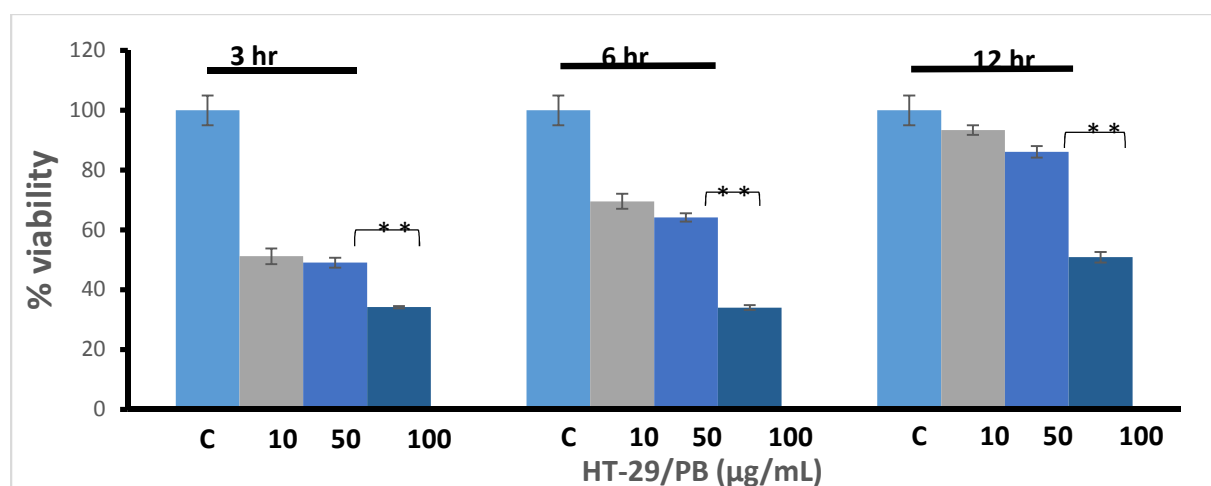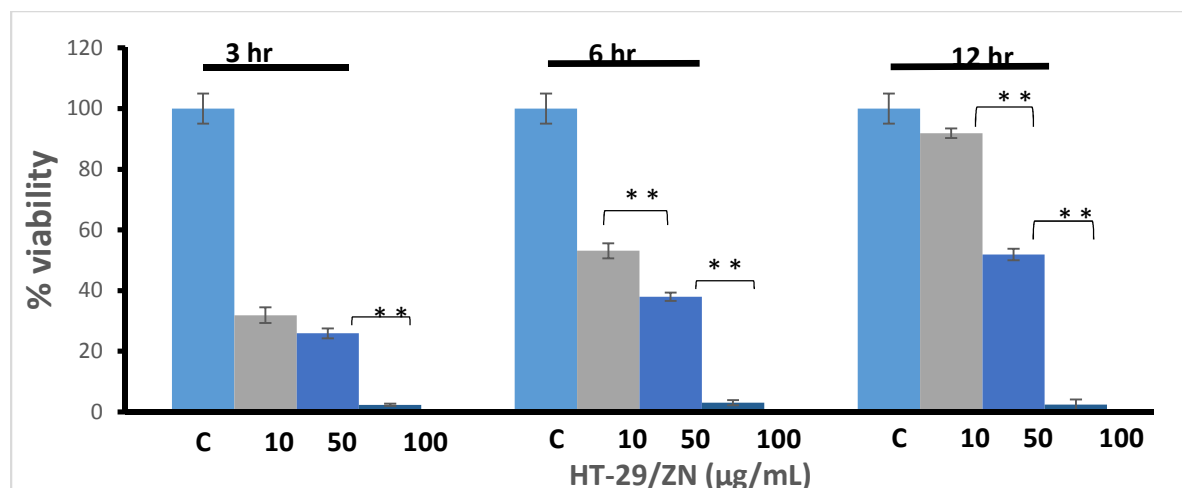
Figure 31: Heavy metal exposure on human lung epithelial HT-29 cells. Viability assays were performed to determine cytotoxicity

We observed a significant decrease (p< 0.01) in cell viability for BEAS-2B cell line at all-time points for the three concentrations tested for zinc (Fig. 29). When exposure to 10µg/ml and 50µg/ml were compared, there was no significant difference in the cell viability at 3h and 6h but a significant difference (p< 0.01) was seen when compared to 100µg/ml of zinc exposure (Fig. 29). BEAS-2B exposure to lead was the most impacted out of all the three-metal exposure tested as cell viability was significantly decreased (p< 0.01) by up to 5-fold for 10 µg/ml and 50 µg/ml and 10-fold for 100 µg/ml (Fig.29). Similarly, normal gut epithelial cells CCD-841 was evaluated for proliferation when exposed to 10 µg/ml, 50 µg/ml, 100 µg/ml, 500 µg/ml and 1000 µg/ml of zinc, lead and manganese. We observed a significant decrease (p< 0.01) in cell viability at all-time points for all metal tested (Fig. 30). When exposure to 10µg/ml and 50µg/ml of zinc and lead were compared, there was no significant difference, and they follow the same results gotten in the treatment of the normal lung cell line (Fig. 29-30). We also determined if our working concentrations had any effect on HT-29 cell viability and observed a significant increase (p< 0.01) in cell viability on a time – dose dependent. We observed that an increase in time leads to a significant increase (p< 0.01) in cell viability (Fig. 31). This effect is opposite when compared to the other normal cell lines and might be as a result of the cancer cell rapidly proliferating.

Since there were no significant difference in cell viability when comparing exposure at 10µg/ml and 50µg/ml for all cell lines and the environmental samples of our metal analysis falls within this measured level, we determined if there will be bacterial response when exposed to 50µg/ml, 100µg/ml and 500µg/ml. In order to assess if exposure to metals will significantly affect bacterial proliferation causing intestinal tract infection or pneumonia, we co-cultured CCD-841, BEAS-2B and HT-29 epithelial cells with SME and SMS in the presence of zinc, lead and manganese (Fig. 32-34). Bacterial proliferation was measured at 0h, 3h and 6h post infection and

the 0h were used as control. We observed that at the 3h time point's exposure to 50μg/ml for CCD-841 cell, a significant increase ($p < 0.01$) in proliferation was observed for both bacterial strains than at exposure to 50μg/ml at 6h end point (Fig. 33).
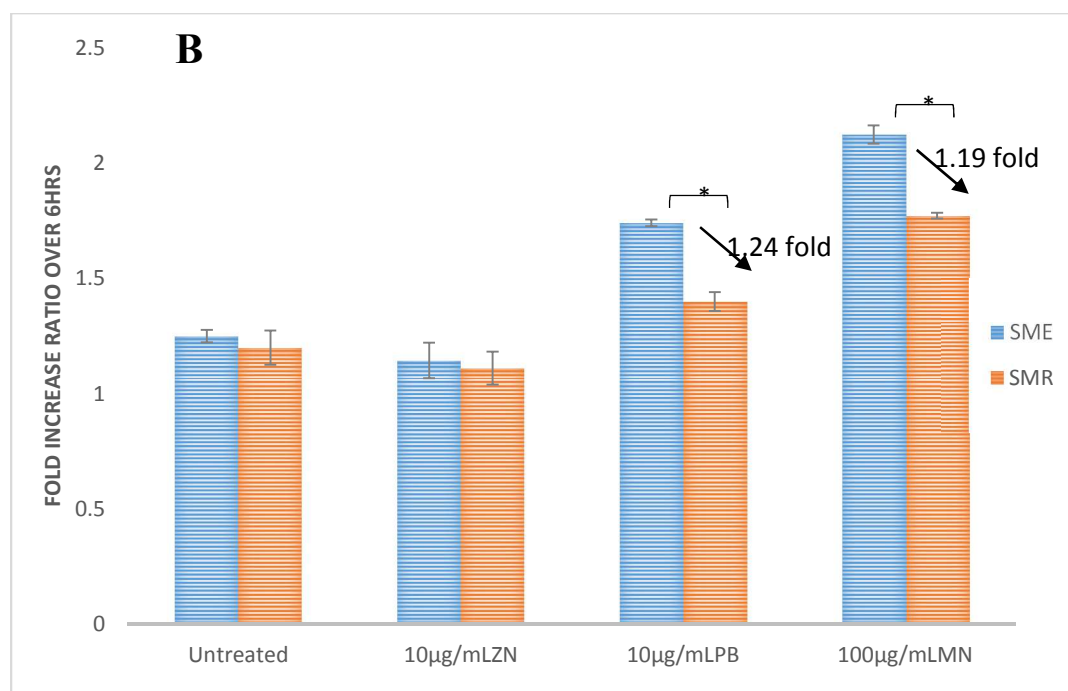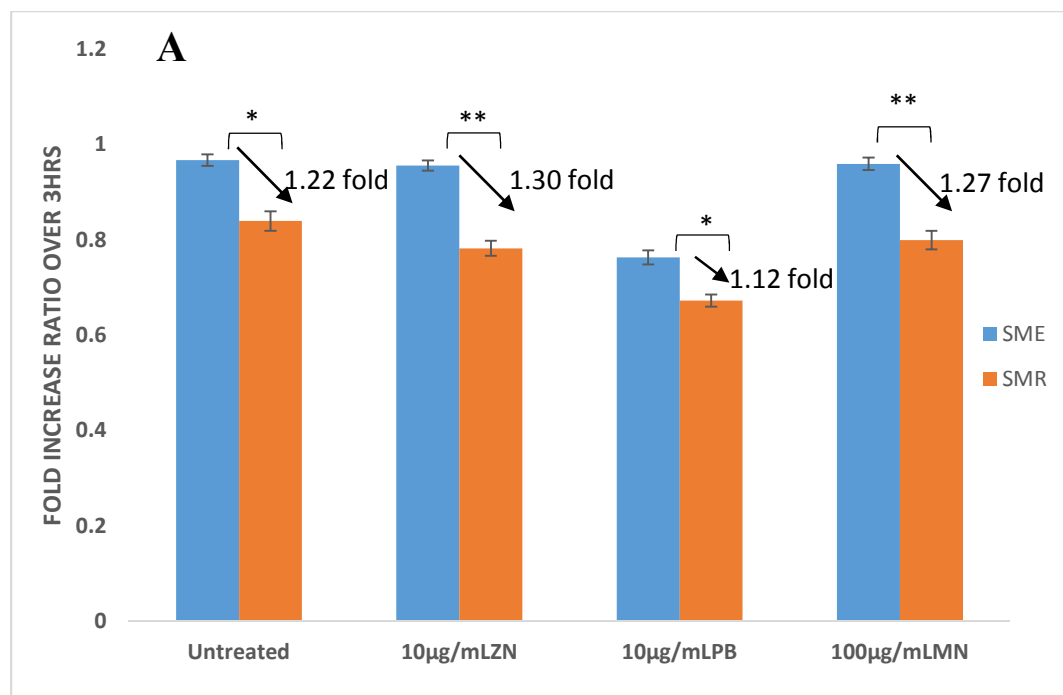
Figure 32: Bacterial co-culture on normal human lung epithelial BEAS-2B cells over (A) 3hrs and (B) 6hrs end point modeling the lung microenvironment (10µg/ml Zn, Pb and 100µg/ml Mn)

More specifically, SME shows significant increase (p< 0.01) in bacterial proliferation than SMS at 6h post infection for all metal exposure. There was also no significant difference in the level of bacterial proliferation for both strains at 3h time point but at 6h, SME exhibited significant increase (p< 0.01) in bacterial proliferation than SMS (Fig. 7). When SME and SMS were infected with CCD-841 cells, exposure to 100μg/ml of zinc and lead significantly reduced (p< 0.01) bacterial proliferation; however, SMS bacterial proliferation was significantly reduced (p< 0.01) than SME at the same concentration and the same 6h end point infection period (Fig. 27).

The above-mentioned findings informed our experimental design for the 6 h co-culture infection model, in which, the lowest metal concentration of each challenge was be used to avoid unnecessary eukaryotic cytotoxicity. In the lung infection model, the environmental isolate exhibited a 1.22-fold significantly higher proliferation over 3 h compared to the reference strain (Fig. 6A) and increased to a 1.44-fold significantly higher proliferation at 6 h (Fig. 6B). Following a 3 h infection period, the environmental isolate maintained significantly higher proliferation than the reference strain despite Zn [10 μg/ml (ppm)], Pb [10 μg/ml (ppm)], and [100 μg/ml (ppm)] Mn-challenge, as seen by 1.30-, 1.12-, and 1.27-fold difference, respectively (Fig 6A). Following a 6 h infection period, only the untreated and Pb-challenged [10 μg/ml (ppm)] environmental isolate had significantly greater proliferation of 1.4- and 1.29-fold respectively (Fig. 6B). To determine whether the environmental isolate was similarly enhanced in its proliferation in the gut environment, HT29 cells were used for a co-culture infection. Unlike the lung infection model, in which the environmental isolate exhibited significantly higher proliferation after 3 h in all challenge conditions, the environmental isolate only experienced significantly
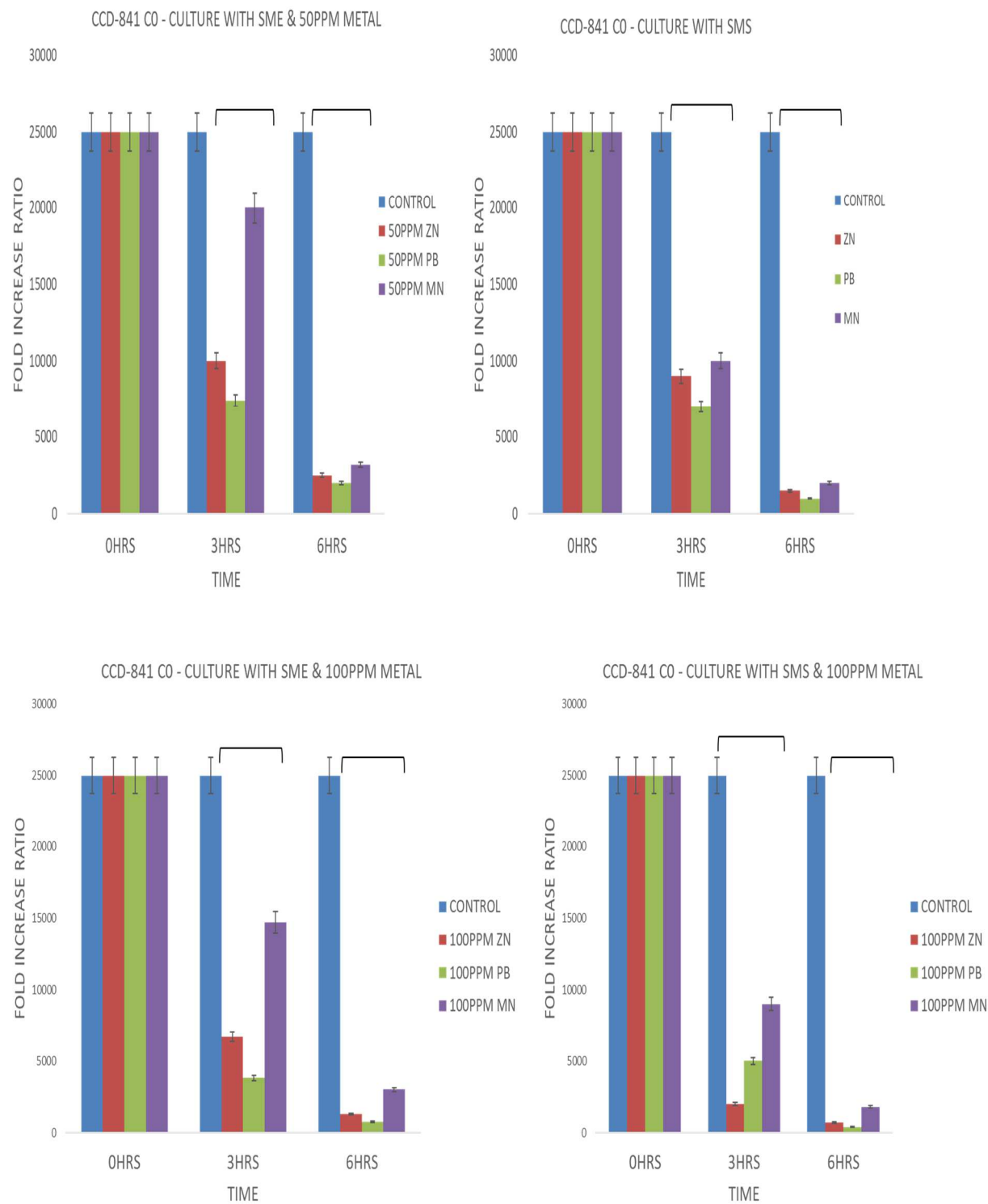
Figure 33: Bacterial co-culture on normal human gut epithelial CCD-841 cells over 3hrs and 6hrs end point modeling the gut microenvironment (10µg/ml Zn, Pb and 100µg/ml Mn)
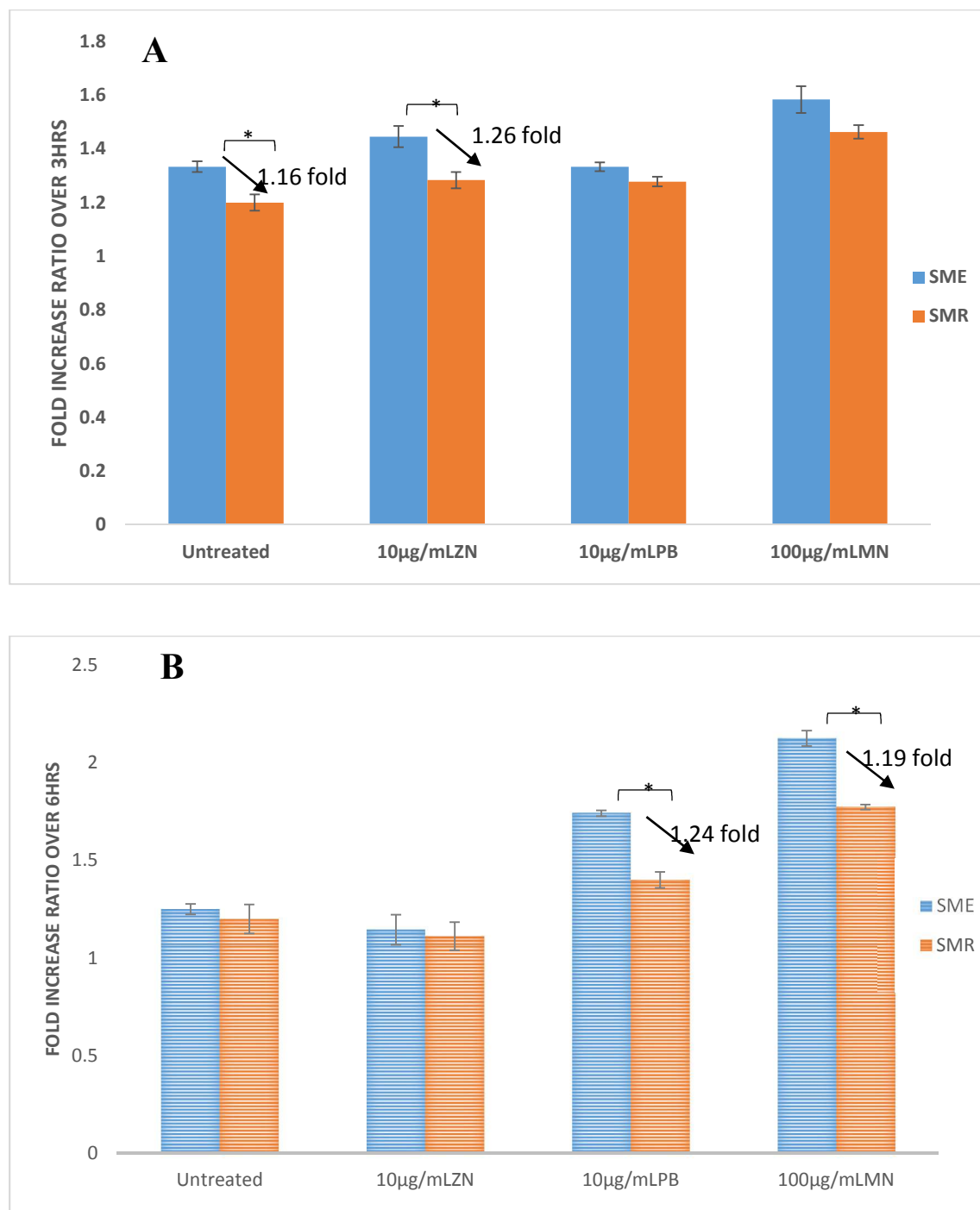
Figure 34: Bacterial co-culture on cancer human gut epithelial HT-29 cells over (A) 3hrs and (B) 6hrs end point modeling the gut microenvironment (10µg/ml Zn, Pb and 100µg/ml Mn)

We also examined the bacterial proliferation with HT-29 cancer gut cells and a significant increase (p< 0.01) in bacterial proliferation was seen in both strains at 3h post infection and exposure to 50μg/ml of zinc and manganese (Fig. 28). To determine whether the environmental isolate was similarly enhanced in its proliferation in the gut environment, HT29 cells were used for a co-culture infection. Unlike the lung infection model, in which the environmental isolate exhibited significantly higher proliferation after 3 h in all challenge conditions, the environmental isolate only experienced significantly.

More specifically, significantly higher proliferation after a 3 h infection was only realized by the environmental isolate in the untreated environment (1.16-fold) and Zn challenge [10 μg/ml (ppm)] environment (Fig. 7A). Interestingly, those significantly enhanced differences were not maintained following a 6 h infection period; rather, significantly enhanced proliferation was only observed in the Pb challenge [10 μg/ml (ppm)] and Mn challenge [100 μg/ml (ppm)] environment, evidenced by 1.24-fold and 1.19-fold differences (Fig. 7B). Taken together, depending on the infection period-length, the *S. marsescens* environmental isolate is enhanced in its proliferative capability in both lung and gut tissues

Interestingly, a significant decrease was seen at exposure of 50μg/ml lead at 6h infection end point while exposure to zinc and manganese was not significantly different. Also, there was no significant difference at 3h post infection when SME and SMS was compared to each other. Similarly, at 100μg/ml exposure to zinc and lead was reduced significantly at both 3h post infection and 6h infection end point

CHAPTER 5

CONCLUSIONS

Houston has experienced three flooding events in a three-year span: 2015 - 2017 (i.e., the Memorial Day flooding in May of 2015, the Tax Day flooding in 2016, and Hurricane Harvey in 2017). We sought to determine microbial loads, identify representative colonies, and assess global population dynamics pre- and post-Harvey. Previous studies have reported bacterial contamination following rainfall (Olds et al. 2017; Islam et al. 2017; Chu et al. 2011; O'Neill et al. 2013; Kistemann et al. 2002; Gelting et al. 2005) at levels high enough to exceed EPA standards. Our findings similarly show that enteric bacterial populations increased following heavy rainfall in several Houston watersheds, likely caused by the redistribution or mobilization of these enteric bacteria pathogens from the watershed to the soil (Dorner et al. 2006; Jean et al. 2006). Contamination of these watersheds can also be caused by a variety of anthropogenic sources such as: proximity to wastewater outfalls, chemical plants, feces from animals, and superfund sites (Lalancette et al. 2014). More specifically, several factors were shown to contribute to high bacterial levels during the wet weather periods such as: wastewater effluent, storm water runoff, treatment facilities, disinfection units, and consistent rain (Desai et al. 2010).

Fong et al. (2007) observed that bacterial pollutants can be transported from wastewater outfalls and municipal discharge, through surface and subsurface flow after intense rain events (Fong et al. 2007). In agreement with this, we observed bacterial transport from upstream to

downstream across some watersheds for Halls watershed (winter 2017), Greens watershed (summer 2017) and Horsepen watershed (winter 2018) enteric bacteria populations. Heavy rainfall has been linked to disease outbreaks such as typhoid fever, diarrhea, and other waterborne diseases (Aud et al. 2004). In that vein, our study isolated and identified opportunistic pathogenic bacteria from the samples analyzed including *S. marcenscens, P. mendocina*, *P. fulva,* and *P. putida.* Further, we identified the *Burkholderia* spp. in the Halls Bayou (~ 2.7-fold higher in winter than summer) in our metagenomic analysis. *Burkholderia cepacia* is a bona fide human pathogen.

Urban watershed recreationalists are at higher risk of contracting gastro-intestinal diseases and other acute respiratory illness than non–recreationalists (DeFlorio-Barker et al. 2018; McLellan et al. 2018) through kayaking, rowing, and other secondary recreation activities (Wiegner et al. 2017; McLellan et al. 2018). Watershed concentrations of enteric bacteria are typically a function of the number of waste-water outfalls, storm drains, and other surface and subsurface runoff discharges. Our study aimed to quantify enteric bacteria and identify pathogenic enteric bacteria associated with waterborne diseases. Interestingly, we observed that enteric bacterial loads were significantly elevated during the 2017 winter (post-Harvey) in Halls, Horsepen, and Mustang Bayous compared to their summer (pre-Harvey) 2017 counterparts. Our 2018 data, one year following the Harvey flooding event, similarly revealed significantly elevated enteric counts in the winter compared to the summer (2018), suggesting that fluctuations in enteric counts are most likely a result of temporal change, seasonal fluctuation, water flow rates, and flooding events**.**

Ultimately, we observed that watersheds closer to superfund and municipal wastewater treatment facility sites contained a higher load of opportunistic pathogenic bacteria, as we expected. Unexpectedly, however, we found higher enteric bacterial loads in the fall relative to

the summer in both 2017 (the year of Hurricane Harvey) and 2018 (one year after the flood). Although we expected some redistribution following the Hurricane Harvey flooding event and potentially higher enteric loads observed in the winter of 2017 as a result, we found higher enteric loads in the winter of 2018 (relative to the summer of 2018) one year later (in a year where there was no flooding event to prompt redistribution. Typically water flow rates in the Houston watershed are slower in the winter as well as the temperature typically being colder than what mesophilic enteric bacteria prefer (37°C). Therefore, reasons why enteric loads were found to be higher in Houston watersheds in the winters compared to the summers over the one-year study are still unclear. Generally speaking, the rural and suburban Houston watersheds such as Horsepen and Cypress Creek watersheds had lower enteric bacterial loads.

Enteric bacterial pathogens are major causes of food-borne gastroenteritis in humans and remain an important public health concern worldwide (Lukinmaa et al. 2014, Natoro et al. 1998). Indicator bacteria, such as *Escherichia coli*, have been shown to be present in various watersheds and also cause harm to both the environment and the health of the residents surrounding these watersheds. Our results demonstrate higher enteric counts during the winter in the majority of Houston watersheds evaluated. *Serratia marcescens*, an opportunistic pathogen and member of the *Enterobacteriaceae* family, was also prevalent in some of the watersheds. Taken together, our data supports the notion that flooding events may cause redistribution of bacterial pathogens at the species-level; however, phyla-level redistributions are much less likely. Heavy metals in urban soils are associated with direct and indirect human health risks. This study examined growth, biofilm formation and oxidative sensitivity of heavy metal (Pb, Zn, and Mn) in urban and rural isolated bacteria of soil samples of Houston watersheds as well as their risks to the gut

environment. Bioavailability of heavy metal concentration were analyzed in the Texas Southern University laboratory by a simplified physiologically based extraction test.

S. marcescens is a formidable opportunistic pathogen capable of causing infections ranging from bacteremia to pneumonia, particularly in the nosocomial setting (González-Juarbe et al. 2015; Weakland et al. 2020). Previously, a *S. marcescens* isolate form the highly contaminated (mercury and uranium) Savannah River Site was found to have both increased metal and antibiotic resistance (Gendy et al. 2020). Such highly resistant opportunistic pathogens are more likely to cause disease outbreaks and could find their way into the nosocomial setting further challenging health workers already grappling with a laundry list of drug resistant organisms present.

In evaluating Houston watershed soils, we also identified an *S. marcescens* strain (Adedoyin et al. 2021) and sought to characterize its growth kinetics, oxidative stress resistance, biofilm production, and virulence potential in both lung and gut infection model systems. Consistent with earlier findings of increased metal resistance (Gendy et al. 2020), the Houston soil-isolate was similarly more resistant to Zn, Pb, and Mn challenge (chosen based on elevated levels measured in Houston soil samples) than a reference strain. Likely a result of environmental adaptation, the Houston soil-isolate was able to tolerate various challenge concentrations of the aforementioned metals and consistently outperformed a *S. marsescens* reference strain in growth curve assays, oxidative stress resistance experiments, biofilm production assays, and both lung and gut infection model systems.

Which, if any, specific metal resistance genes play (a) role(s) in subsequent challenges remains unknown; however, a recent proteomic study of Lauria-Bertani grown *S. marcescens* revealed some 15,000 unique peptides belonging to over 2,500 protein groups. Several of these groups include chemotaxis genes as well as beta lactamase resistance genes (Gangadharappa et al.

al 2020). It is possible that several genes from either of the aforementioned groups could be playing a role during lung and/or gut infections/interactions, and that metal exposure results in their direct overexpression. In that same vein, a comparative genomic study of a Savannah River Site environmentally isolated *S. marcescens* strain and various reference strains revealed 360 distinct genes involved in drug and/or trace metal resistance (Gendy et al. 2020). It is possible that the Houston-isolated *S. marcescens* is also in possession of unique genes as well, enabling survival in the local, heavily polluted watershed soils. It has already been shown that glucose metabolism and capsule production drive virulence of *S. marcescens* during bacteremia in murine models (Anderson et al. 2017); therefore, it conceivable that some of those participating genes could also become upregulated in environmental strains challenged by metal exposure.

S. marcescens, an opportunistic pathogen increasingly causing nosocomial and community infections, can be found in local watersheds. In those environments, *S. marcescens* can become exposed to various environmental toxicants, including trace metals. Adaptations to these elevated toxicant levels can promote enhanced virulence. An adapted *S. marcescens* strain with enhanced biofilm production and oxidative stress resistance can cause increased virulence and poses a significant threat to human health. These findings confirm that a Houston watershed soil *S. marcescens* isolate had increased virulence potential (relative to a reference strain) and experienced enhanced proliferation in both lung and gut infection models. Taken together, routine bacterial surveillance of local watersheds is warranted and should be aimed at characterizing increased antibiotic resistance and virulence potential of environmentally isolated bacterial pathogens.

REFERENCE

Adedoyin FT, Bhaskar MSB, Rosenzweig JA (2021) Characterization of Bacterial Populations in Urban and Rural Houston Watershed Soil Samples Following a Flooding Event. Frontiers in Environmental Microbiology 7 (1) 22-34.

Ahmed, W., Hamilton, K., Toze, S., Cook, S., & Page, D. (2019). A review on microbial contaminants in storm water runoff and outfalls: Potential health risks and mitigation strategies. *The Science of the total environment*, *692*, 1304–1321. https://doi.org/10.1016/j.scitotenv.2019.07.055

Ahemad, M. (2019). Remediation of metalliferous soils through the heavy metal resistant plant growth promoting bacteria: paradigms and prospects. *Arabian Journal of Chemistry*, *12*(7), 1365-1377.

Arnone, R. D., & Perdek Walling, J. (2007). Waterborne pathogens in urban watersheds. *Journal of Water and Health*, *5*(1), 149-162.

Auld, H., MacIver, D., & Klaassen, J. (2004). Heavy rainfall and waterborne disease outbreaks: the Walkerton example. *Journal of Toxicology and Environmental Health, Part A*, *67*(20-22), 1879-1887.

Barberán, A., Bates, S. T., Casamayor, E. O., & Fierer, N. (2012). Using network analysis to explore co-occurrence patterns in soil microbial communities. *The ISME journal*, *6*(2), 343-351.

Bado, M., Kwende, S., Shishodia, S., & Rosenzweig, J. A. (2017). Impact of dust exposure on mixed bacterial cultures and during eukaryotic cell co-culture infections. *Applied Microbiology and Biotechnology*, *101*(18), 7027-7039.

Behera, M., Dandapat, J., & Rath, C. C. (2014). Effect of heavy metals on growth response and antioxidant defense protection in Bacillus cereus. *Journal of basic microbiology*, *54*(11), 1201-1209.

Branda SS, Chu F, Kearns DB, Losick R, Kolter R (2006) A major protein component of the Bacillus subtilis biofilm matrix. Molecular microbiology 59(4):1229-38 doi:10.1111/j.1365-2958.2005.05020.x

Breton J, Daniel C, Vignal C, Body-Malapel M, Garat A, Plé C, Foligné B. Does oral exposure to cadmium and lead mediate susceptibility to colitis? The dark-and-bright sides of heavy metals in gut ecology. Sci Rep. 2016 Jan 11; 6:19200. doi: 10.1038/srep19200. PMID: 26752005; PMCID: PMC4707487.

Brinkmeyer, R., Amon, R. M., Schwarz, J. R., Saxton, T., Roberts, D., Harrison, S. & Duan, S. (2015). Distribution and persistence of Escherichia coli and Enterococci in stream bed and bank sediments from two urban streams in Houston, TX. *Science of the Total Environment*, *502*, 650-658.

Cao S, Feehley TJ, Nagler CR (2014) The role of commensal bacteria in the regulation of sensitization to food allergens. FEBS letters 588(22):4258-66 doi:10.1016/j.febslet.2014.04.026

Çelebi, A., Şengörür, B., & Kløve, B. (2014). Human health risk assessment of dissolved metals in groundwater and surface waters in the Melen watershed, Turkey. *Journal of Environmental Science and Health, Part A*, *49*(2), 153-161.

Chellam, S., Sharma, R. R., Shetty, G. R., & Wei, Y. (2008). Nanofiltration of pretreated Lake Houston water: disinfection by-product speciation, relationships, and control. *Separation and Purification Technology*, *64*(2), 160-169.

Chiang, P. C., Wu, T. L., Kuo, A. J., Huang, Y. C., Chung, T. Y., Lin, C. S., ... & Su, L. H. (2013). Outbreak of Serratia marcescens postsurgical bloodstream infection due to contaminated intravenous pain control fluids. International Journal of Infectious Diseases, 17(9), e718-e722.

Chu, Y., Salles, C., Tournoud, M. G., Got, P., Troussellier, M., Rodier, C., & Caro, A. (2011). Faecal bacterial loads during flood events in Northwestern Mediterranean coastal rivers. *Journal of Hydrology*, *405*(3-4), 501-511.

Curtis PD, Atwood J, 3rd, Orlando R, Shimkets LJ (2007) Proteins associated with the Myxococcus xanthus extracellular matrix. Journal of bacteriology 189(21):7634-42 doi:10.1128/JB.01007-07

Devaraj A, Justice SS, Bakaletz LO, Goodman SD (2015) DNABII proteins play a central role in UPEC biofilm structure. Molecular microbiology doi:10.1111/mmi.12994

Desai, A. M., Rifai, H., Helfer, E., Moreno, N., & Stein, R. (2010). Statistical investigations into indicator bacteria concentrations in Houston metropolitan watersheds. *Water Environment Research*, *82*(4), 302-318.

Desai, A. M., & Rifai, H. S. (2013). Escherichia coli concentrations in urban watersheds exhibit diurnal sag: Implications for water☐quality monitoring and assessment. *JAWRA Journal of the American Water Resources Association*, *49*(4), 766-779.

Dorner, S. M., Anderson, W. B., Slawson, R. M., Kouwen, N., & Huck, P. M. (2006). Hydrologic modeling of pathogen fate and transport. *Environmental science & technology*, *40*(15), 4746-4753

ESRI. 2014. Arc GIS Desktop-Environmental Systems Research Institute: Release 10.3. Redlands, CA, USA.

Faulkner, M. J., & Helmann, J. D. (2011). Peroxide stress elicits adaptive changes in bacterial metal ion homeostasis. *Antioxidants & redox signaling*, *15*(1), 175-189.

Ferris, M. J., Norori, J., Zozaya-Hinchliffe, M., & Martin, D. H. (2007). Cultivation-independent analysis of changes in bacterial vaginosis flora following metronidazole treatment. *Journal of clinical microbiology*, *45*(3), 1016-1018.

Ferris, M. J., Norori, J., Zozaya-Hinchliffe, M., & Martin, D. H. (2007). Cultivation-independent analysis of changes in bacterial vaginosis flora following metronidazole treatment. *Journal of clinical microbiology*, *45*(3), 1016-1018.k

Ferreira CM, Vieira AT, Vinolo MA, Oliveira FA, Curi R, Martins Fdos S (2014) The central role of the gut microbiota in chronic inflammatory diseases. Journal of immunology research 2014:689492 doi:10.1155/2014/689492

Flemming HC, Wingender J 2010. The biofilm matrix. *Nat Rev Microbiol* 8: 623–633 [PubMed] [Google Scholar]

Fong, T. T., Mansfield, L. S., Wilson, D. L., Schwab, D. J., Molloy, S. L., & Rose, J. B. (2007). Massive microbiological groundwater contamination associated with a waterborne outbreak in Lake Erie, South Bass Island, Ohio. *Environmental health perspectives*, *115*(6), 856-864.

Gallaher TK, Wu S, Webster P, Aguilera R (2006) Identification of biofilm proteins in non-typeable Haemophilus Influenzae. BMC microbiology 6:65 doi:10.1186/1471-2180-6-65

Gangadharappa BS, Rajashekarappa S, Sathe G (2020) Proteomic profiling of *Serratia marcescens* by high-resolution mass spectrometry. Bioimpacts. 10(2):123-135.

Gendy S, Chauhan A, Agarwal M, Pathak A, Rathore RS, Jaswal R (2020) Is Long-Term Heavy Metal Exposure Driving Carriage of Antibiotic Resistance in Environmental Opportunistic Pathogens: A Comprehensive Phenomic and Genomic Assessment: 10.3389/fmicb.2020.01923.

Geuking MB, Koller Y, Rupp S, McCoy KD (2014) The interplay between the gut microbiota and the immune system. Gut microbes 5(3):411-8 doi:10.4161/gmic.29330

Gelting, R., Sarisky, J., Selman, C., Otto, C., Higgins, C., Bohan, P. O., ... & Meehan, P. J. (2005). Use of a systems-based approach to an environmental health assessment for a waterborne disease outbreak investigation at a snowmobile lodge in Wyoming. *International journal of hygiene and environmental health*, *208*(1-2), 67-73

González-Juarbe N, Mares CA, Hinojosa CA, Medina JL, Cantwell A, Dube PH, Orihuela CJ, Bergman MA (2015) Requirement for Serratia marcescens cytolysin in a murine model of hemorrhagic pneumonia. Infect Immun. 83(2):614-24.

Goto, D. K., & Yan, T. (2011). Genotypic diversity of Escherichia coli in the water and soil of tropical watersheds in Hawaii. *Appl. Environ. Microbiol.*, *77*(12), 3988-3997.

Gough, H. L., & Stahl, D. A. (2011). Microbial community structures in anoxic freshwater lake sediment along a metal contamination gradient. *The ISME journal*, *5*(3), 543-558.

Handbook of Texas Online, Robert Wooster, "BAYOU CITY," accessed October 29, 2019, http://www.tshaonline.org/handbook/online/articles/etb01. Uploaded on June 12, 2010. Modified on May 26, 2016. Published by the Texas State Historical Association.

Handbook of Texas Online, "MUSTANG BAYOU," accessed May 09, 2020, http://www.tshaonline.org/handbook/online/articles/rhm05. Uploaded on June 15, 2010. Published by the Texas State Historical Association.

Harris County Flood Control District HCFCD. (2015). *Streambank Stabilization Handbook: A Guide for harris county Landowners*. Retrieved from https://texasriparian.org/wp-content/uploads/2013/02/HCFCD-Streambank-Stabilization-Handbook.pdf

Harris County Flood Control District HCFCD. (2020). Buffalo Bayou. *Harris County Flood Control District*. Retrieved from https://www.hcfcd.org/Find-Your-Watershed/Buffalo-Bayou

Harris County Flood Control District HCFCD. (2020). Halls Bayou. *Harris County Flood Control District*. Retrieved from https://www.hcfcd.org/Find-Your-Watershed/Halls-Bayou

Harris County Flood Control District HCFCD. (2020). Hunting Bayou. *Harris County Flood Control District*. Retrieved from https://www.hcfcd.org/Find-Your-Watershed/Hunting-Bayou

Houston-Galveston Area Council (2002) Regional Land Cover Data. Houston-Galveston Area Council: Houston, Texas, http://www.h-gac. com/rds/land_use/default.aspx.

Houston-Galveston Area Council (2008). Bacteria TMDLs for Halls Bayou Halls Bayou http://www.h-gac.com/watershed-based-plans/documents/houston-metro/houston-metro_11-10-08_presentation.pdf

Houston-Galveston Area Council (2015). How is the Water? *H-GAC, Basin Highlights Report*. Retrieved from https://www.h-gac.com/clean-rivers-program/documents/2015%20BHR%20FINAL_Abridged%20Version.pdf

Hussein, K. A., & Joo, J. H. (2013). Heavy metal resistance of bacteria and its impact on the production of antioxidant enzymes. *African Journal of Microbiology Research*, *7*(20), 2288-2296.

Imlay, J. A. (2015). Transcription factors that defend bacteria against reactive oxygen species. *Annual review of microbiology*, *69*, 93-108.

Imlay, J. A. (2019). Where in the world do bacteria experience oxidative stress? *Environmental microbiology*, *21*(2), 521-530.

Islam, M. M., Hofstra, N., & Islam, M. A. (2017). The impact of environmental variables on faecal indicator bacteria in the Betna river basin, Bangladesh. *Environmental Processes*, *4*(2), 319-332.

Jane Buckle, Chapter 7 - Infection, Editor(s): Jane Buckle, Clinical Aromatherapy (Third Edition), Churchill Livingstone, 2015, Pages 130-167, ISBN 9780702054402, https://doi.org/10.1016/B978-0-7020-5440-2.00007(https://www.sciencedirect.com/science/article/pii/B9780702054402000073)

Jean, J. S., Guo, H. R., Chen, S. H., Liu, C. C., Chang, W. T., Yang, Y. J., & Huang, M. C. (2006). The association between rainfall rate and occurrence of an enterovirus epidemic due to a contaminated well. *Journal of applied microbiology*, *101*(6), 1224-1231.

Joo HS, Otto M (2012) Molecular basis of in vivo biofilm formation by bacterial pathogens. Chemistry & biology 19(12):1503-13 doi:10.1016/j.chembiol.2012.10.022

Jeamsripong, S., Chuanchuen, R., & Atwill, E. R. (2018). Assessment of Bacterial Accumulation and Environmental Factors in Sentinel Oysters and Estuarine Water Quality from the Phang Nga Estuary Area in Thailand. *International journal of environmental research and public health*, *15*(9), 1970. https://doi.org/10.3390/ijerph15091970

Kistemann, T., Claßen, T., Koch, C., Dangendorf, F., Fischeder, R., Gebel, J. & Exner, M. (2002). Microbial load of drinking water reservoir tributaries during extreme rainfall and runoff. *Appl. Environ. Microbiol.*, *68*(5), 2188-2197

Khan I, Yasir M, Azhar EI, Kumosani T, Barbour EK, Bibi F, Kamal MA (2014) Implication of gut microbiota in human health. CNS & neurological disorders drug targets 13(8):1325-33

Kostakioti, M., Hadjifrangiskou, M., & Hultgren, S. J. (2013). Bacterial biofilms: development, dispersal, and therapeutic strategies in the dawn of the postantibiotic era. *Cold Spring Harbor perspectives in medicine*, *3*(4), a010306.

Kotzampassi K, Giamarellos-Bourboulis EJ, Stavrou G (2014) Obesity as a consequence of gut bacteria and diet interactions. ISRN obesity 2014:651895 doi:10.1155/2014/651895

Lawal A, Jejelowo O, Chopra AK, Rosenzweig JA (2011) Ribonucleases and bacterial virulence. Microbial biotechnology 4(5):558-71 doi:10.1111/j.1751-7915.2010.00212.

Lalancette, C., Papineau, I., Payment, P., Dorner, S., Servais, P., Barbeau, B., & Prévost, M. (2014). Changes in Escherichia coli to Cryptosporidium ratios for various fecal pollution sources and drinking water intakes. *Water research*, *55*, 150-161.

Lee, D. Y., Lee, H., Trevors, J. T., Weir, S. C., Thomas, J. L., & Habash, M. (2014). Characterization of sources and loadings of fecal pollutants using microbial source tracking assays in urban and rural areas of the Grand River Watershed, Southwestern Ontario. *Water research*, *53*, 123-131.

Link, D. D., Walter, P. J., & Kingston, H. M. (1999). Wastewater standards and extraction chemistry in validation of microwave-assisted EPA method 3015A. *Environmental science & technology*, *33*(14), 2469-2473.

Lukinmaa, S., NAKARI, U. M., Eklund, M., & Siitonen, A. (2004). Application of molecular genetic methods in diagnostics and epidemiology of food□borne bacterial pathogens. *Apmis*, *112*(11□12), 908-929.

Madsen E. L. (2011). Microorganisms and their roles in fundamental biogeochemical cycles. *Curr Opin Biotechnol* 22:456–464 [CrossRef][PubMed] [Google Scholar]

Mahurpawar, M. (2015). Effects of heavy metals on human health. *International Journal of Reseacrh-Granthaalayah, ISSN-23500530*, 2394-3629.

Mhuantong, W., Wongwilaiwalin, S., Laothanachareon, T., Eurwilaichitr, L., Tangphatsornruang, S., Boonchayaanant, B. & Khan, E. (2015). Survey of microbial diversity in flood areas during Thailand 2011 flood crisis using high-throughput tagged amplicon pyrosequencing. *PloS one*, *10*(5).

Nataro, J. P., & Kaper, J. B. (1998). Diarrheagenic escherichia coli. *Clinical microbiology reviews*, *11*(1), 142-201.

Ochieng JB, Boisen N, Lindsay B, Santiago A, Ouma C, Ombok M, Fields B, Stine OC, Nataro JP (2014) Serratia marcescens is injurious to intestinal epithelial cells. Gut Microbes. 2014;5(6):729-36.

Olds, H. T., Corsi, S. R., Dila, D. K., Halmo, K. M., Bootsma, M. J., & McLellan, S. L. (2018). High levels of sewage contamination released from urban areas after storm events: A quantitative survey with sewage specific bacterial indicators. *PLoS medicine*, *15*(7), e1002614. https://doi.org/10.1371/journal.pmed.1002614

Olivera, F., & DeFee, B. B. (2007). Urbanization and Its Effect On Runoff in the Whiteoak Bayou Watershed, Texas 1. *JAWRA Journal of the American Water Resources Association*, *43*(1), 170-182.

O'Neill, S., Adhikari, A. R., Gautam, M. R., & Acharya, K. (2013). Bacterial contamination due to point and nonpoint source pollution in a rapidly growing urban center in an arid region. *Urban Water Journal*, *10*(6), 411-421.

Patwa, L. G., Fan, T. J., Tchaptchet, S., Liu, Y., Lussier, Y. A., Sartor, R. B., & Hansen, J. J. (2011). Chronic intestinal inflammation induces stress-response genes in commensal Escherichia coli. *Gastroenterology*, *141*(5), 1842-1851.

Prabhakaran, P., Ashraf, M. A., & Aqma, W. S. (2016). Microbial stress response to heavy metals in the environment. *Rsc Advances*, *6*(111), 109862-109877.

Pandey, P. K., Kass, P. H., Soupir, M. L., Biswas, S., & Singh, V. P. (2014). Contamination of water resources by pathogenic bacteria. *AMB Express*, *4*, 51. https://doi.org/10.1186/s13568-014-0051-x

Pandey, P. K., Soupir, M. L., Haddad, M., & Rothwell, J. J. (2012). Assessing the impacts of watershed indexes and precipitation on spatial in-stream E. coli concentrations. *Ecological indicators*, *23*, 641-652.

Quigg, A., Broach, L., Denton, W., & Miranda, R. (2009). Water quality in the Dickinson Bayou watershed (Texas, Gulf of Mexico) and health issues. *Marine Pollution Bulletin*, *58*(6), 896-904.

Rifai, H. (2007). Total Maximum Daily Loads for Fecal Bacteria in the Dickinson Bayou Final Historical Data Review and Analysis Report Revision http://www.tceq.state.tx.us/compliance/monitoring/water/quality/data/08twqi/twqi08.htm Texas Commission on Environmental Quality.

Rehman, K., Fatima, F., Waheed, I., & Akash, M. S. H. (2018). Prevalence of exposure of heavy metals and their impact on health consequences. *Journal of cellular biochemistry*, *119*(1), 157-184.

Robles Alonso V, Guarner F (2013) Linking the gut microbiota to human health. The British journal of nutrition 109 Suppl 2:S21-6 doi:10.1017/S0007114512005235

Rosenzweig JA, Chopra AK (2013) The exoribonuclease Polynucleotide Phosphorylase influences the virulence and stress responses of yersiniae and many other pathogens. Frontiers in cellular and infection microbiology 3:81 doi:10.3389/fcimb.2013.00081

Rogers, G. O., & Defee Ii, B. B. (2005). Long-term impact of development on a watershed: early indicators of future problems. *Landscape and Urban Planning*, *73*(2-3), 215-233.

Sipes, J. L., & Zeve, M. K. (2012). *The Bayous of Houston*. Arcadia Publishing.

Sneck-Fahrer, D. A., Milburn, M. S., East, J. W., & Oden, J. H. (2005). *Water-Quality Assessment of Lake Houston near Houston, Texas, 2000-2004* (No. 2005-5241). US Geological Survey.

Shahid, M., Pourrut, B., Dumat, C., Nadeem, M., Aslam, M., & Pinelli, E. (2014). Heavy-metal-induced reactive oxygen species: phytotoxicity and physicochemical changes in plants. In *Reviews of Environmental Contamination and Toxicology Volume 232* (pp. 1-44) Springer, Cham.

Suraju, M. O., Lalinde-Barnes, S., Sanamvenkata, S., Esmaeili, M., Shishodia, S., & Rosenzweig, J. A. (2015). The effects of indoor and outdoor dust exposure on the growth, sensitivity to oxidative-stress, and biofilm production of three opportunistic bacterial pathogens. *Science of the Total Environment*, *538*, 949-958.

Stocker, M. D., Rodriguez-Valentin, J. G., Pachepsky, Y. A., & Shelton, D. R. (2016). Spatial and temporal variation of fecal indicator organisms in two creeks in Beltsville, Maryland. *Water Quality Research Journal of Canada*, *51*(2), 167-179.

Teague, A., Christian, J., & Bedient, P. (2013). Radar rainfall application in distributed hydrologic modeling for Cypress Creek watershed, Texas. *Journal of Hydrologic Engineering*, *18*(2), 219-227.

Texas Coastal Watershed Program. 2008. Land Use Classification GIS layer. Available at www.urban-nature.org

Texas Commission on Environmental Quality Page 1 Chapter 307 - Texas Surface Water Quality Standards Rule Project No. 2016-002-307-OW. https://www.tceq.texas.gov/waterquality/standards/2018-surface-water-quality-standards. https://www.tceq.texas.gov/assets/public/waterquality/standards/tswqs2018/2018swqs_all sections_nopreamble.pdf. https://www.tceq.texas.gov/assistance/water/wastewater/ww-bac-t.html

Thomas, P., Sekhar, A. C., Upreti, R., Mujawar, M. M., & Pasha, S. S. (2015). Optimization of single plate-serial dilution spotting (SP-SDS) with sample anchoring as an assured method for bacterial and yeast cfu enumeration and single colony isolation from diverse samples. *Biotechnology Reports*, *8*, 45-55.

Thomas VC, Thurlow LR, Boyle D, Hancock LE (2008) Regulation of autolysis-dependent extracellular DNA release by Enterococcus faecalis extracellular proteases influences biofilm development. Journal of bacteriology 190(16):5690-8 doi:10.1128/JB.00314-08

Tiefenthaler, L. L., Stein, E. D., & Lyon, G. S. (2009). Fecal indicator bacteria (FIB) levels during dry weather from Southern California reference streams. *Environmental monitoring and assessment*, *155*(1-4), 477-492.

United States Environmental Protection Agency *(USEPA). (2000). "Bacterial indicator tool user's guide." EPA-832-B-01-003, Washington, D.C.*

U.S. EPA 2012a. Water Quality Standards Handbook: Second Edition. EPA-823-B-12-002; March 2012. Retrieved November 13, 2012 from http://water.epa.gov/scitech/swguidance/standards/handbook/index.cfm

U.S. EPA 2012b. Method 1611: Enterococci in Water by TaqMan® Quantitative Polymerase Chain Reaction (qPCR) Assay. EPA-821-R-12-008. https://www.epa.gov/sites/production/files/2015-10/documents/rwqc2012.pdf

U.S. Geological Survey. Geographic Names Phase I data compilation (1976-1981). 31-Dec-1981. Primarily from U.S. Geological Survey 1:24,000-scale topographic maps (or 1:25K, Puerto Rico 1:20K) and from U.S. Board on Geographic Names files. In some instances, from 1:62,500 scale or 1:250,000 scale maps.

Van Loon, A. F., Ploum, S. W., Parajka, J., Fleig, A. K., Garnier, E., Laaha, G., & Van Lanen, H. A. J. (2015). Hydrological drought types in cold climates: quantitative analysis of causing factors and qualitative survey of impacts. *Hydrology and Earth System Sciences*, *19*(4), 1993.

Weakland DR, Smith SN, Bell B, Tripathi A, Mobley HLT (2020) The Serratia marcescens Siderophore Serratiochelin Is Necessary for Full Virulence during Bloodstream Infection. Infect Immun. 88(8): e00117-20.

Wilkes, G., Brassard, J., Edge, T. A., Gannon, V., Gottschall, N., Jokinen, C. C., Jones, T. H., Khan, I. U., Marti, R., Sunohara, M. D., Topp, E., & Lapen, D. R. (2014). Long-term monitoring of waterborne pathogens and microbial source tracking markers in paired agricultural watersheds under controlled and conventional tile drainage

management. *Applied and environmental microbiology*, *80*(12), 3708–3720. https://doi.org/10.1128/AEM.00254-14

Whitman, R. L., Nevers, M. B., & Byappanahalli, M. N. (2006). Examination of the watershed-wide distribution of Escherichia coli along Southern Lake Michigan: an integrated approach. *Applied and environmental microbiology*, *72*(11), 7301–7310. https://doi.org/10.1128/AEM.00454-06

Wu, C. H., Sercu, B., Van de Werfhorst, L. C., Wong, J., DeSantis, T. Z., Brodie, E. L., Hazen, T. C., Holden, P. A., & Andersen, G. L. (2010). Characterization of coastal urban watershed bacterial communities leads to alternative community-based indicators. *PloS one*, *5*(6), e11285. https://doi.org/10.1371/journal.pone.0011285

Wu, J., Rees, P., & Dorner, S. (2011). Variability of E. coli density and sources in an urban watershed. *Journal of water and health*, *9*(1), 94-106.

Zuroff TR, Gu W, Fore RL, Leschine SB, Curtis WR (2014) Insights into Clostridium phytofermentans biofilm formation: aggregation, microcolony development and the role of extracellular DNA. Microbiology 160(Pt 6):1134-43 doi:10.1099/mic.0.078014-0.
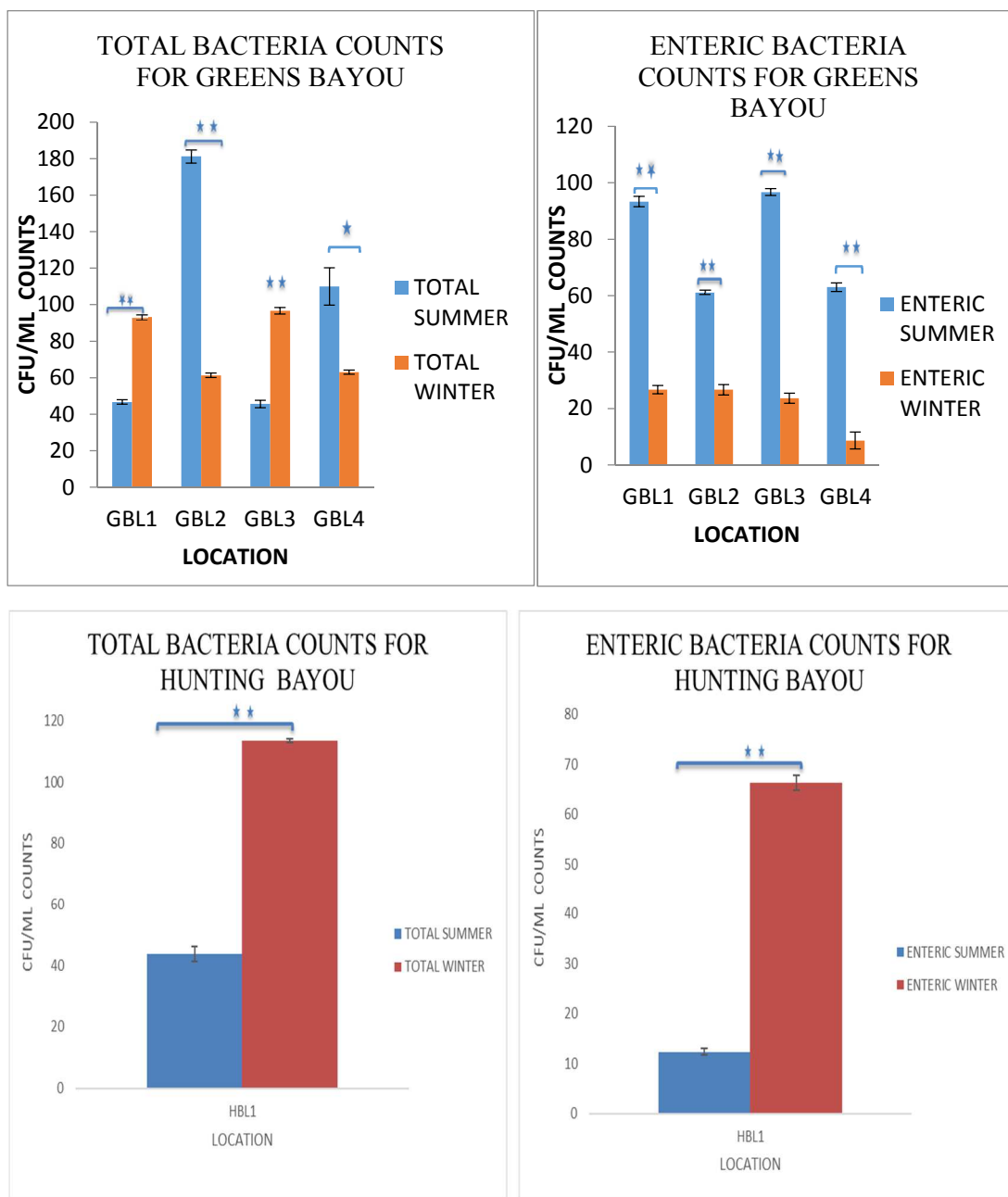
Figure 35: Total bacterial and enteric counts for Greens and Hunting. This experiment was run in triplicate and statistical analysis was determined using the Student's T-test, with p < 0.05 denoted by one asterisk and p < 0.01 denoted by two asterisks.
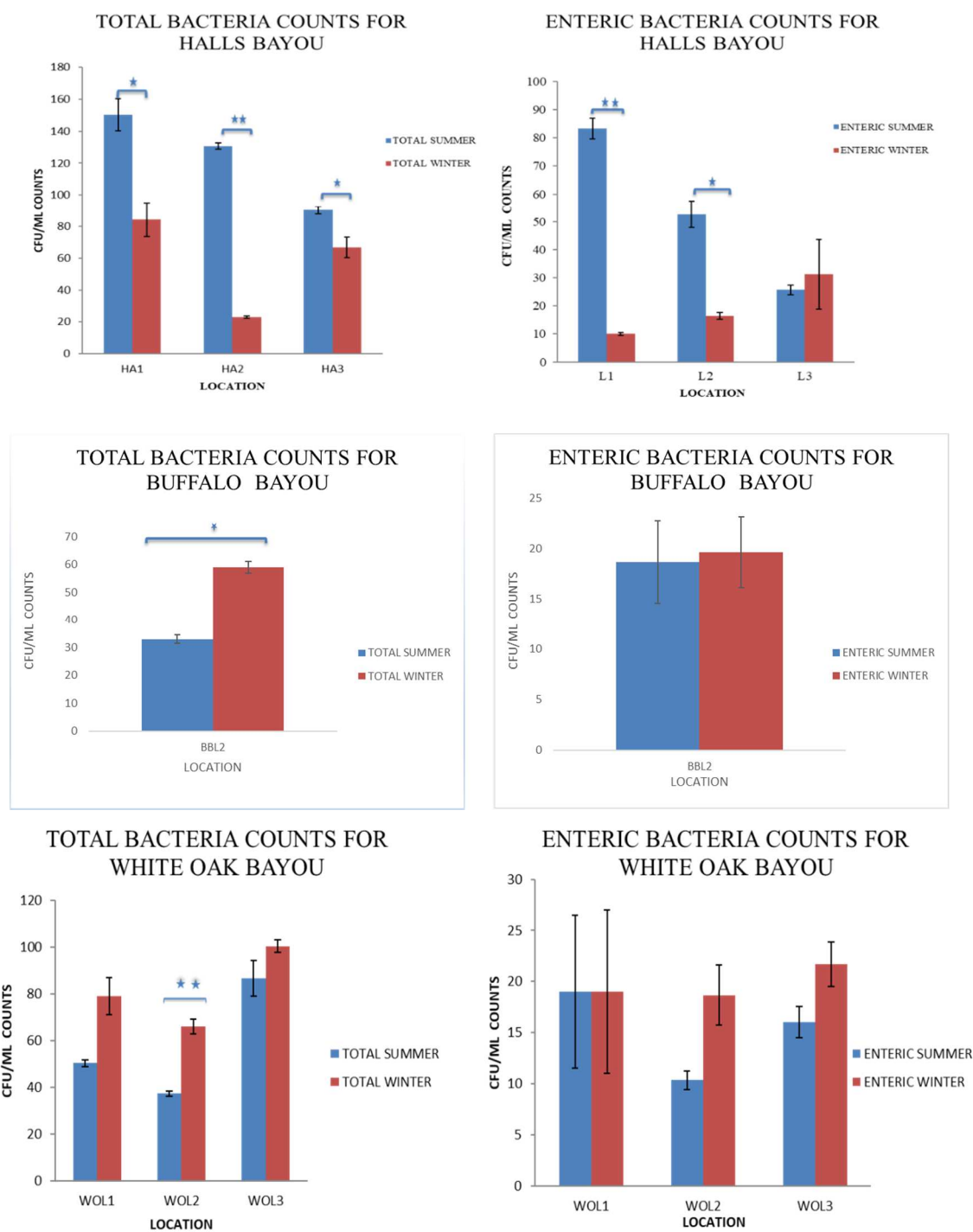
Figure 36: Total and enteric bacterial counts for Halls, Buffalo, and White Oaks Bayous. This experiment was run in triplicate and statistical analysis was determined using the Student's T-test, with $p < 0.05$ denoted by one asterisk and $p < 0.01$ denoted by two asterisks.
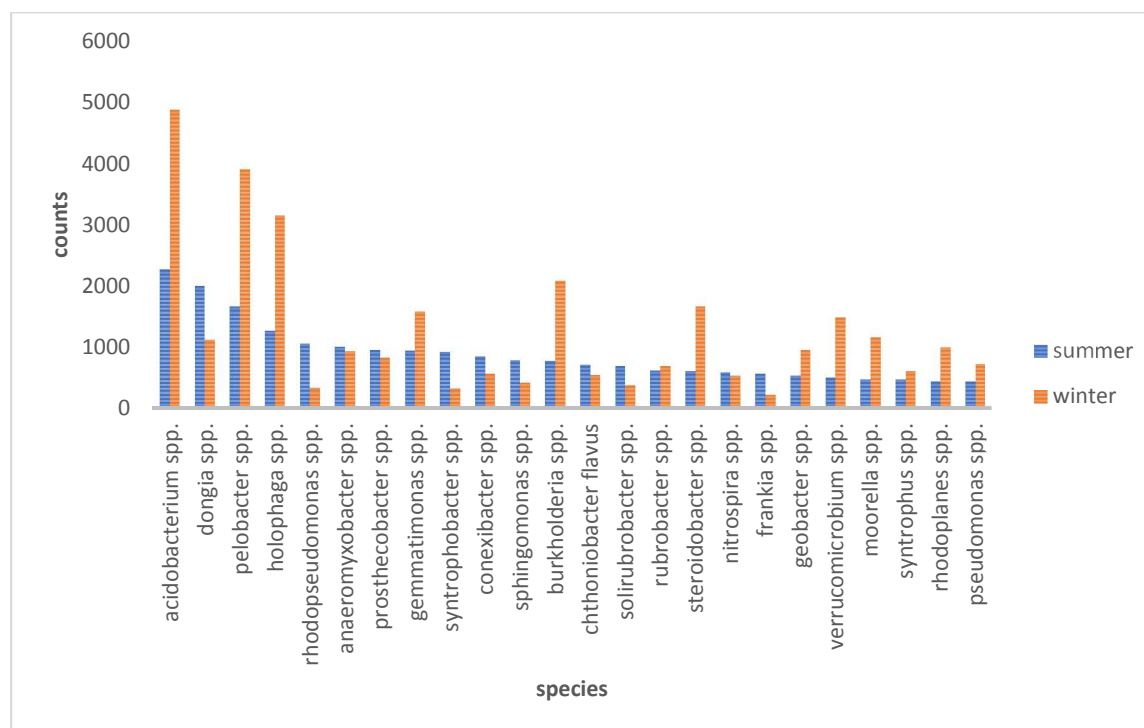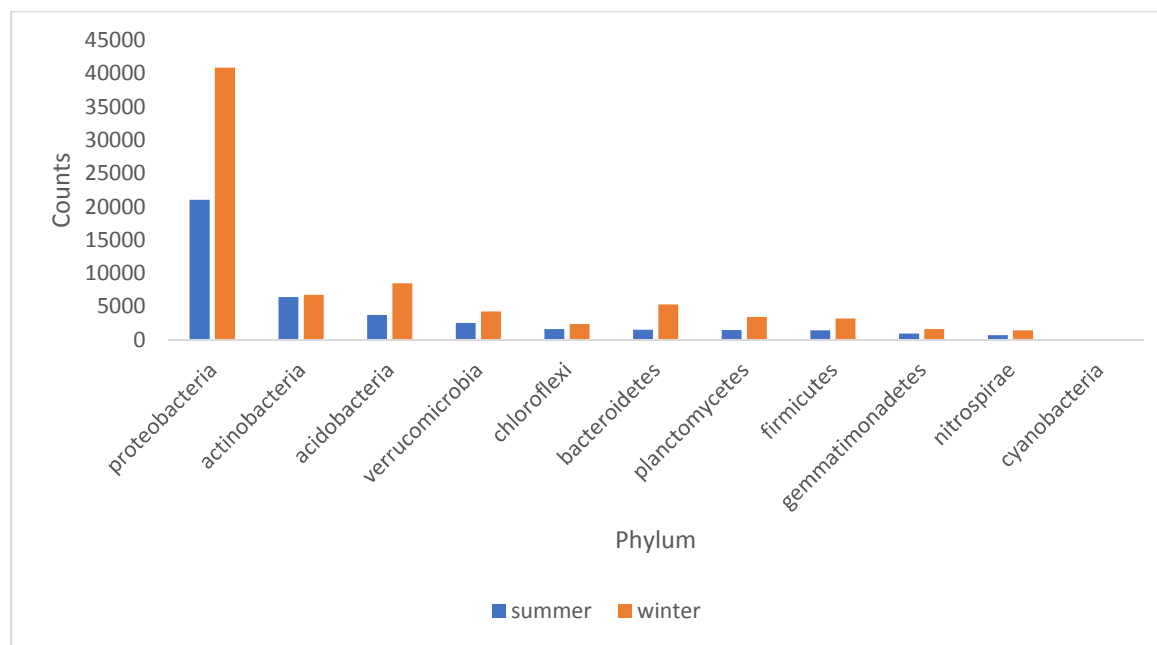
Figure 37: Operational Taxonomical Unit (OTU) percentage distribution from Halls Bayou soil samples during the summer and winter in 2017 for (A) Phylum and (B) species.
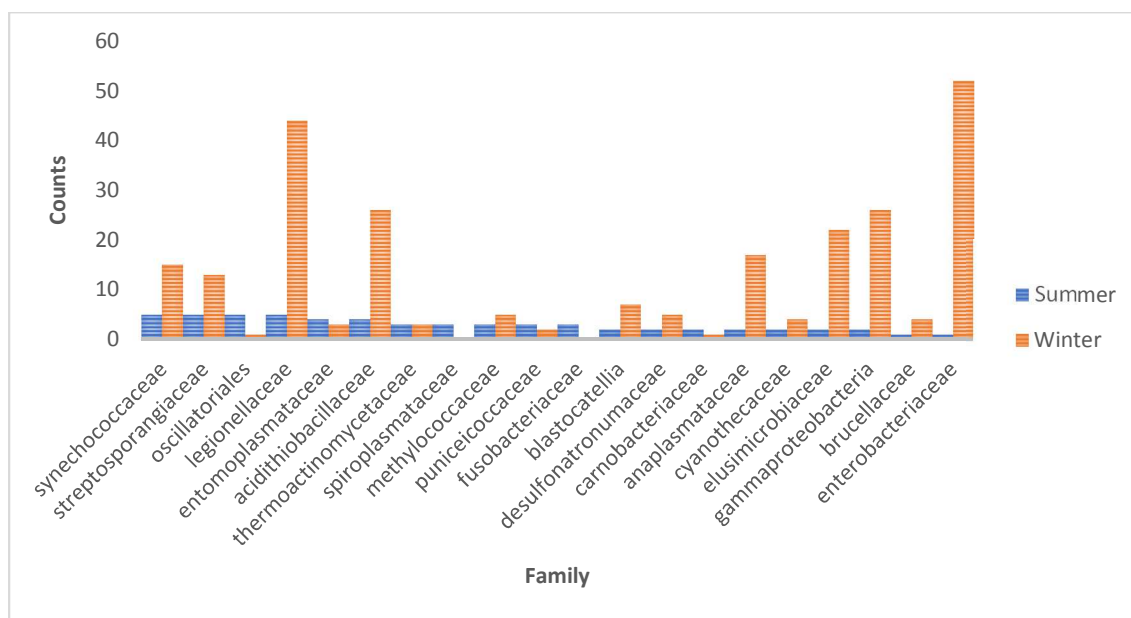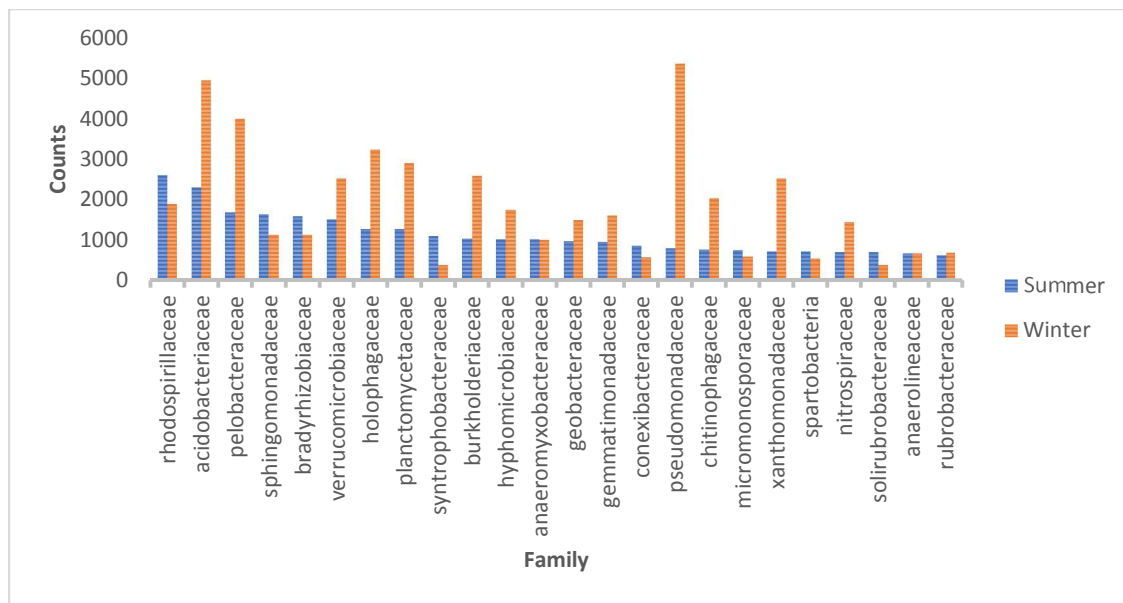
Figure 38: Operational Taxonomical Unit (OTU) percentage distribution from Halls Bayou soil samples during the summer and winter in 2017 for family
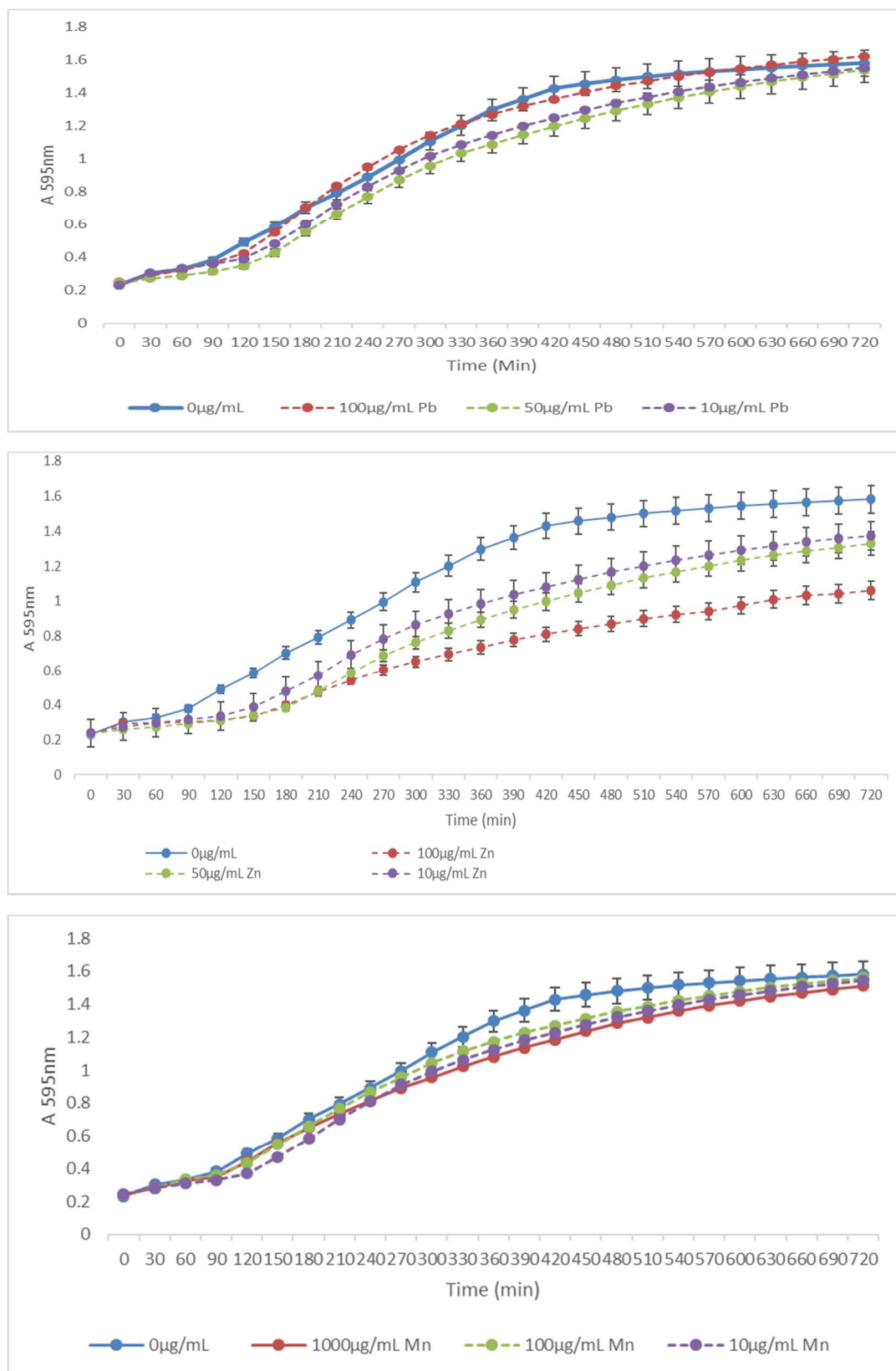
Figure 39: SME growth kinectics in the presence of toxicants (Zn,Pb and Mn)
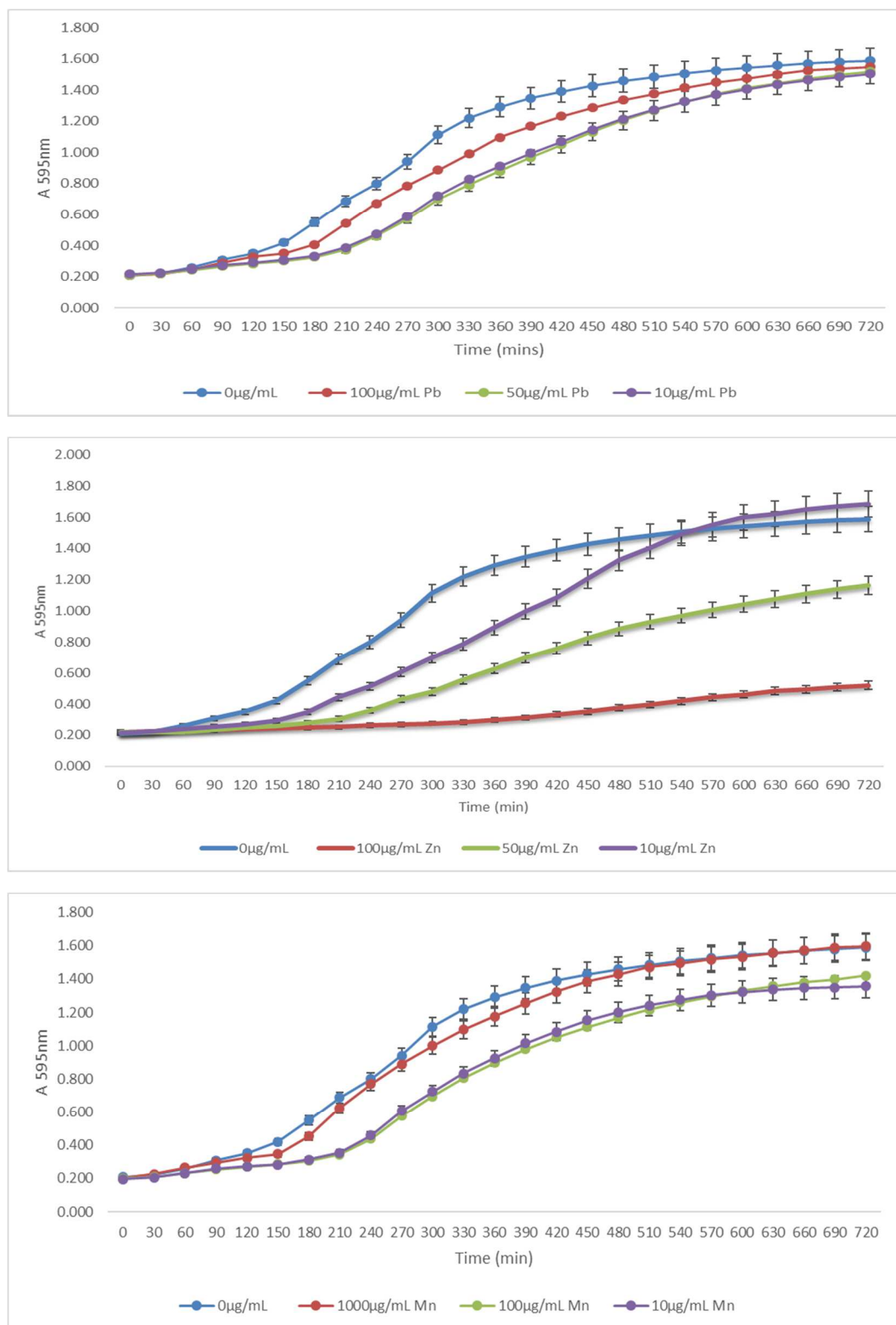
Figure 40: SMS growth kinectics in the presence of toxicants (Zn,Pb and Mn)
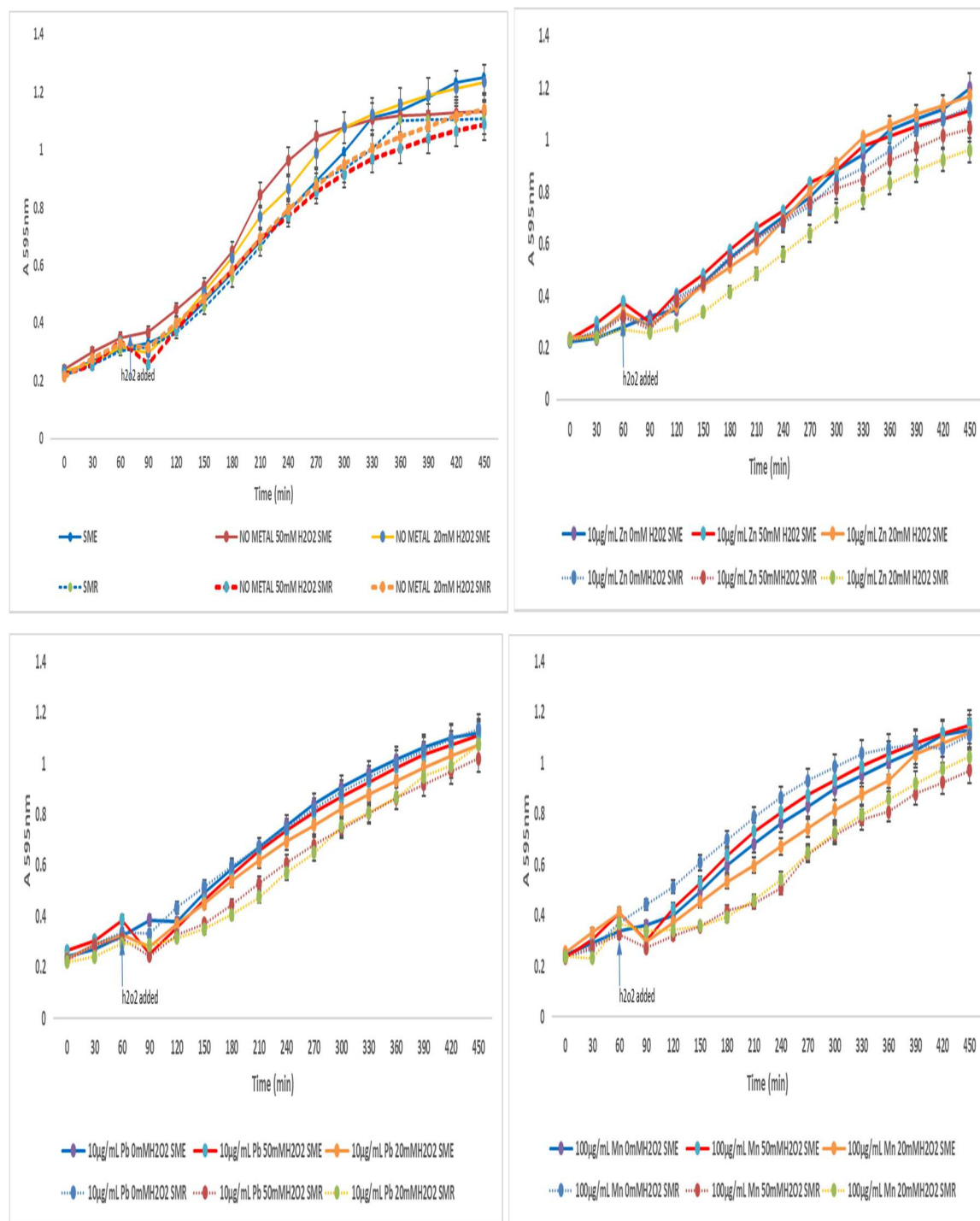
Figure 41: Oxidative stress sensitivity of SME and SMR in the presence of toxicants (10µg/ml Zn, Pb and 100µg/ml Mn)
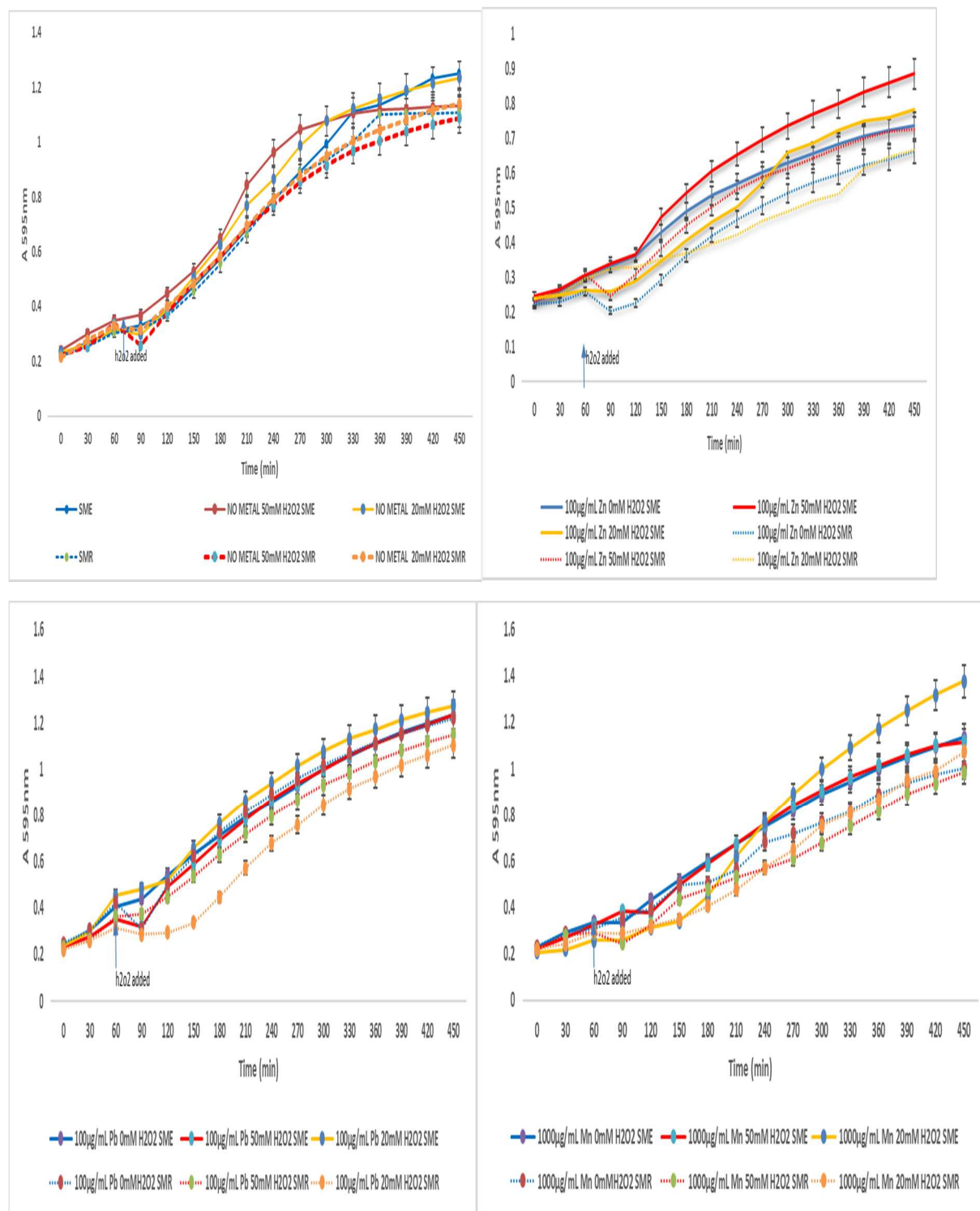
Figure 42: Oxidative stress sensitivity of SME and SMR in the presence of toxicants (100μg/ml Zn, Pb and 1000μg/ml Mn)
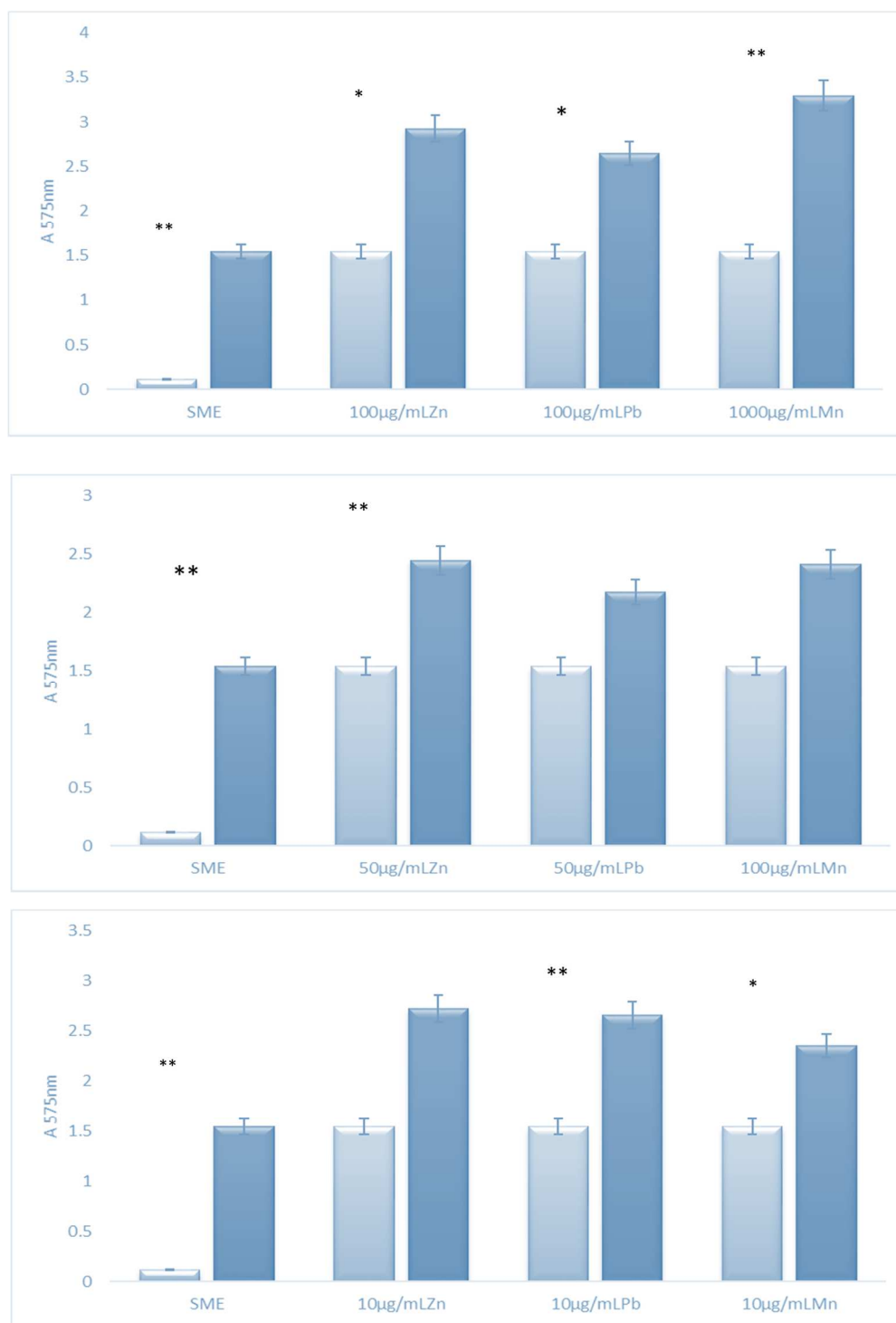
Figure 43: Biofilm production of *Serratia marcescen*s strains to heavy metal exposure.
*Serratia marcescen*s environmental isolate (SME) was exposed to 10 μg/ml, 50 μg/ml and 100 μg/ml of zinc, lead and 100 μg/ml, 500 μg/ml and 1000 μg/ml manganese.

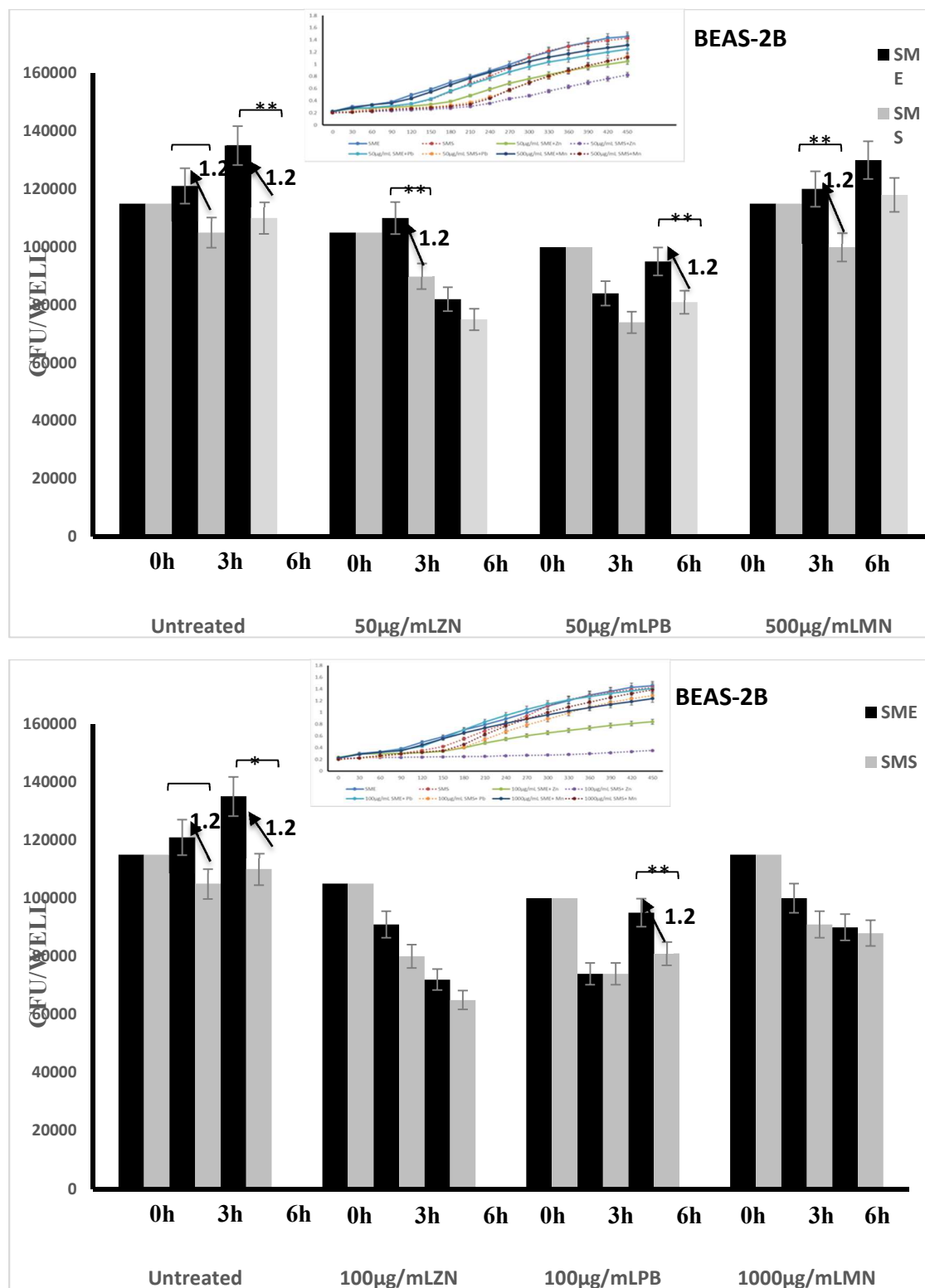Figure 44: Biofilm production of *Serratia marcescen*s strains to heavy metal exposure.
*Serratia marcescen*s surrogate strain (SMS) was exposed to 10 µg/ml, 50 µg/ml and 100 µg/ml of zinc, lead and 100 µg/ml, 500 µg/ml and 1000 µg/ml manganese.

Figure 45: Bacterial co-culture on normal human lung epithelial BEAS-2B cells over 3hrs and 6hrs

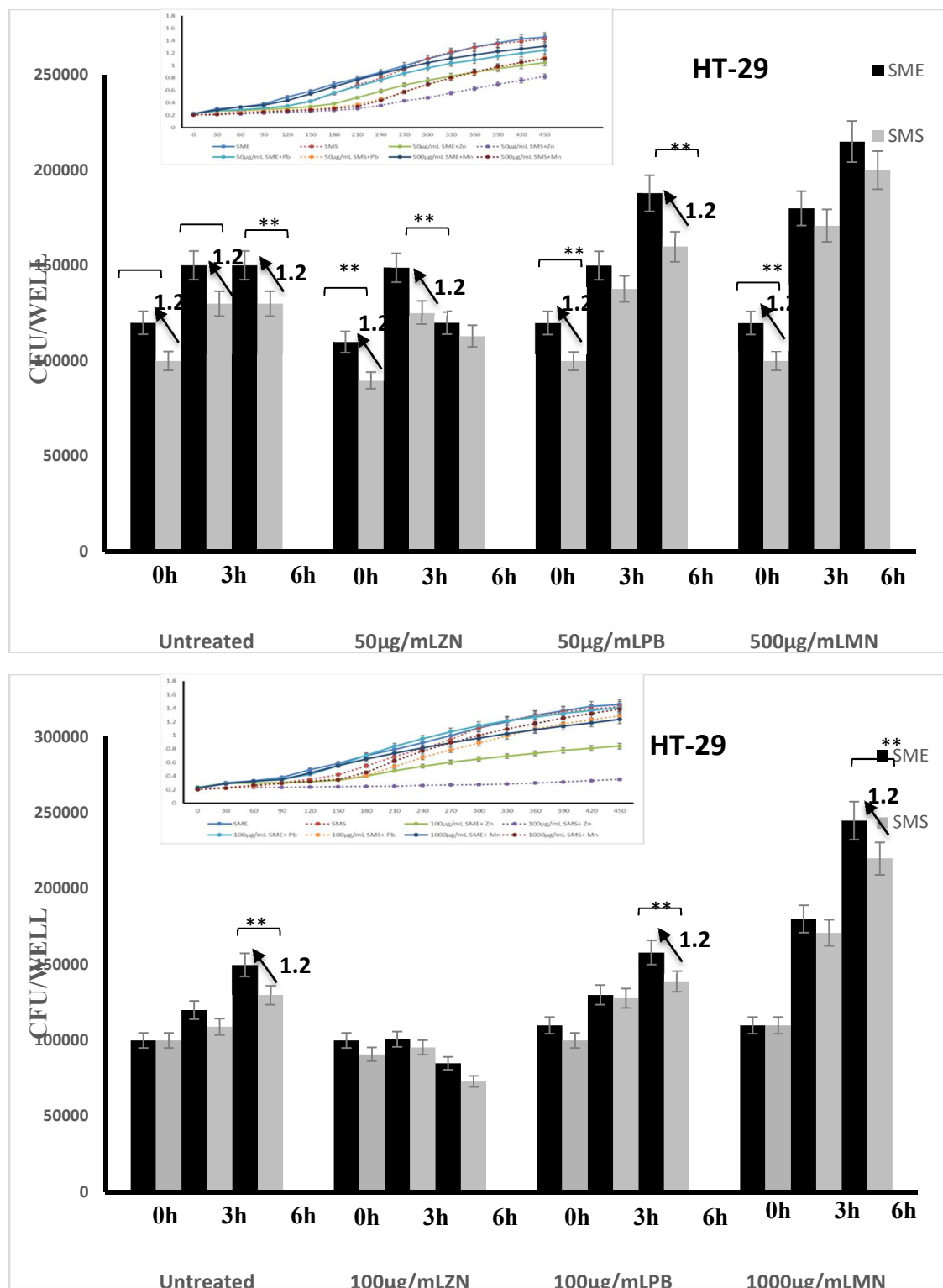end point modeling the lung microenvironment (100µg/ml Zn, Pb and 1000µg/ml Mn)

Figure 46: Bacterial co-culture on cancer gut epithelial HT-29 cells over 3hrs and 6hrs end point

modeling the gut microenvironment (100µg/ml Zn, Pb and 1000µg/ml Mn)
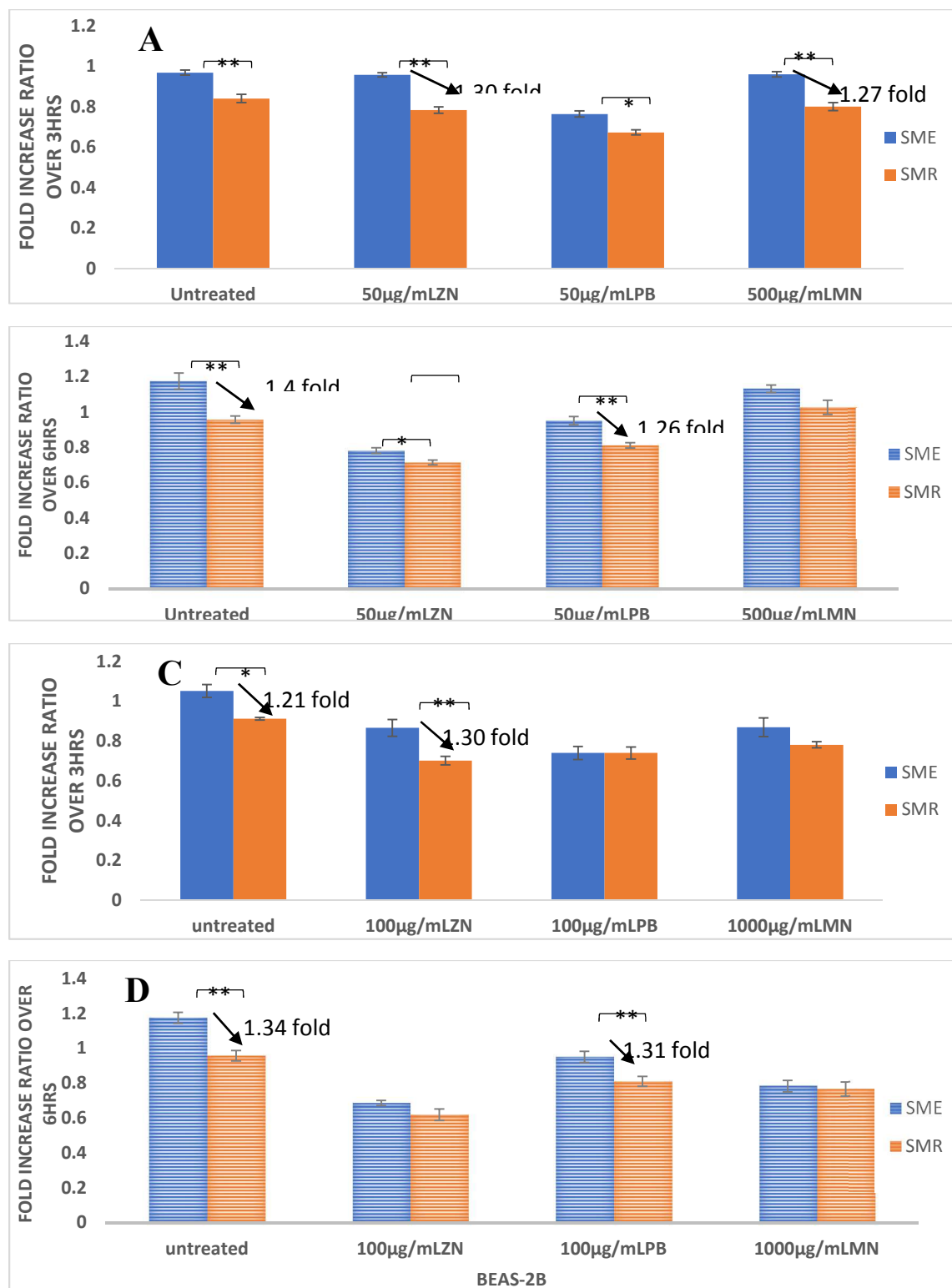
Figure 47: Bacterial co-culture on normal human lung epithelial BEAS-2B cells over 3hrs and 6hrs
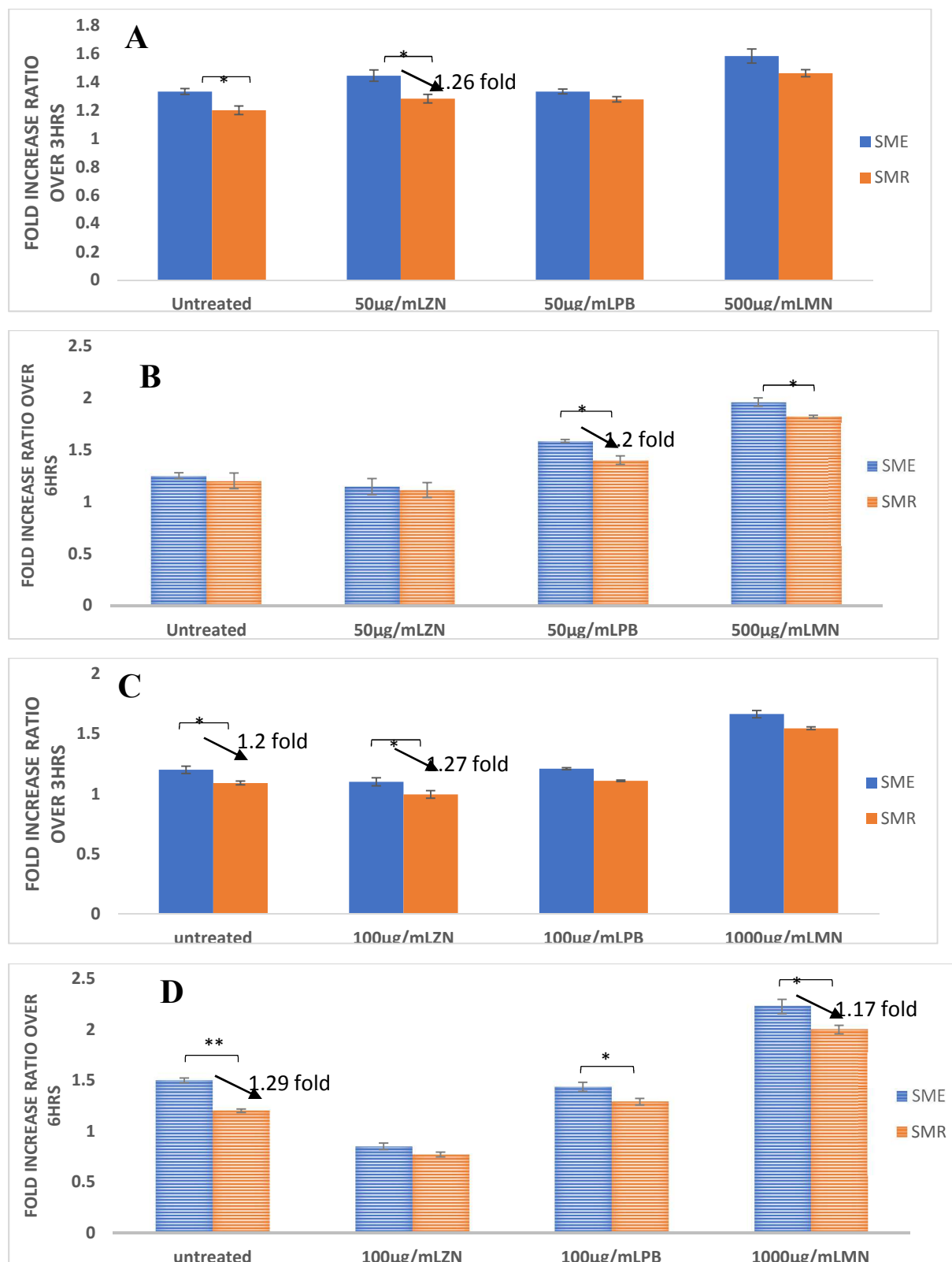
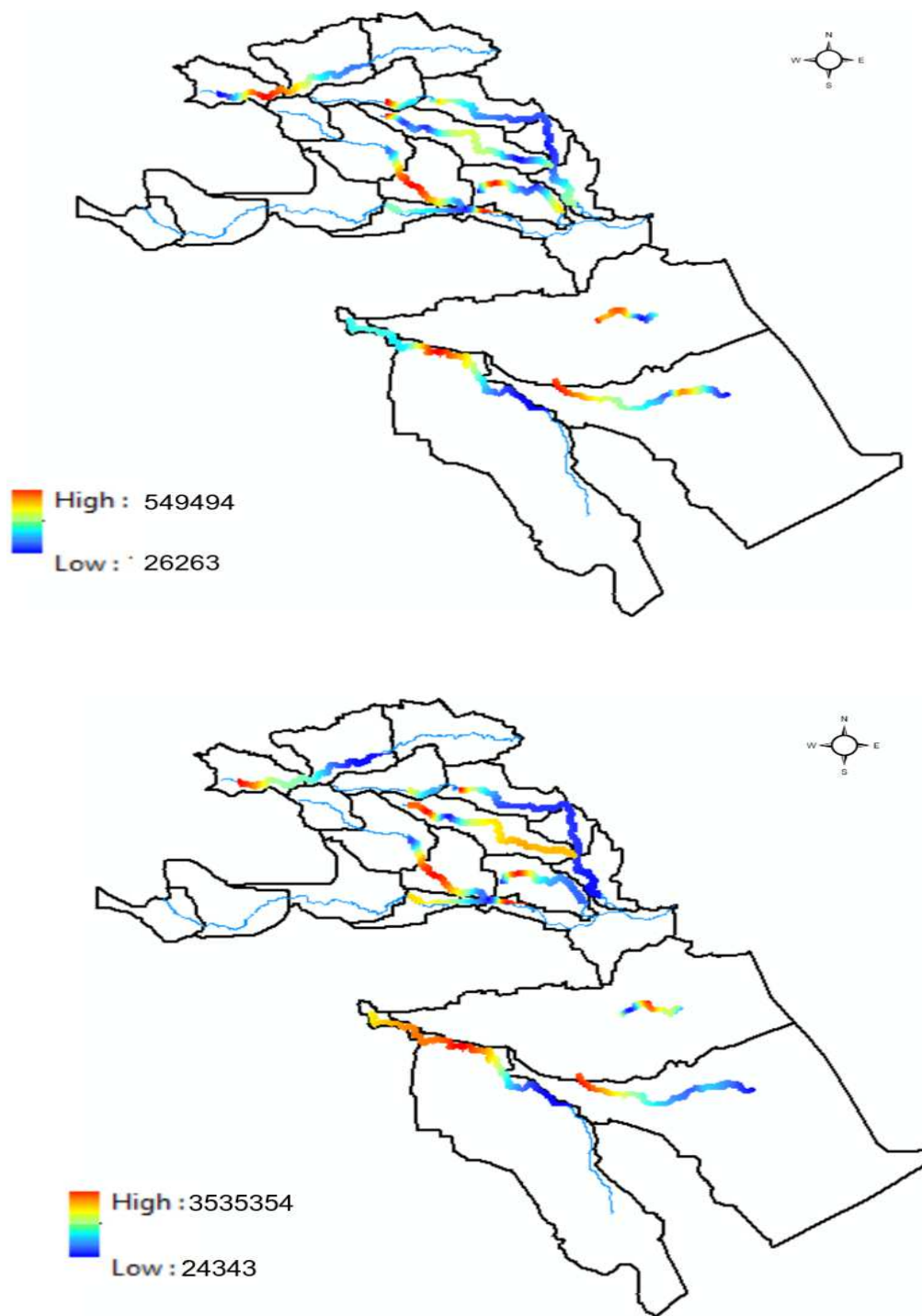Figure 48: Bacterial co-culture on cancer gut epithelial HT-29 cells over 3hrs and 6hrs end point

Figure 49: Interpolation map showing the total bacteria population over time for (A) summer 2017 and 2018.; total bacteria population over time for (B) winter 2017 and 2018.